## PMFermiCOLPEm Resource

**From:** Govan, Tekia
**Sent:** Thursday, March 21, 2013 11:19 AM
**To:** Chakravorty, Manas
**Cc:** 'carl@cjcassoc.com'; 'Manuel Miranda'; FermiCOL Resource
**Subject:** FW: DTE/S&L SASSI2010 V&V References (1 of 2)
**Attachments:** References for SASSI2010 V&V p 1-56.pdf

---

**From:** Michael K Brandon [mailto:brandonm@dteenergy.com]
**Sent:** Thursday, March 21, 2013 11:13 AM
**To:** Govan, Tekia
**Subject:** DTE/S&L SASSI2010 V&V References (1 of 2)

Tekia

Per your request, attached are the references from the public domain used in the V&V being audited.

Due to the size this is 1 of 2 files that I will forward

None of this information is proprietary.

Mike Brandon
Licensing - Manager
DTE Energy/MEP/Nuclear Development
313.235.0443

**Hearing Identifier:** Fermi_COL_Public
**Email Number:** 1173

**Mail Envelope Properties** (F5A4366DF596BF458646C9D433EA37D7EEA8E3859C)

**Subject:** FW: DTE/S&L SASSI2010 V&V References (1 of 2)
**Sent Date:** 3/21/2013 11:18:33 AM
**Received Date:** 3/21/2013 11:18:43 AM
**From:** Govan, Tekia

**Created By:** Tekia.Govan@nrc.gov

**Recipients:**
"'carl@cjcassoc.com'" <carl@cjcassoc.com>
Tracking Status: None
"'Manuel Miranda'" <mmiranda@bnl.gov>
Tracking Status: None
"FermiCOL Resource" <FermiCOL.Resource@nrc.gov>
Tracking Status: None
"Chakravorty, Manas" <Manas.Chakravorty@nrc.gov>
Tracking Status: None

**Post Office:** HQCLSTR01.nrc.gov

| Files | Size | Date & Time |
|---|---|---|
| MESSAGE | 523 | 3/21/2013 11:18:43 AM |
| References for SASSI2010 V&V p 1-56.pdf | 4158408 | |

**Options**
**Priority:** Standard
**Return Notification:** No
**Reply Requested:** No
**Sensitivity:** Normal
**Expiration Date:**
**Recipients Received:**

Nuclear Engineering and Design 36 (1976) 325–340


# VIBRATIONS OF A RIGID DISC ON A LAYERED VISCOELASTIC MEDIUM

J. Enrique LUCO
*Department of Applied Mechanics and Engineering Sciences,*
*University of California, San Diego, La Jolla, California 92093, USA*

Received 17 January 1976

A method of obtaining the dynamic impedance functions for a rigid circular foundation placed on a layered viscoelastic half-space is presented. Both hysteretic and Voigt models of internal damping are considered. The results obtained indicate that the presence of internal damping introduces important changes in the dynamic response of the foundation for vertical, rocking and horizontal steady-state excitation.

## 1. Introduction

A key step in the evaluation of the effects of soil–structure interaction on the earthquake response of a structure is the computation of the force–displacement relationship for the foundation. Several such relationships, expressed in terms of impedance or compliance functions, are available at the present time [1]. However, most of these studies are restricted to a model of soil corresponding to a non-dissipative, purely elastic medium. In these studies no material or internal damping is considered and, consequently, the only source of energy dissipation corresponds to the geometric attenuation, also called radiation damping.

The objective of this study is to incorporate the effects of material damping in the analysis of the harmonic response of a rigid circular foundation placed on a layered medium. The need for incorporating the material damping in the solution of this problem arises from the important effects that internal damping has, particularly when large strains are involved or when the medium representing the soil is layered. In this study two types of material damping are considered: viscous Voigt-type damping and hysteretic-type damping. Three types of harmonic excitations are investigated: vertical force, rocking moment and horizontal force. In all cases relaxed conditions on the contact between the circular foundation and the supporting medium are assumed.

In a previous study, Veletsos and Verbic [2] considered the harmonic response of a circular foundation placed on a viscoelastic half-space. The procedure used by them was based on establishing analytical approximations to the numerically obtained solutions for the elastic problem and in extending these approximations to the viscoelastic case by use of the correspondence principle. Such approach cannot be extended to the analysis of layered media for which the impedance functions may present strong fluctuations as a function of frequency. The studies reported in refs. [3]–[5], although more general with regard to the incorporation of material damping, are based on an assumed stress distribution at the contact between the foundation and the soil.

The method of solution employed here follows, except for consideration of the material damping, the procedure used by the author [6] to solve the problem for a non-dissipative layered medium.

## 2. Formulation of the problem

### *2.1. Statement of the problem*

In what follows, a study is made of the forced harmonic vibrations of a rigid circular footing of radius $a$ placed on the surface of a layered viscoelastic medium. The layered medium consists of $N-1$ parallel layers resting on a viscoelastic half-space. Both the layers and the half-space are assumed to be homogeneous and

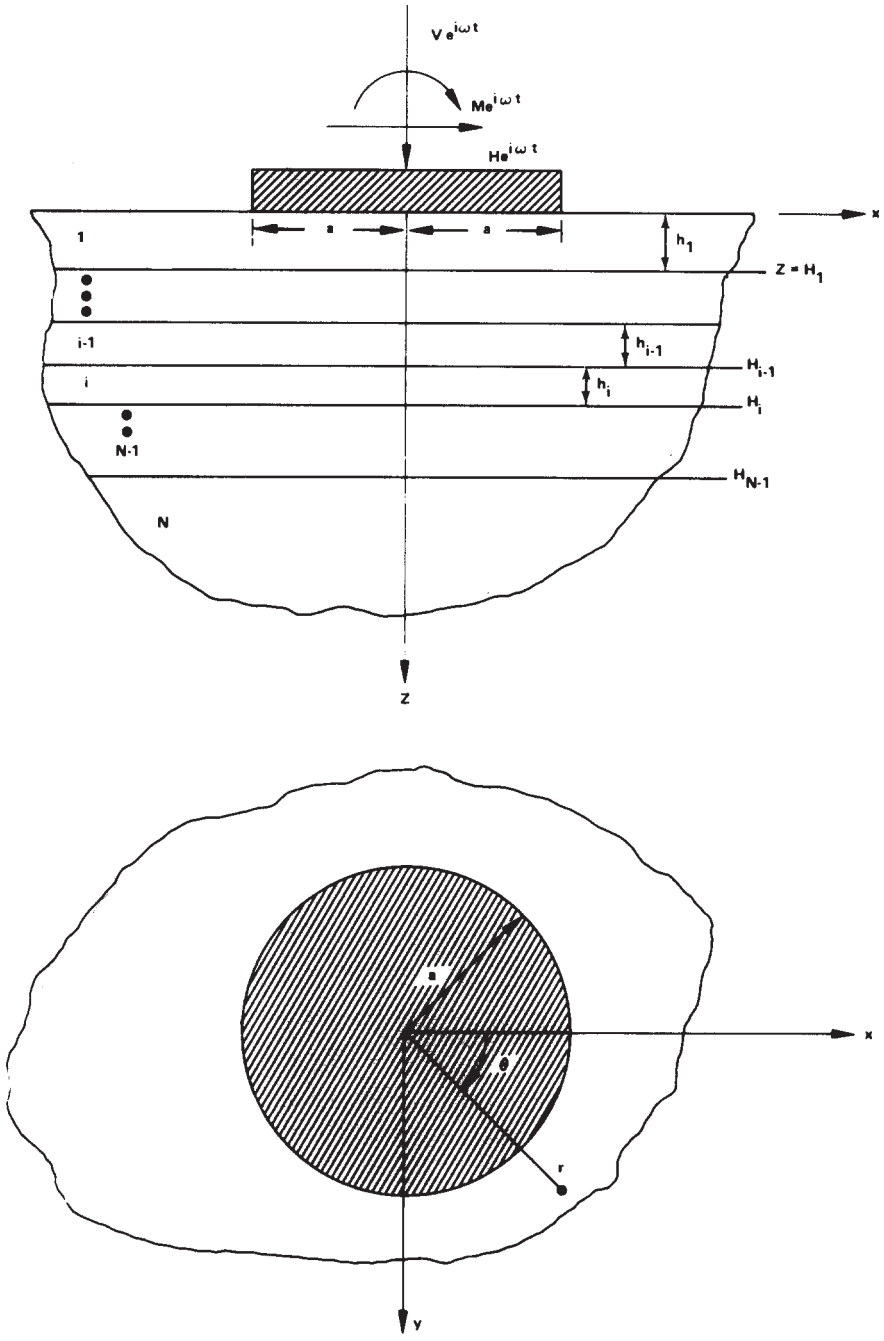


Fig. 1. Description of the model.

isotropic with densities $\rho_i$, shear moduli $G_i$, and Poisson's ratios $\sigma_i (i = 1, 2, ..., N)$, respectively. In addition, depending on the type of internal friction considered, the relative viscosity coefficient $(G_i'/G_i)$ (for Voigt-type dissipation), or, the hysteretic damping coefficient $\xi_i = \omega G_i'/2G_i$ (for hysteretic-type dissipation) are assumed to be known for each one of the media forming the soil deposit. The geometry of the model

and the coordinate systems used are shown in fig. 1.

A welded type of contact is assumed to exist between adjacent layers. Thus, the stresses and displacements are continuous across each interface. The contact between the foundation and the surface of the top layer is assumed to be relaxed, i.e. the contact is frictionless for vertical and rocking vibrations and pressureless for horizontal vibrations.

The boundary conditions at $z = 0$ expressed in terms of displacement and stress components in cylindrical coordinates are:

(a) vertical vibrations

$$u_z(r, \theta, 0) = \Delta_v e^{i\omega t}, \qquad 0 \leqslant r \leqslant a; \quad (1a)$$

$$\sigma_{zz}(r, \theta, 0) = 0, \qquad r > a, \quad (1b)$$

$$\sigma_{zr}(r, \theta, 0) = \sigma_{z\theta}(r, \theta, 0) = 0, \qquad 0 < r < \infty; \quad (2)$$

(b) rocking vibrations

$$u_z(r, \theta, 0) = \alpha r \cos\theta\, e^{i\omega t}, \qquad 0 \leqslant r \leqslant a; \quad (3a)$$

$$\sigma_{zz}(r, \theta, 0) = 0, \qquad r > a, \quad (3b)$$

$$\sigma_{zr}(r, \theta, 0) = \sigma_{z\theta}(r, \theta, 0) = 0, \qquad 0 < r < \infty; \quad (4)$$

(c) horizontal vibrations

$$u_r(r, \theta, 0) = \Delta_H \cos\theta\, e^{i\omega t},$$

$$u_\theta(r, \theta, 0) = -\Delta_H \sin\theta\, e^{i\omega t}, \qquad 0 \leqslant r \leqslant a, \quad (5)$$

$$\sigma_{zr}(r, \theta, 0) = \sigma_{z\theta}(r, \theta, 0) = 0, \qquad r > a; \quad (6)$$

$$\sigma_{zz}(r, \theta, 0) = 0, \qquad 0 < r < \infty. \quad (7)$$

In the above equations, $\Delta_v$ is the amplitude of the vertical displacement of the center of the rigid foundation; $\alpha$ is the amplitude of the rocking angle about the $y$ axis ($\theta = \pi/2$); $\Delta_H$ is the amplitude of the horizontal displacement of the foundation in the direction of the $x$ axis ($\theta = 0$); and $\omega$ is the frequency of the steady-state vibrations.

The continuity conditions at the interface $z = H_i$ are

$$u_r^i(r, \theta, H_i) = u_r^{i+1}(r, \theta, H_i), \quad (8a)$$

$$u_\theta^i(r, \theta, H_i) = u_\theta^{i+1}(r, \theta, H_i), \quad (8b)$$

$$u_z^i(r, \theta, H_i) = u_z^{i+1}(r, \theta, H_i) \qquad (i = 1, 2, ..., N-1), \quad (8c)$$

$$\sigma_{zr}^i(r, \theta, H_i) = \sigma_{zr}^{i+1}(r, \theta, H_i), \quad (9a\text{–}c)$$

$$\sigma_{z\theta}^i(r, \theta, H_i) = \sigma_{z\theta}^{i+1}(r, \theta, H_i),$$

$$\sigma_{zz}^i(r, \theta, H_i) = \sigma_{zz}^{i+1}(r, \theta, H_i) \qquad (i = 1, 2, ..., N-1),$$

where the superscript $i$ indicates the $i$th layer. In addition, the displacement and stress components in the underlying half-space must tend to zero as $(r^2 + z^2)$ tends to infinity.

### 2.2. Types of energy dissipation

In this study two types of energy dissipation are considered, namely, the Voigt viscous model and the hysteretic model.

The stress–strain relationships for harmonic vibrations of a solid with Voigt-type damping are of the form [7]

$$\sigma_{zz} = (\lambda + i\omega\lambda')\Theta + 2(\mu + i\omega\mu')\epsilon_{zz}, \quad (10a)$$

$$\sigma_{zx} = 2(\mu + i\omega\mu')\epsilon_{xz}, \quad (10b)$$

where

$$\Theta = \epsilon_{xx} + \epsilon_{yy} + \epsilon_{zz}. \quad (10c)$$

In eqs. (10a) and (10b), $\omega$ is the frequency of the excitation; $\lambda$ and $\mu$ are Lame's constants; and $\lambda'$, $\mu'$ are the viscosities. It is clear from eqs. (10a) and (10b) that the viscoelastic problem may be solved, if the solution for the corresponding purely elastic problem is known, by substituting in the elastic solution $\lambda$ and $\mu$ by the complex moduli

$$\lambda^* = \lambda(1 + i\omega\lambda'/\lambda) \quad \text{and} \quad \mu^* = \mu(1 + i\omega\mu'/\mu). \quad (11a, b)$$

To simplify the problem it is assumed that

$$\lambda'/\lambda = \mu'/\mu. \quad (12)$$

In this case the remaining complex constants are given by

$$E^* = \frac{(3\lambda^* + 2\mu^*)\mu^*}{\lambda^* + \mu^*} = E(1 + i\omega\mu'/\mu),$$

$$k^* = \lambda^* + \tfrac{2}{3}\mu^* = k(1 + i\omega\mu'/\mu), \quad (13a, b)$$

$$\sigma^* = \lambda^*/[2(\lambda^* + \mu^*)] = \sigma, \quad (13c)$$

where $E$, $k$ and $\sigma$ are Young's modulus, the bulk modulus, and Poisson's ratio, respectively. The assumption given by eq. (12) has the advantage that the Poisson's ratio for the viscoelastic medium is real and equal to the Poisson's ratio of the corresponding elastic medium. One disadvantage, however, is the fact that the bulk modulus is complex and consequently there are losses associated with changes of volume.

Equation (10b) indicates that for shear deformations the stress–strain relationship could be described by an ellipse. The energy loss per cycle is given by the area of the ellipse and the corresponding 'specific loss' is

$$\Delta W/W = 2\pi(\omega\mu'/\mu)\,, \tag{14}$$

where $W$ is the elastic energy stored when the strain is a maximum. Equation (14) indicates that for a Voigt solid the 'specific loss', or the energy loss per cycle, is proportional to the frequency of the excitation. The elliptical stress–strain loop in this case is a direct result of the viscosity of the medium.

Laboratory tests on soils indicate that the 'specific loss' $\Delta W/W$ is independent of the frequency of the excitation and that the stress–strain loop is not an ellipse [8–12]. It appears then that the mechanism of energy loss in soils is not of the viscous type but rather is a direct result of the anelastic behaviour of soils. In spite of this anelastic behaviour an approximate approach is to assume that the soil may be treated in a similar way as a viscoelastic medium, except that in this case the complex shear modulus $\mu^*$ and the 'specific loss' are taken to be equal to

$$\mu^* = \mu(1 + 2i\xi) \quad \text{and} \quad \Delta W/W \equiv 4\pi\xi\,, \tag{15,16}$$

where $\xi$ is a damping constant independent of frequency. This model of internal damping is also called constant hysteretic-type damping. The damping constant $\xi$ is analogous to the percentage of critical damping under resonant conditions, or during free vibrations [8]. The hysteretic damping constant $\xi$ is strain dependent: values for low strain may be less than 0.02, while for high strains $\xi$ may reach values of 0.15 or 0.20.

In what follows the shear modulus $\mu$ is designated by $G$, and the shear viscosity $\mu'$ is designated by $G'$.

### 2.3. Integral representation

A solution of the equations of motion in cylindrical coordinates satisfying the conditions at the interface between layers, as well as the conditions at infinity, may be obtained by the application of the correspondence principle to a representation derived by Sezawa and reported in ref. [13] and [14].

The displacement and stress components of interest, at $z = 0$, are given by

$$u_r(r, \theta, 0) = a\,u_r^*(r')\cos(n\theta)\,,$$

$$u_\theta(r, \theta, 0) = a u_\theta^*(r')\sin(n\theta)\,,$$

$$u_z(r, \theta, 0) = a u_z^*(r')\cos(n\theta)\,, \tag{17}$$

$$\sigma_{zr}(r, \theta, 0) = G_1\,\sigma_{zr}^*(r')\cos(n\theta)\,,$$

$$\sigma_{z\theta}(r, \theta, 0) = G_1\,\sigma_{z\theta}^*(r')\sin(n\theta)\,,$$

$$\sigma_{zz}(r, \theta, 0) = G_1\,\sigma_{zz}^*(r')\cos(n\theta)\,, \tag{18}$$

where $n = 0$ for vertical vibrations; $n = 1$ for rocking and horizontal vibrations; $r' = r/a$; and

$$u_r^*(r') \pm u_\theta^*(r') = \mp 2\int_0^\infty \{k[\Delta_{11}(k)C_1(k) + \Delta_{12}(k)C_2(k)]/\Delta_R \mp \Delta_{33}C_3(k)/\Delta_L\} J_{n\pm1}(a_0 k r')\,\mathrm{d}k\,, \tag{19}$$

$$u_z^*(r') = 2\int_0^\infty k\{[\Delta_{21}(k)C_1(k) + \Delta_{22}(k)C_2(k)]/\Delta_R\} J_n(a_0 k r')\,\mathrm{d}k\,, \tag{20}$$

$$\sigma_{zr}^*(r') \pm \sigma_{z\theta}^*(r') = \pm 2a_0\int_0^\infty [kC_1(k) \mp C_3(k)] J_{n\pm1}(a_0 k r')\,\mathrm{d}k\,, \tag{21}$$

$$\sigma_{zz}^*(r') = 2a_0\int_0^\infty kC_2(k) J_n(a_0 k r')\,\mathrm{d}k\,. \tag{22}$$

In eqs. (19)–(22), $a_0 = \omega a/\beta_1$ is a dimensionless frequency defined in terms of the shear wave velocity $\beta_1$ of the top layer. The functions $\Delta_{ij}(i,j = 1,2)$, $\Delta_R$, $\Delta_{33}$ and $\Delta_L$, appearing in eqs. (19)–(22), depend on the properties of the soil column and are given in the appendix. The functions $C_1(k)$, $C_2(k)$ and $C_3(k)$ are to be determined by the boundary conditions at $z = 0$. For vertical and rocking vibrations, eqs. (2) and (4) together with eq. (21) imply that

$$C_1(k) = C_3(k) = 0 \,. \tag{23}$$

Similarly, for horizontal vibrations, eqs. (7) and (22) imply that

$$C_2(k) = 0 \,. \tag{24}$$

Before imposing the remaining boundary conditions, it is convenient to introduce the following substitution [6, 14]:

(a) vertical vibrations

$$C_2(k) = -\left[\frac{\Delta_V \kappa_1^2}{\pi a(1-\sigma_1)}\, a_0\right] \int_0^1 \phi_V(t)\cos(a_0 kt)\,\mathrm{d}t \,; \tag{25}$$

(b) rocking vibrations

$$C_2(k) = -\left[\frac{2\alpha\kappa_1^2}{\pi(1-\sigma_1)}\, a_0\right] \int_0^1 \phi_R(t)\sin(a_0 kt)\,\mathrm{d}t \,; \tag{26}$$

(c) horizontal vibrations

$$C_1(k) = \left[\frac{2\Delta_H \kappa_1^2}{\pi a(2-\sigma_1)}\, a_0\right] \times \int_0^1 \{\phi_1(t)\cos(a_0 kt) - \phi_2(t)\,[\cos(a_0 kt) - \sin(a_0 kt)/a_0 kt)]\}\mathrm{d}t \,, \tag{27}$$

$$C_3(k) = -\left[\frac{2\Delta_H \kappa_1^2}{\pi a(2-\sigma_1)}\, a_0 k\right] \times \int_0^1 \{-\phi_1(t)\cos(a_0 kt) - (1-\sigma_1)\phi_2(t) \times [\cos(a_0 kt) - \sin(a_0 kt)/a_0 kt]\}\,\mathrm{d}t \,, \tag{28}$$

where $\phi_V(t)$, $\phi_R(t)$, and $\phi_1(t)$, $\phi_2(t)$ are functions to be determined by eqs (1), (3) and (5), respectively. In eqs (25)–(28), $\kappa_1^2 = (1 + \mathrm{i}\omega G_1'/G_1)^{-1}$ for Voigt-type damping, and $\kappa_1^2 = (1 + 2\mathrm{i}\xi_1)^{-1}$ for hysteretic-type damping. The substitutions indicated above satisfy directly the stress boundary conditions prescribed in eqs (1b), (3b) and (6).

## 3. Integral equations and impedance functions

Substitution from eqs. (25)–(28), together with eqs (23) and (24), into eqs (17), (19) and (20), and imposition of the remaining displacement boundary conditions, leads to the following integral equations for the unknown functions $\phi_V(t)$, $\phi_R(t)$, $\phi_1(t)$ and $\phi_2(t)$:

(a) vertical vibrations

$$\phi_V(t) + \int_0^1 K(t,t')\phi_V(t')\,\mathrm{d}t' = 1 \qquad (0 \leqslant t \leqslant 1) \,, \tag{29}$$

where

$$K(t,t') = L_1(|t-t'|) + L_1(t+t') \,, \tag{30}$$

$$L_1(t) = -\frac{a_0}{\pi}\int_0^\infty \left[\frac{k\Delta_{22}}{(1-\sigma_1)\Delta_R \kappa_1^2} + 1\right]\cos(a_0 kt)\,\mathrm{d}k; \tag{31}$$

(b) rocking vibrations

$$\phi_R(t) + \int_0^1 K(t,t')\phi_R(t')\,\mathrm{d}t' = t \qquad (0 \leqslant t \leqslant 1) \,, \tag{32}$$

where

$$K(t,t') = L_1(|t-t'|) - L_1(t+t') \,. \tag{33}$$

The function $L_1(t)$ in eq. (33) is defined by eq. (31).

(c) Horizontal vibrations

$$\phi_1(t) + \int_0^1 [K_{11}(t,t')\phi_1(t') + K_{12}(t,t')\phi_2(t')]\,\mathrm{d}t' = 1 \qquad (0 \leqslant t \leqslant 1) \,, \tag{34}$$

$$(1-\sigma_1)\phi_2(t)+\int_0^1 [K_{21}(t,t')\phi_1(t')+ +K_{22}(t,t')\phi_2(t')]\,dt'=0 \qquad (0\leqslant t\leqslant 1)\,, \quad (35)$$

where

$$K_{11}(t,t')=\frac{2a_0}{\pi}\left(\frac{1}{2-\sigma_1}\right)\int_0^1 [(1-\sigma_1)H_1(k)+H_2(k)] \times \cos(a_0kt)\cos(a_0kt')\,dk\,, \quad (36)$$

$$K_{12}(t,t')=-\frac{2a_0}{\pi}\left(\frac{1-\sigma_1}{2-\sigma_1}\right)\int_0^\infty [H_1(k)-H_2(k)] \times \cos(a_0kt)\left[\cos(a_0kt')-\frac{\sin(a_0kt')}{a_0kt'}\right]dk\,, \quad (37)$$

$$K_{21}(t,t')=-\frac{2a_0}{\pi}\left(\frac{1-\sigma_1}{2-\sigma_1}\right)\int_0^\infty [H_1(k)-H_2(k)] \times \left[\cos(a_0kt)-\frac{\sin(a_0kt)}{a_0kt}\right]\cos(a_0kt')\,dk\,, \quad (38)$$

$$K_{22}(t,t')=\frac{2a_0}{\pi}\left(\frac{1-\sigma_1}{2-\sigma_1}\right)\int_0^\infty [H_1(k)+(1-\sigma_1)H_2(k)] \times \left[\cos(a_0kt)-\frac{\sin(a_0kt)}{a_0kt}\right]\left[\cos(a_0kt')-\frac{\sin(a_0kt')}{a_0kt'}\right]dk\,, \quad (39)$$

and

$$H_1(k)=\frac{k}{\kappa_1^2(1-\sigma_1)}\frac{\Delta_{11}}{\Delta_R}-1\,, \quad (40)$$

$$H_2(k)=\frac{k\Delta_{33}}{\kappa_1^2\Delta_L}-1. \quad (41)$$

The integral equations (29), (32), (34) and (35) are of the Fredholm type and have a form suitable for numerical solution. Once these integral equations have been solved, the entire displacement and stress field may be evaluated by substitution from eqs (25)–(28) into eqs (19)–(22). In particular, the total vertical load $V$, the rocking moment about the $y$ axis $M$, and the total horizontal load in the $x$ direction $H$ may be found to be given by

$$V=\frac{4G_1a\Delta_v e^{i\omega t}}{(1-\sigma_1)\kappa_1^2}\int_0^1 \phi_v(t)\,dt\,, \quad (42)$$

$$M=\frac{8G_1a^3\alpha e^{i\omega t}}{(1-\sigma_1)\kappa_1^2}\int_0^1 t\phi_R(t)\,dt\,, \quad (43)$$

$$H=\frac{8G_1a\Delta_H e^{i\omega t}}{(2-\sigma_1)\kappa_1^2}\int_0^1 \phi_1(t)\,dt\,. \quad (44)$$

Equations (42)–(44) constitute the force-displacement relationship for the circular foundation. It should be mentioned that in deriving these equations the terms coupling the horizontal and rocking vibrations have been neglected.

It is convenient to write eqs (42)–(44) in the following form:

$$V=\frac{4G_1a}{1-\sigma_1}[k_{VV}(a_0)+ia_0c_{VV}(a_0)]\Delta_v e^{i\omega t}\,, \quad (45)$$

$$M=\frac{8G_1a^3}{3(1-\sigma_1)}[k_{MM}(a_0)+ia_0c_{MM}(a_0)]\alpha e^{i\omega t}\,, \quad (46)$$

$$H=\frac{2G_1a}{2-\sigma_1}[k_{HH}(a_0)+ia_0c_{HH}(a_0)]\Delta_H e^{i\omega t}\,, \quad (47)$$

where

$$k_{VV}(a_0)=\int_0^1 \mathrm{Re}[\phi_v(t)/\kappa_1^2]\,dt\,,$$

$$c_{VV}(a_0)=\frac{1}{a_0}\int_0^1 \mathrm{Im}[\phi_v(t)/\kappa_1^2]\,dt\,, \quad (48)$$

$$k_{MM}(a_0)=3\int_0^1 \mathrm{Re}[t\phi_R(t)/\kappa_1^2]\,dt\,,$$

$$c_{MM}(a_0)=\frac{3}{a_0}\int_0^1 \mathrm{Im}[t\phi_R(t)\kappa_1^2]\,dt\,, \quad (49)$$

$$k_{HH}(a_0)=\int_0^1 \mathrm{Re}[\phi_1(t)/\kappa_1^2]\,dt\,,$$

$$c_{HH}(a_0)=\frac{1}{a_0}\int_0^1 \mathrm{Im}[\phi_1(t)/\kappa_1^2]\,dt\,. \quad (50)$$

The terms inside the square brackets in eqs. (45)–(47) are the normalized impedance functions for vertical , rocking and horizontal vibrations; the factors outside the parentheses correspond to the static values ($a_0 = 0$) of the impedance functions for an elastic half-space having the properties of the top layer. The functions $k_{VV}(a_0)$, $k_{MM}(a_0)$ and $k_{HH}(a_0)$, corresponding to the real part of the impedance functions, will be called 'equivalent stiffness coefficients', while the functions $c_{VV}(a_0)$, $c_{MM}(a_0)$ and $c_{HH}(a_0)$, proportional to the imaginary part of the impedance functions, will be designated 'equivalent damping coefficients'. Both the equivalent stiffness and damping coefficients are functions not only of the dimensionless frequency $a_0$ but also depend on the properties of the different media forming the soil column.

In solving the problem for horizontal vibrations, a further approximation has been introduced by assuming that $\phi_2(t)$ is sufficiently small so that the integral equations (34) and (35) may be reduced to

$$\tilde{\phi}_1(t) + \int_0^1 K_{11}(t, t')\tilde{\phi}_1(t')\,\mathrm{d}t = 1 \qquad (0 \leqslant t \leqslant 1)\,, \tag{51}$$

where the kernel $K_{11}(t, t')$ is given by eq. (36). The basis for this approximation is that for the case of a uniform half-space, the function $\phi_2(t)$ is much smaller than $\phi_1(t)$; particularly for the static case $\phi_2(t) = 0$. The above approximation is equivalent to the requirement that $\sigma_{zy} = 0$ under the foundation and thus corresponds to a further relaxation of the boundary conditions.

## 4. Numerical solution

The numerical procedure used to solve the integral equations (29), (32) and (51), consists of reducing these equations to a system of algebraic equations that are solved by standard methods. A key step in this procedure is the evaluation of the kernels $K(t, t')$ given by eqs (30), (33) and (36). In the case of a medium with no internal friction the functions $\Delta_R$ and $\Delta_L$ have zeros for real values of $k$ and consequently the integrands in eqs (31) and (36) are singular at these points. This situation complicates the numerical evaluation of the kernels. However, if there is internal friction then the zeros of $\Delta_R$ and $\Delta_L$ are complex and consequently the numerical evaluation of the kernels is simplified. The kernels are evaluated numerically using Filon's method of integration up to a sufficiently large value of $k$; the rest is evaluated analytically by using the asymptotic forms of the integrands for large $k$.

## 5. Some numerical results

The procedure described above has been used to obtain the rocking, horizontal and vertical impedance functions for a rigid circular foundation placed on a uniform viscoelastic half-space. The corresponding equivalent stiffness and damping coefficients for a hysteretically damped half-space are shown in figs. 2–4 versus the dimensionless frequency $a_0$ for values of $\xi = 0.05$, 0.15 and 0.25 (crosses, triangles and circles, respectively). The approximate results obtained by Veletsos and Verbic [2] are also shown in these figures by means of segmented and continuous lines. Inspection of figs. 2–4 indicates that both sets of results follow the same trends although some differences in numerical values may be observed. These differences stem from the simplified analytic expressions used by Veletsos and Verbic to represent the undamped stiffness and damping coefficients. In general, the effect of the hysteretic damping on the impedance functions is represented by a marked reduction of the equivalent stiffness coefficients for high frequencies, together with a marked increase of the equivalent damping coefficients specially for low frequencies. In particular the equivalent damping coefficients tend to $2\xi/a_0$ as $a_0$ tends to zero.

Similar comparisons are presented in figs. 5–7 for the case of a rigid circular foundation placed on a uniform viscoelastic half-space with Voigt-type damping. The numerical results shown correspond to values of the dimensionless viscosity $\beta G'/aG = 0.1$, 0.3 and 0.5. It may be seen that the Voigt model of energy dissipation leads to larger effects on the impedance functions, particularly for high values of the dimensionless frequency $a_0$. On the other hand, the equivalent damping coefficients tend to finite values as $a_0$ tends to zero in opposition to the behavior observed for a hysteretically damped half-space.

The effects of internal damping on the rocking,

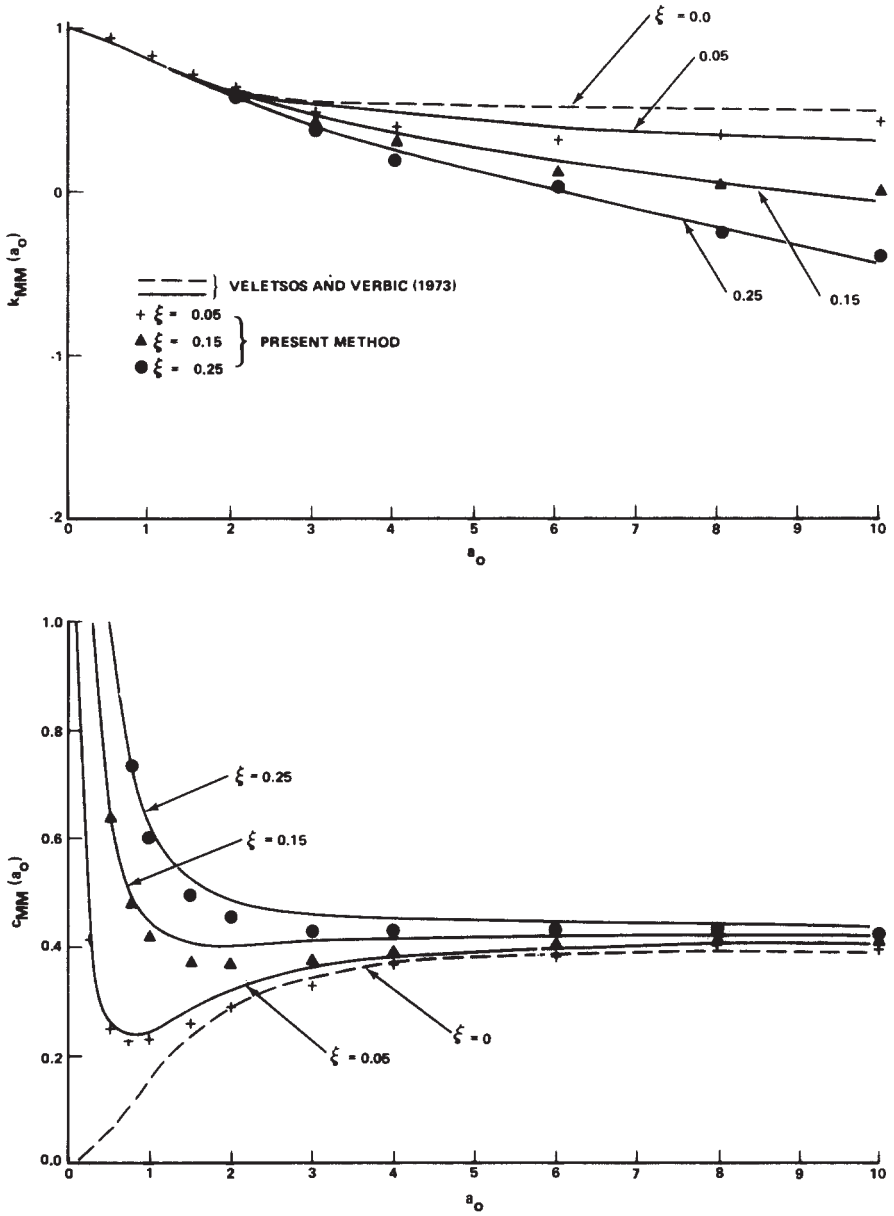


Fig. 2. Rocking impedance function for a hysteretically damped half-space ($\sigma = 1/3$).

horizontal and vertical impedance functions for a rigid circular foundation supported on a layered medium are illustrated in figs. 8–10, respectively. In this case the hysteretically damped medium representing the soil consists of a viscoelastic layer of thickness $h$ and properties $\beta_1$, $\rho_1$, $\sigma_1$ and $\xi_1$, resting on viscoelastic half-space with properties $\beta_2$, $\rho_2$, $\sigma_2$ and $\xi_2$. The results presented correspond to the particular values $\beta_1 = 0.8\,\beta_2$, $\rho_1 = 0.85\,\rho_2$, $\sigma_1 = \sigma_2 = 0.25$, and $\xi_1 = \xi_2 = 0.05$; comparisons are made with the corresponding undamped results ($\xi_1 = \xi = 0$) for values of $h/a = 0.5$ and 33. The impedance functions shown in figs. 8–10 have been normalized by the corresponding static impedances for a uniform elastic half-space

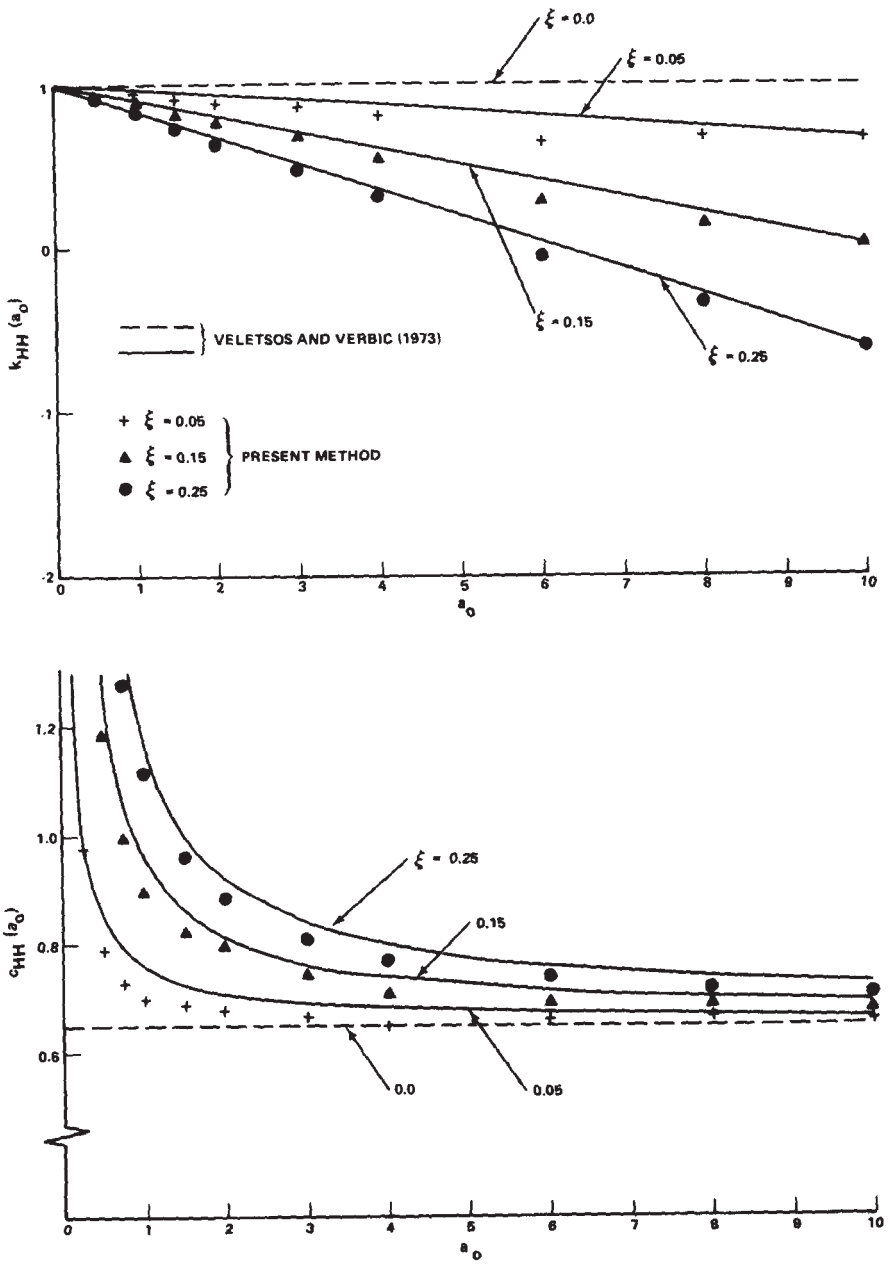


Fig. 3. Horizontal impedance function for a hysteretically damped half-space ($\sigma = 1/3$).

having the properties of the top layer. The results shown indicate that for this particular setting the effects of internal damping on the equivalent stiffness coefficients are minor; however, the equivalent damping coefficients experience a large increase, particularly for low frequencies.

## 6. Conclusions

A procedure to obtain the dynamic impedance functions for a rigid circular foundation placed on a layered viscoelastic medium has been presented. The numerical results obtained indicate that the presence

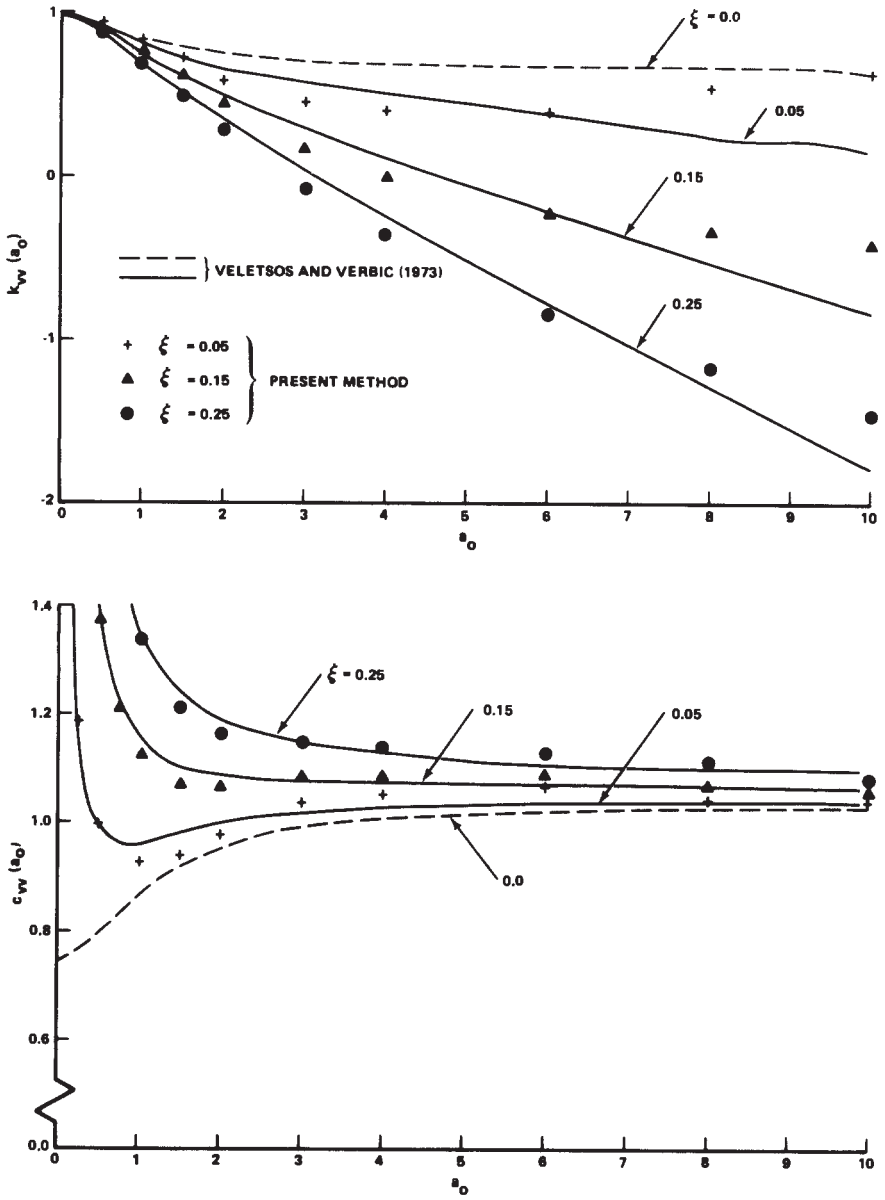


Fig. 4. Vertical impedance function for a hysteretically damped half-space ($\sigma$ = 1/3).

of internal damping in the supporting medium leads to marked changes in the impedance functions for a rigid foundation. In particular, the equivalent damping coefficients may experience large increases indicating that the effects of internal damping in the soil should be included when studying the dynamic response of foundations or the dynamic interaction between structures and the ground.

**Acknowledgments**

The work reported here was part of an extensive study on soil–structure interaction conducted by Bechtel Power Corporation. The writer wishes to express his appreciation to A.H. Hadjian for his helpful suggestions.

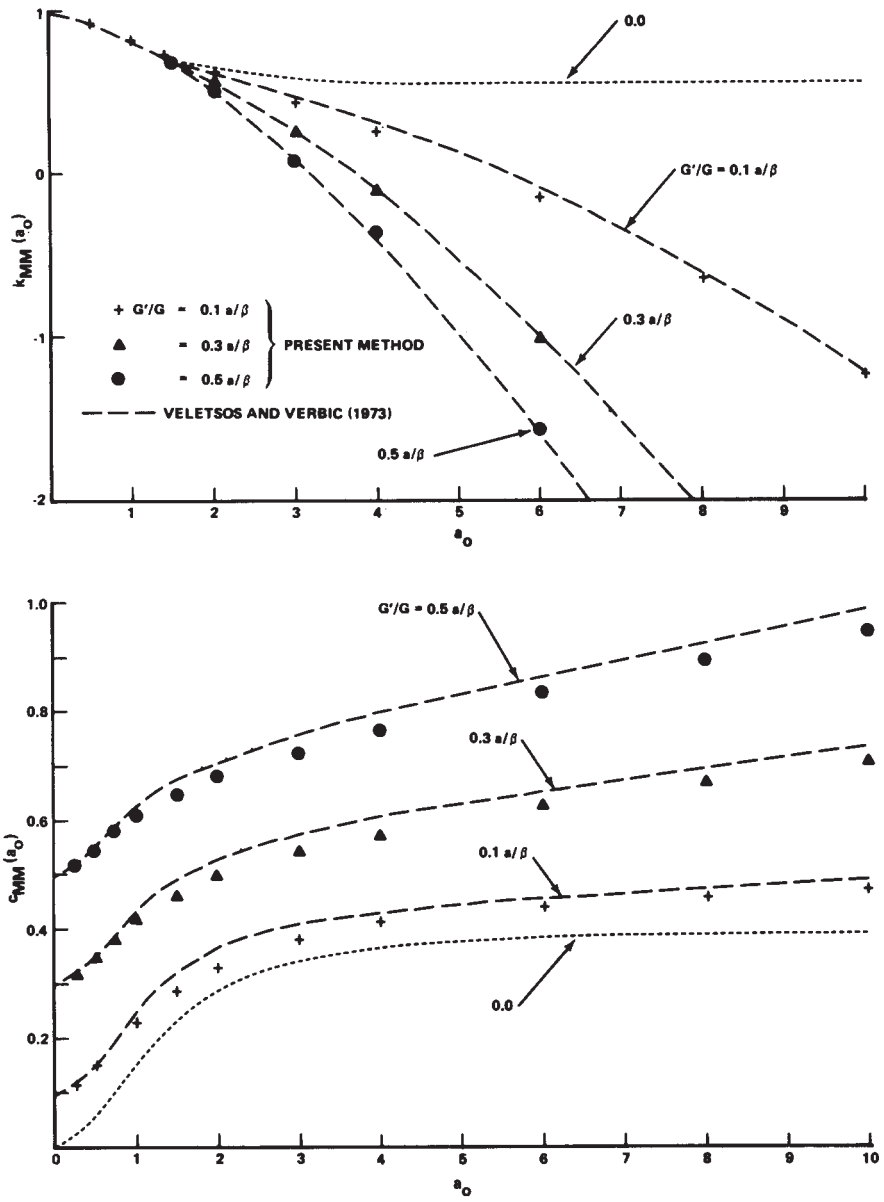


Fig. 5. Rocking impedance function for a viscoelastic half-space (Voigt model, $\sigma = 1/3$).

## Appendix: Transfer matrices

The functions $\Delta_{ij}(k)$ $(i,j = 1,2)$ and $\Delta_R(k)$ entering in eqs. (19) and (20) are defined by

$$\begin{bmatrix} \Delta_{11}(k) & \Delta_{12}(k) \\ \Delta_{21}(k) & \Delta_{21}(k) \end{bmatrix}$$

$$= (T^*_{11}A + T^*_{12}B)\,\mathrm{adj}(T^*_{21}A + T^*_{22}B)\,, \tag{A1}$$

and

$$\Delta_R = \det(T^*_{21}A + T^*_{22}B)\,, \tag{A2}$$

where

$$[A] = \begin{bmatrix} -k & \nu'_N \\ \nu_N & -k \end{bmatrix}, \tag{A3}$$

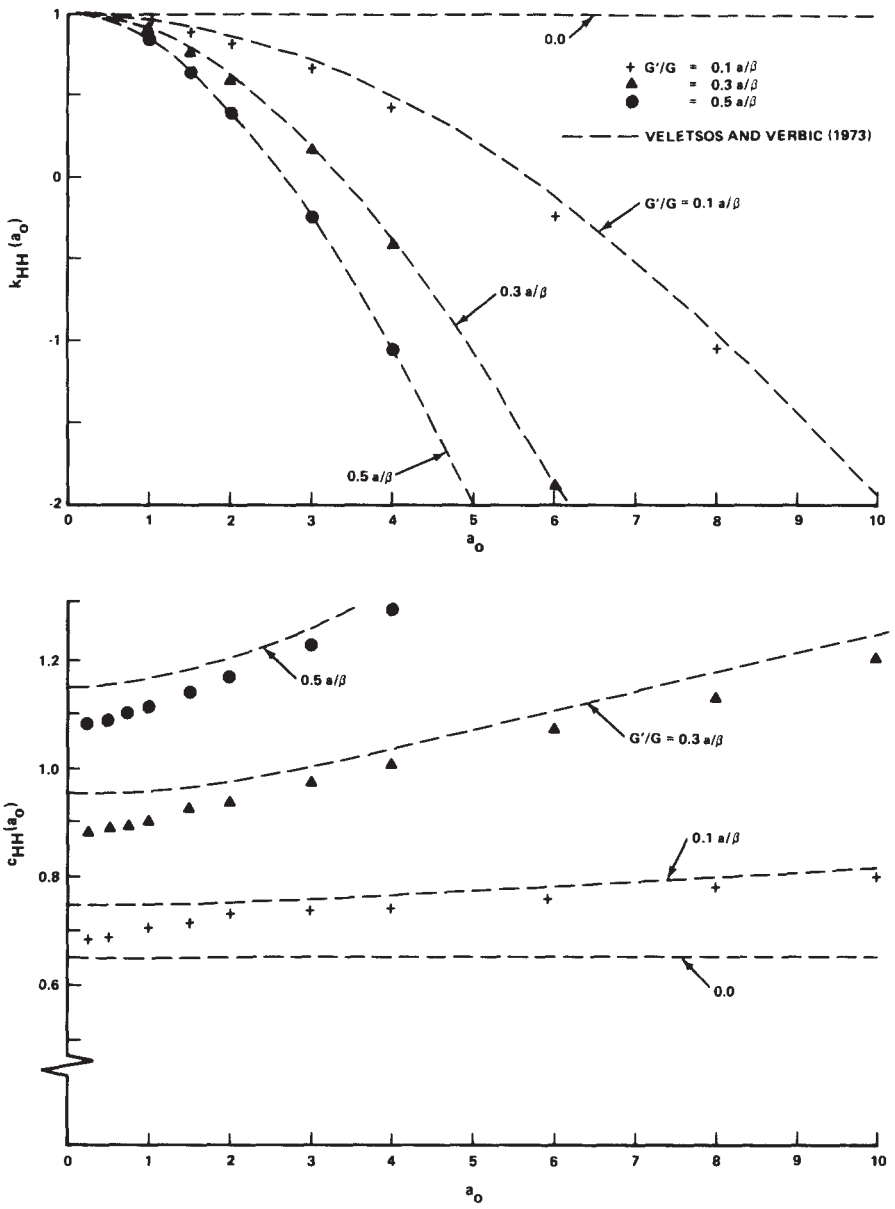


Fig. 6. Horizontal impedance function for a viscoelastic half-space (Voigt model, $\sigma = 1/3$).

$$[B] = \frac{G_N^*}{G_1}\begin{bmatrix} -2\nu_N k & (2k^2 - \kappa_N^2) \\ -(2k^2 - \kappa_N^2) & 2\nu'_N\kappa \end{bmatrix}, \qquad \text{(A4)}$$

and $T_{ij}^*(i,j = 1,2)$ are the submatrices of the total transfer matrix $T^*$ associated with the set of layers overlying the base half-space. The total transfer matrix $T^*$,

$$[T^*] = \left[\begin{array}{c|c} T_{12}^* & T_{11}^* \\ \hline T_{21}^* & T_{22}^* \end{array}\right] \qquad \text{(A5)}$$

may be obtained in terms of the transfer matrices for each layer $T_j(j = 1, N-1)$ by means of the following

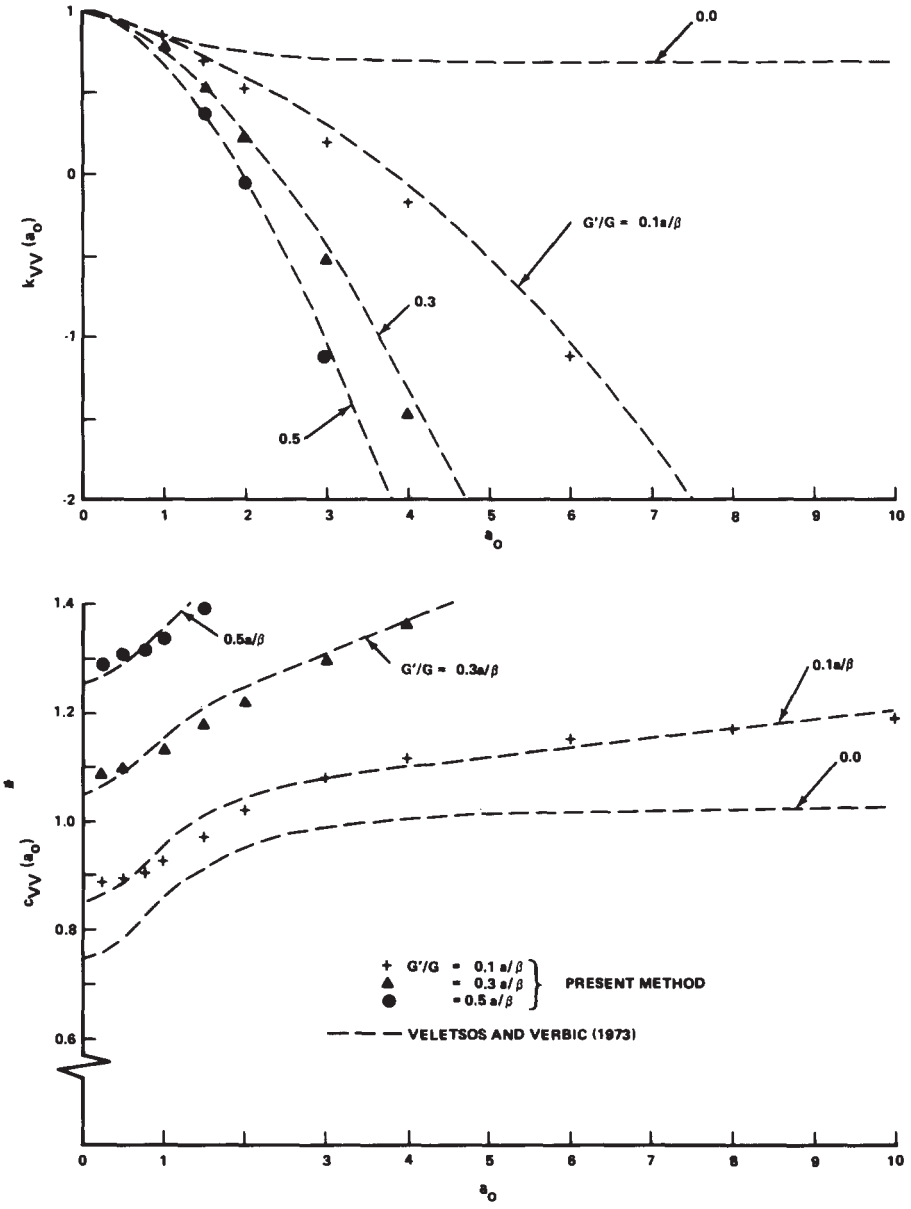


Fig. 7. Vertical impedance function for a viscoelastic half-space (Voigt model, $\sigma = 1/3$).

product:

$$[T^*] = [T_1]\,[T_2] \ldots [T_j] \ldots [T_{N-1}]\,. \tag{A6}$$

The transfer matrix for the $j$th layer is in turn given by

$$[T_j] = \begin{bmatrix} T^j_{11} & T^j_{12} \\ T^j_{21} & T^j_{22} \end{bmatrix}, \tag{A7}$$

where

$$T^j_{11} = -\frac{1}{\kappa_j^2}\begin{bmatrix} -2k^2 CH_j + (2k^2 - \kappa_j^2)CHP_j & -k(2k^2 - \kappa_j^2)SH_j + 2k\nu_j'^2 SHP_j \\ 2k\nu_j^2 SH_j - k(2k^2 - \kappa_j^2)SHP_j & (2k^2 - \kappa_j^2)CH_j - 2k^2 CHP_j \end{bmatrix},$$

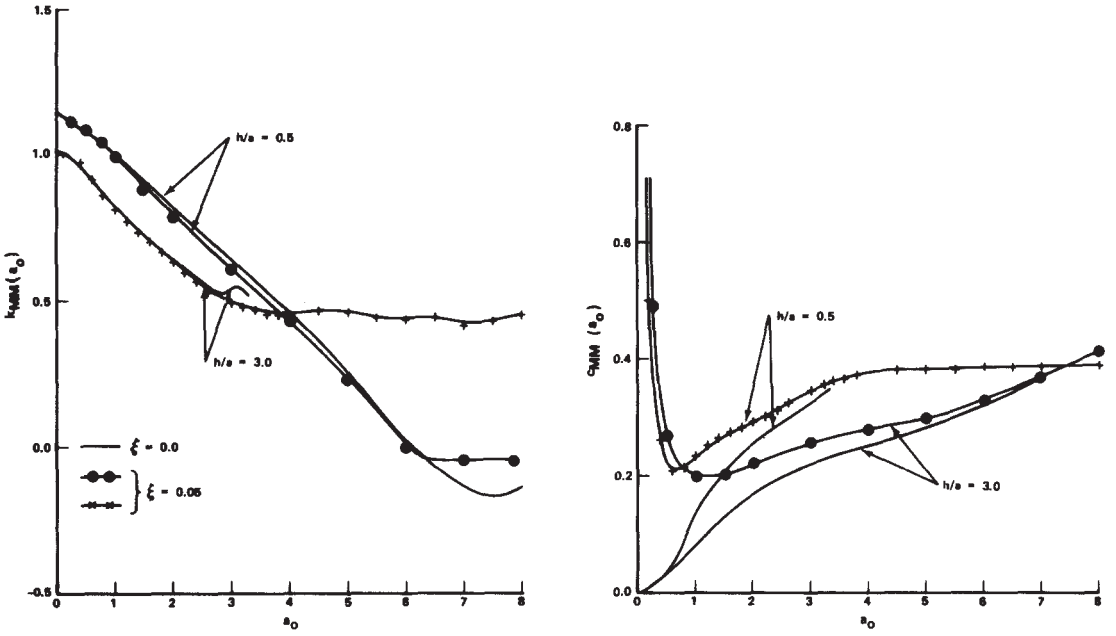


Fig. 8. Rocking impedance function for a layered hysteretically damped medium.

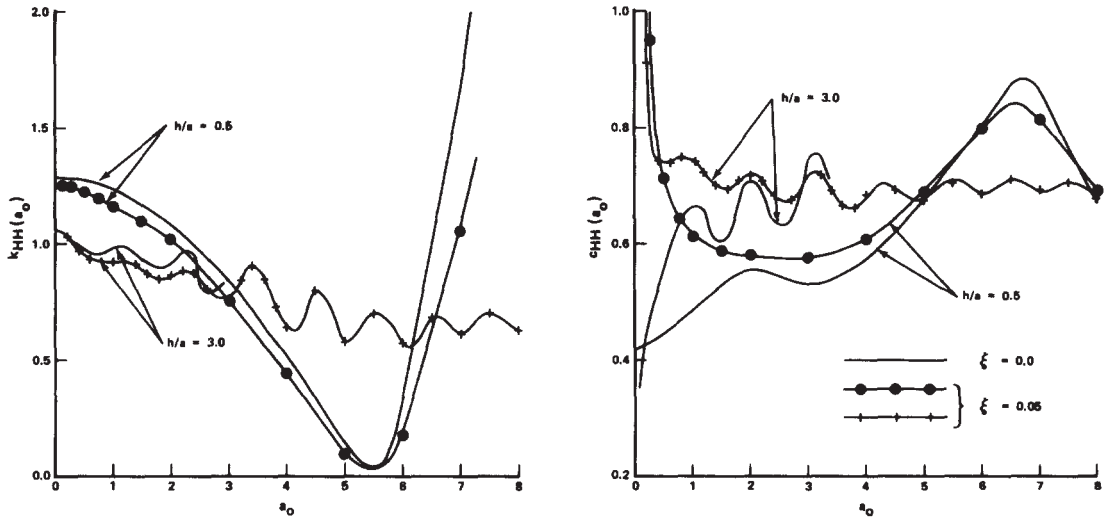


Fig. 9. Horizontal impedance function for a layered hysteretically damped medium.

$$T_{12}^{j} = -\left(\frac{\rho_1}{\rho_j}\right)\begin{bmatrix} -k^2 SH_j + \nu_j'^2 SHP_j & k(CH_j - CHP_j) \\ k(CH_j - CHP_j) & -\nu_j^2 SH_j + k^2 SHP_j \end{bmatrix}, \tag{A8}$$

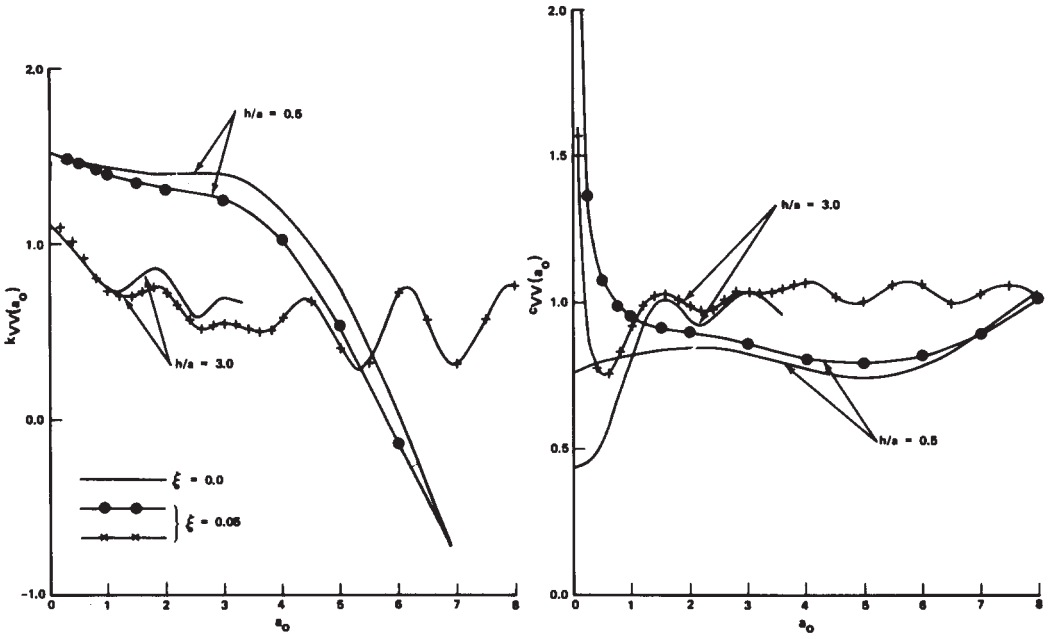


Fig. 10. Vertical impedance function for a layered hysteretically damped medium.

$$T_{21}^{j} = -\frac{1}{\kappa_j^4}\left(\frac{\rho_j}{\rho_1}\right)\begin{bmatrix} -4\nu_j^2 k^2 SH_j + (2k^2-\kappa_j^2)^2 SHP_j & -2k(2k^2-\kappa_j^2)(CH_j - CHP_j) \\ -2k(2k^2-\kappa_j^2)(CH_j - CHP_j) & -(2k^2-\kappa_j^2)^2 SH_j + 4\nu_j'^2 k^2 SHP_j \end{bmatrix},$$

$$T_{22}^{j} = -\frac{1}{\kappa_j^2}\begin{bmatrix} -2k^2 CH_j + (2k^2-\kappa_j^2)CHP_j & 2k\nu_j^2 SH_j - k(2k^2-\kappa_j^2)SHP_j \\ -k(2k^2-\kappa_j^2)SH_j + 2\nu_j'^2 k SHP_j & (2k^2-\kappa_j^2)CH_j - 2k^2 CHP_j \end{bmatrix}.$$

The different terms entering in eqs. (A3)–(A8) are defined by

$$\nu_j = (k^2 - \gamma_j^2\kappa_j^2)^{1/2}, \qquad \nu_j' = (k^2-\kappa_j^2)^{1/2},$$

$$\gamma_j^2 = (1-2\sigma_j)/2(1-\sigma_j), \quad \kappa_j^2 = G_1\rho_j/G_j^*\rho_1,$$

$$G_j^* = G_j(1 + i\omega G_j'/G_j) \quad \text{or} \quad G_j^* = G_j(1+2i\xi_j),$$

$$SH_j = \sinh(a_0\nu_j\lambda_j)/\nu_j, \qquad SHP_j = \sinh(a_0\nu_j'\lambda_j)/\nu_j', \tag{A9}$$

$$CH_j = \cosh(a_0\nu_j\lambda_j), \qquad CHP_j = \cosh(a_0\nu_j'\lambda_j),$$

$$\lambda_j = h_j/a, \qquad a_0 = \omega a/\beta_1,$$

where $\sigma_j$, $\rho_j$, $G_j$, $G_j'/G_j$, and $h_j$ are, respectively, Poisson's ratio, density, shear modulus, relative viscosity and thickness of the $j$th layer. In the last two equations of (A9), $a$ is the radius of the circular foundation, $\omega$ is the frequency of the steady-state vibrations and $\beta_1$ is the shear wave velocity of the top layer. The first form of $G_j^*$ corresponds to the Voigt-type damping, while the second corresponds to the hysteretic-type damping; $\xi_j$ being the hysteretic damping constant for the $j$th layer.

The functions $\Delta_{33}(k)$ and $\Delta_L(k)$ entering in eq. (19) are defined by

$$\Delta_{33}(k) = L_{11}^* + L_{12}^*\nu_N' G_N^*/G_1, \tag{A10}$$

$$\Delta_L(k) = L_{21}^* + L_{22}^*\nu_N' G_N^*/G_1, \tag{A11}$$

where $L_{ij}^*(i,j=1,2)$ are the elements of the transfer matrix $L^*$. The transfer matrix $L^*$,

$$[L^*] = \begin{bmatrix} L_{11}^* & L_{12}^* \\ L_{21}^* & L_{22}^* \end{bmatrix}, \tag{A12}$$

is defined in terms of the transfer matrices for each layer by

$$[L^*] = [L_1] \cdot [L_2] \ldots [L_j] \ldots [L_{N-1}] , \qquad \text{(A13)}$$

in which

$$[L_j] = \begin{bmatrix} CHP_j & (G_1/G_j^*)SHP_j \\ (G_j^*/G_1)\nu_j'^2 SHP_j & CHP_j \end{bmatrix} . \qquad \text{(A14)}$$

## References


[1] A.H. Hadjian, J.E. Luco and N.C. Tsai, Soil–structure interaction: continuum or finite element? Nucl. Eng. Des. 31 (2) (1974) 151–167.

[2] A.S. Veletsos and B. Verbic, Vibration of viscoelastic foundations, Report 18, Department of Civil Engineering, Rice University, Houston, Texas, Apr. (1973).

[3] T. Kobori, R. Minai, T. Suzuki and K. Kusakabe, Dynamic ground compliance of rectangular foundation on a semi-infinite viscoelastic medium, Annual report, Disaster Prevention Research Institute of Kyoto University, No. 11A (1968) 349–367.

[4] T. Kobori, R. Minai and T. Suzuki, The dynamical ground compliance of a rectangular foundation on a viscoelastic stratum, Bull. Disaster Prev. Res. Inst., Kyoto University, 20, Mar. (1971) 389–329.

[5] T. Kobori and T. Suzuki, Foundation vibrations on a viscoelastic multilayered medium, Proc. Third Japan Earthquake Engineering Symposium, Tokyo (1970) 493–499.

[6] J.E. Luco, Impedance functions for a rigid foundation on a layered medium, Nucl. Eng. Des. 31 (2) (1974) 204–207.

[7] H. Kolsky, Stress Waves in Solids, Dover, New York (1963).

[8] R. Dobry, Damping in soils: its hysteretic nature and the linear approximation, Research Report R70-14, MIT, Department of Civil Engineering, Cambridge, Mass. (1970).

[9] B.O. Hardin and V.P. Drnevich, Shear modulus and damping in soils: measurements and parameter effects, Proc. Amer. Soc. Civ. Eng. 98 (SM6) (1972) 603–624.

[10] R.J. Krizek and A.G. Franklin, Energy dissipation in soft clay, Proc. Int. Symp. on Wave Propagation and Dynamic Properties of Earth Materials, University of New Mexico Press, Albuquerque (1967) 797–807.

[11] F.E. Richard, J.R. Hall and R.D. Woods, Vibration of Soils and Foundations, Prentice-Hall, New York (1970).

[12] H.B. Seed and I.M. Idriss, Soil moduli and damping factors for dynamic response analysis, Report, EERC 70-10, University of California, Berkeley (1970).

[13] G.N. Bycroft, Forced vibrations of a rigid circular plate on a semi-infinite elastic space or on an elastic stratum, Phil. Trans. Roy. Soc. London 248 (1956) 327–368.

[14] J.E. Luco and R.A. Westmann, Dynamic response of circular footings, J. Eng. Mech. Div., ASCE 97 (EM5), Oct. (1971) 1381–1395.

Reference 81

217 SEISMIC RESPONSE OF CYLINDRICAL EMBEDDED FOUNDATIONS TO RAYLEIGH WAVE

by Michio Iguchi*

ABSTRACT

The dynamic harmonic response of a rigid cylindrical foundation embedded in a homogeneous elastic half-space and subjected to Rayleigh waves are studied. The numerical results indicate that increase of embedment depth pronouncedly decrease the amplitudes of the vertical and rocking motions. Also, the horizontal seismic forces acting on the embedments exhibit a marked decrease with increase of frequencies.

## INTRODUCTION

The dynamic response of a rigid massless foundation to seismic waves are generally referred to as the foundation input motions or merely as the input motions. The analysis of the input motions becomes the key step in evaluation of the dynamic response of structure to seismic excitations. In the analysis of the earthquake response of structures, it has been assumed that the seismic waves impinge vertically on the foundation. However, it has been reported that the analysis based on the assumption of vertical incidence may not explain the actual observational results of seismic motions on structures (5, 12). On the other hand, it has been shown that the surface waves contribute to major part of the seismic motions (10). From such a point of view, many studies have been conducted on the dynamic responses of foundations not only to the non-vertically incident shear waves but to the surface waves. Most of these studies, however, are restricted to the analysis of rigid flat foundations supported on a soil surface (e.g., Kobori et al. (6), Luco and Wong (9) and Wong and Luco (11)) and very few have been addressed to the analysis of the three-dimensional embedded foundations (1, 2, 3, 4, 7, 8).

This paper describes the analysis of the dynamic responses of rigid cylindrical foundation embedded in a homogeneous elastic half-space and subjected to Rayleigh wave. The analysis is based on an approximate procedure proposed by Iguchi (3). In numerical calculations, the effects of embedment depth and mass of foundation on the dynamic responses are investigated. Also, some results of the seismic forces and moment acting on the embedments during earthquake are illustrated.

## ANALYSIS OF INPUT MOTIONS

The coordinate system and the geometry of a cylindrical foundation embedded in a homogeneous elastic medium are illustrated in Fig. 1; the radius and embedment depth of the cylinder are denoted by a and h, respectively. The seismic excitation considered here is Rayleigh wave which propagates in the opposite direction of the x-axis as shown in Fig. 1. In formulation of the input motions, it is assumed that the cylindrical foundation is perfectly bonded to the surrounding soil. Also, harmonic response is considered and time factor $\exp(i\omega t)$, with circular frequency $\omega$ will be omitted in formulations what follows.

*Assoc. Prof., Faculty of Science and Engineering, Science Univ. of Tokyo.

Cake. No. 03.7.316-2

Page B.3

The horizontal and vertical components of free-field motions of Rayleigh wave in the y- and z-directions, denoted by $u_y^f$ and $u_z^f$ respectively, can be expressed in terms of the cylindrical coordinate system $(r, \theta, z)$ as follows.

$$u_y^f(r, \theta, z) = R_H\{2\kappa^2 e^{\alpha z} - (2\kappa^2 - 1)e^{\beta z}\}$$
$$\left[J_o(kr) + 2\sum_{n=1}^{\infty}\{J_{2n}(kr)\cos 2n\theta - iJ_{2n-1}(kr)\sin(2n-1)\theta\}\right] \quad (1)$$

$$u_z^f(r, \theta, z) = R_v\{2\kappa^2 e^{\beta z} - (2\kappa^2 - 1)e^{\alpha z}\}$$
$$\left[J_o(kr) + 2\sum_{n=1}^{\infty}\{J_{2n}(kr)\cos 2n\theta - iJ_{2n-1}(kr)\sin(2n-1)\theta\}\right] \quad (2)$$

where $R_H$ and $R_v$ denote the horizontal and vertical amplitudes of Rayleigh wave, respectively, on the surface of an elastic half-space and

$$\alpha = k\sqrt{1 - \nu^2/\kappa^2}, \quad \beta = k\sqrt{1 - 1/\kappa^2}, \quad k = \omega/V_R \quad (3)$$

in which $V_R$ is Rayleigh wave velocity and

$$\nu^2 = V_s^2/V_p^2 = \frac{1 - 2\upsilon}{2 - 2\upsilon}, \quad \kappa^2 = V_s^2/V_R^2 \quad (4)$$

$V_p$ and $V_s$ denote the longitudinal and shear wave velocities, respectively, and $\upsilon$ is the Poisson's ratio of soil. It can be shown that $R_H$ and $R_v$ are correlated by following equation.

$$R_v = -i\frac{2}{(\beta/k)^2 + 1}\frac{\alpha}{k}R_H = -i\frac{(\beta/k)^2 + 1}{2}\frac{k}{\beta}R_H \quad (5)$$

And $\kappa$ is the real root of Rayleigh equation.

$$(2\kappa^2 - 1)^2 - 4\kappa^2\sqrt{\kappa^2 - \nu^2}\sqrt{\kappa^2 - 1} = 0 \quad (6)$$

For a Poisson's ratio $\upsilon = 0.25$, $R_v = -1.4679\, i\, R_H$ and $V_R = 0.91940\, V_s$.

When Rayleigh wave impinges on a massless rigid cylindrical foundation embedded in an elastic soil, the resulting motions of the foundation may be described by two horizontal displacements in the y- and z-directions and one rotation with respect to the x-axis, which are denoted by $\Delta_y^*$, $\Delta_z^*$ and $\Phi_x^*$, respectively. These motions are defined at the center of top surface of the foundation. Based on an approximate procedure proposed by Iguchi (3) for evaluation of the input motions, these three components may be expressed in the following form.

$$\begin{bmatrix}\Delta_y^* \\ \Delta_z^* \\ \Phi_x^*\end{bmatrix} = \begin{bmatrix}A & & S_x \\ & A & \\ S_x & & J_{px}\end{bmatrix}^{-1}\begin{bmatrix}\Delta_y^f \\ \Delta_z^f \\ \Phi_x^f\end{bmatrix} - \begin{bmatrix}K_{HH} & & -K_{HM} \\ & K_{vv} & \\ -K_{HM} & & K_{MM}\end{bmatrix}^{-1}\begin{bmatrix}F_y^f \\ F_z^f \\ M_x^f\end{bmatrix} \quad (7)$$

where A, $S_x$ and $J_{px}$ are the area, the first and the second moments of area with respect to the x-axis, respectively, of the contact surface between the cylinder and the soil. These are found to be given by

$$A = \pi a(a + 2h), S_x = \pi ah(a + h), J_{px} = \pi a\left[h(a^2 + \tfrac{2}{3}h^2) + a(\tfrac{1}{4}a^2 + h^2)\right] \quad (8)$$

$K_{HH}$, $K_{vv}$, $K_{MM}$ and $K_{HM}$ are the horizontal, vertical, rocking and coupling impedance functions, respectively. These functions for the cylindrical foundations have been evaluated by Day (1) for some embedment ratios h/a

and a Poisson's ratio $\upsilon = 0.25$. Also $\Delta_y^f$, $\Delta_z^f$ and $\Phi_x^f$ in Eq. (7) represent resultant displacements in the y- and z-directions and rotation with respect to the x-axis, respectively, of the free-field motions generated on the contact surface between the embedment and the soil. These displacements may be evaluated by following equations.

$$\Delta_y^f = \int_0^{2\pi}\left[\int_{-h}^{0} a\, u_y^f(a, \theta, z)dz + \int_0^a r\, u_y^f(r, \theta, -h)dr\right]d\theta \tag{9}$$

$$\Delta_z^f = \int_0^{2\pi}\left[\int_{-h}^{0} az u_z^f(a, \theta, z)dz + \int_0^a hr u_z^f(r, \theta, -h\, dr\right]d\theta \tag{10}$$

$$\Phi_x^f = \int_0^{2\pi}\left[-\int_{-h}^{0} az u_y^f(a, \theta, z)dz + \int_0^a hr u_y^f(r, \theta, -h)dr\right]d\theta$$

$$+ \int_0^{2\pi}\left[\int_{-h}^{0} a^2 \sin\theta\, u_z^f(a, \theta, z)dz + \int_0^a r^2 \sin\theta\, u_z^f(r, \theta, -h)dr\right]d\theta \tag{11}$$

Finally, $F_y^f$, $F_z^f$ and $M_x^f$ in Eq. (7) represent resultant forces in the y- and z-directions and moment with respect to the x-axis, respectively, of the free-field tractions generated on the contact surface of the embedment. These forces and moment can be evaluated by

$$F_y^f = -\int_0^{2\pi}\left[\int_{-h}^{0} a\left\{\sin\theta\, \tau_{rr}^f(a, \theta, z) + \cos\theta\, \tau_{r\theta}^f(a, \theta, z)\right\}dz\right]d\theta$$

$$+ \int_0^{2\pi}\left[\int_0^a r\left\{\sin\theta\, \tau_{zr}^f(r, \theta, -h) + \cos\theta\, \tau_{z\theta}^f(r, \theta, -h)\right\}dr\right]d\theta \tag{12}$$

$$F_z^f = -\int_0^{2\pi}\left[\int_{-h}^{0} a\, \tau_{rz}^f(a, \theta, z)dz - \int_0^a r\, \tau_{zz}^f(r, \theta, -h)dr\right]d\theta \tag{13}$$

$$M_x^f = \int_0^{2\pi}\left[\int_{-h}^{0}\left\{az\left(\sin\theta\, \tau_{rr}^f(a, \theta, z) + \cos\theta\, \tau_{r\theta}^f(a, \theta, z)\right)\right.\right.$$

$$\left.\left. - a^2 \sin\theta\, \tau_{rz}^f(a, \theta, z)\right\}dz\right]d\theta$$

$$+ \int_0^{2\pi}\left[\int_0^a\left\{hr\left(\sin\theta\, \tau_{zr}^f(r, \theta, -h) + \cos\theta\, \tau_{z\theta}^f(r, \theta, -h)\right)\right.\right.$$

$$\left.\left. + r^2 \sin\theta\, \tau_{zz}^f(r, \theta, -h)\right\}dr\right]d\theta \tag{14}$$

where $\tau_{rr}^f$ etc. are the stress components on the side or bottom of the foundation associated with the free-field motions. These stresses can be evaluated by the well known formulas in the theory of elasticity. These integrations are found to be expressed in the explicit forms and thus, the input motions can be readily calculated by Eq. (7).

Inspecting Eq. (7) reveals that the first term of the left hand side corresponds to a weighted average of the free-field motions and the second to the effect of diffracted waves by the presence of the rigid foundation (3). For a flat foundation supported on a soil surface, the second term of Eq. (7) disappears since the tractions on a soil surface associated with the free-field motions become zeros. However, for an embedded foundation the second term is to play an important roll in estimation of the input motions (3).

## ANALYSIS OF DYNAMIC RESPONSE

Once the foundation input motions are obtained, the dynamic response of the foundations with consideration of effect of the mass can be evalu-

ated. Assuming that the mass of the foundation is uniformly distributed, and in absence of external forces the dynamic displacement responses in the y- and z-directions and rocking response with respect to the x-axis, denoted by $\Delta_y$, $\Delta_z$ and $\Phi_x$ respectively, can be expressed in the form of

$$\begin{bmatrix} \Delta_y \\ \Delta_z \\ a\Phi_x \end{bmatrix} = \left( [I] - \pi a_o^2 \delta \frac{M_o}{M_s} [K]^{-1} [M] \right)^{-1} \begin{bmatrix} \Delta_y^* \\ \Delta_z^* \\ a\Phi_x^* \end{bmatrix} \tag{15}$$

where [I] is a unit matrix, [K] is the impedance matrix already appeared in Eq. (7) and [M] is a non-dimensional mass matrix defined by

$$[M] = \begin{bmatrix} 1 & & \delta/2 \\ & 1 & \\ \delta/2 & & 1/4 + \delta^2/3 \end{bmatrix} \tag{16}$$

$M_o$ and $M_s$ in Eq. (15) represent the total mass of the foundation and mass of soil of the same volume with the embedment.

The analysis of seismic forces and moment acting on the embedment during earthquakes will be of interest. Denoting the seismic forces in the y- and z-directions by $F_y^s$ and $F_z^s$ respectively, and moment with respect to the x-axis by $M_x^s$, these values can be expressed by

$$\begin{bmatrix} F_y^s \\ F_x^s \\ M_x^s/a \end{bmatrix} = M_o \omega^2 \begin{bmatrix} 1 & & \delta/2 \\ & 1 & \\ & & 1/4 + \delta^2/12 \end{bmatrix} \begin{bmatrix} \Delta_y \\ \Delta_z \\ a\Phi_x \end{bmatrix} \tag{17}$$

It should be noted here that the seismic moment is defined at the centroid of cylinder. Combining Eqs. (15) and (17), the seismic forces and moment can be readily calculated.

## NUMERICAL RESULTS

Input Motions: In calculation of the input motions based on Eq. (7), the results of impedance functions evaluated by Day (1) for a Poisson's ratio of soil $\upsilon = 0.25$ are used. The calculated results of modulus of normalized input motions $|\Delta_y^*/R_H|$, $|\Delta_z^*/R_H|$ and $|a\Phi_x^*/R_H|$ are shown in Figs. 2(a), (b) and (c) versus the dimensionless frequency $a_o = a\omega/V_s$ for four values of embedment ratios $\delta = h/a = 0$, 0.5, 1.0 and 2.0. Since the input motions are defined as the dynamic response of massless rigid foundation to seismic waves, the mass of the foundation is disregarded in the results. From the results shown in Figs. 2(a) and (b), it may be observed that for low frequencies the horizontal and vertical input motions approach the amplitudes corresponding to the free-field motions on a soil surface. As the frequency increase, these two components decrease remarkably in amplitudes. Regarding the effect of embedment depth, the results indicate that the vertical input motions decrease as $\delta$ becomes large in the frequency range $a_o < 2$. However, as to the horizontal input motion the effect of embedment depth is not so distinct. The results shown in Fig. 2(c) indicate that the rocking input motion is remarkable for a flat foundation supported on a soil surface and exhibits pronounced decrease in amplitudes with increase of $\delta$. It should be noted, though not illustrated in figure, that the horizontal and rocking input

motions are almost in phase, and the vertical motion is out of phase with the horizontal component of free-field surface motion. It is of interest to compare the results presented here with the corresponding results to the horizontally incident SH wave (4) on the condition that the horizontal amplitudes of the free-field surface motion are same for both waves. For the case of horizontal input motions, the results to Rayleigh wave excitations are comparable to those to the SH wave. On the other hand, as for the rocking input motions, the results to Rayleigh wave excitation for $\delta >$ 0.5 are five to ten times larger than the corresponding results to SH wave.

Effect of Mass: Seismic response of the embedded foundations with consideration of the mass can be computed with use of Eq. (15). Numerical results of modulus of the horizontal, vertical and rocking responses are shown in Figs. 3(a), (b) and (c) versus the dimensionless frequency $a_o$ for four values of non-dimensional mass ratios $M_o/M_s$ = 0, 0.5, 1.0 and 1.5, and for an embedment ratio $\delta$ = 1. The horizontal response shown in Fig. 3(a) is with respect to the top surface of the foundation. The results shown in Figs. 3 indicate that the effect of mass on the dynamic responses is notable for horizontal and rocking motions, and less for the vertical motion.

Seismic Forces and Moment: Perhaps the most interesting response of the embedded foundation is the seismic forces and moment acting on the embedments during earthquakes. The seismic forces and moment are equivalent to the inertia forces and moment of the embedments, and can be evaluated from Eq. (17) together with Eq. (15). The calculated results of modulus of dimensionless horizontal seismic forces are shown in Figs. 4 versus the dimensionless frequency $a_o$ for three values of embedment ratios $M_o/M_s$ = 0.5, 1.0 and 1.5, and for $\delta$ = 0.5, 1.0 and 2.0. These normalized results may be interpreted as the conventional seismic coefficients for the embedments supposing that the horizontal accelerations on the soil surface be $\omega^2 R_H$ = 980gals in all frequencies. The results shown in Figs. 4 indicate that the horizontal seismic forces decrease remarkably with increase of frequency. One of the most interesting characteristics observed from the results shown in Figs. 4 is that the seismic coefficients are almost independent on the mass ratio $M_o/M_s$. The results of dimensionless seismic moment are shown in Fig. 5 versus the non-dimensional frequency $a_o$ for $M_o/M_s$ = 0.5, 1.0 and 1.5 and for $\delta$ = 1.0. It should be noted that the embedded foundation is to be subjected to a certain amount of seismic moment in addition to the lateral force.

## CONCLUSIONS

The dynamic responses of the cylindrical rigid foundation embedded in an elastic half-space have been studied for horizontally propagating Rayleigh wave. It has been found that the horizontal, vertical and rocking motions are induced on the foundation. The horizontal and vertical input motions exhibit a remarkable decrease with increase of frequency. The embedment depth of cylinder has a marked effect on the vertical component and no distinct effect on the horizontal motion at the top of the foundation. The amplitude of rocking input motion tends to increase in the frequency range $0 < a_o < 2$ for a flat foundation and $0 < a_o < 1$ for the embedment ratio $\delta = h/a = 2$. The maximum amplitude of the rocking motions tend to decrease with increasing embedment ratio. The results of horizontal seismic coefficients for embedded cylinder obtained

here have indicated the pronounced decrease in magnitudes with increase of frequency. The coefficient tends to decrease with increase of the embedment ratio. It may be also concluded that the embedded foundation is to be subjected to the seismic moment in addition to the lateral seismic forces.

## REFERENCES

(1) Day, S. M., "Finite Element Analysis of Seismic Scattering Problems," Thesis presented to the Univ. of Calif., at San Diego, in partial fulfilment of the requirements for the degree of Doctor of Philosophy, 1977.

(2) Dominguez, J., "Response of Embedded Foundations to Travelling Waves," Report No. R78-24, Dept. of Civil Engrg, MIT, Cambrige, Mass., 1978.

(3) Iguchi, M., "An approximate analysis of input motions for rigid embedded foundations," Trans. of Architect. Inst. of Japan, No. 315, May, pp61-75, 1982.

(4) Iguchi, M., "Approximate analysis of seismic response for embedded foundations subjected to travelling seismic waves," Proc. 7th European Conf. on Earthq. Engrg, (Athens), 1982. (to appear).

(5) Ishii, K., M. Iguchi and T. Hirose, "A study on torsional vibration of symmetrical structures based on observational seismic records," Proc. 6th Japan Earthq. Engrg Symp., (Tokyo), 1982. (to be submitted).

(6) Kobori, T., R. Minai and Y. Shinozaki, "Vibration of a rigid circular disc on an elastic half-space subjected to plane waves," Theoretical and Applied Mechanics, Vol. 31, pp109-119, Univ. of Tokyo Press, 1973.

(7) Lee, V. W. and M. D. Trifunac, "Body wave excitation of embedded hemisphere," Jour. of Engrg Mech. Div., ASCE, Vol. 108, EM3, June, pp546-563, 1982.

(8) Luco, J. E., "Torsional response of structures for SH waves: The case of hemispherical foundations," Bull. of Seism. Soc. Am., Vol. 66, No. 1, pp109-123, February, 1976.

(9) Luco, J. E. and H. L. Wong, "Dynamic response of rectangular foundations for Rayleigh wave excitation," Proc. 5th World Conf. on Earthq. Engrg, (Rome), 1973.

(10) Trifunac, M. D. "Response envelope spectrum and interpretation of strong earthquake ground motion," Bull. of Seism. Soc. Am., Vol. 61, No. 2, pp343-356, April, 1971.

(11) Wong, H. L. and J. E. Luco, "Dynamic response of rectangular foundations to obliquely incident seismic waves," Earthq. Engrg Struct. Dyn., Vol. 6, pp3-16, 1977.

(12) Yamahara, H. "Ground motions during earthquakes and the input loss of earthquake power to an excitation of buildings," Soil and Foundation, Vol. 10, No. 2, Japan Soc. of Soil Mech. and Foundation Engrg, 1970.

Calc. No. 03.7.916-2.0
Page B.8

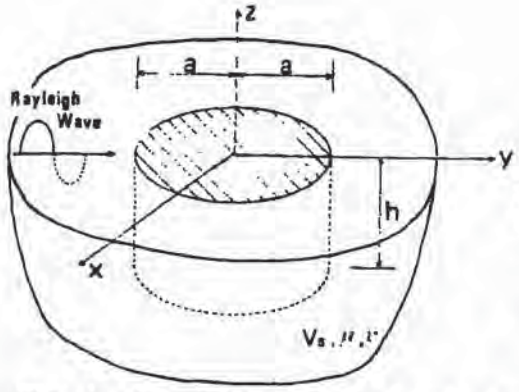


Fig. 1 Description of the Problem Geometry and Coordinate System.

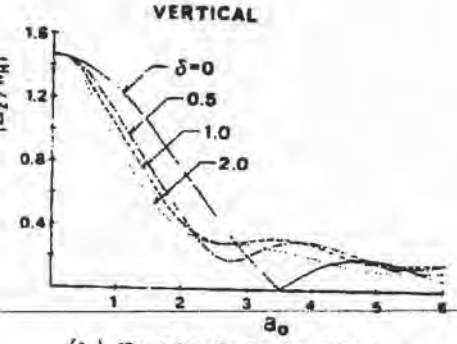


(b) Vertical Input Motion.

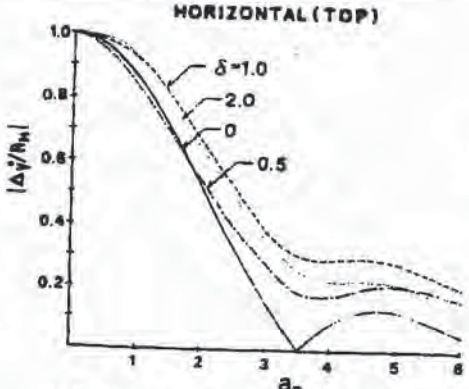


(a) Horizontal Input Motion.

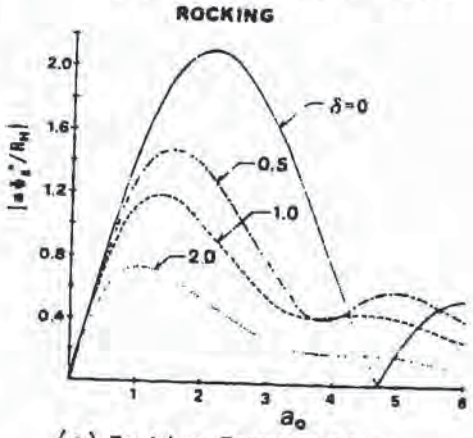


(c) Rocking Input Motion.

Fig. 2 Effect of Embedment Ratio on the Input Motions. ($\nu$ = 0.25)

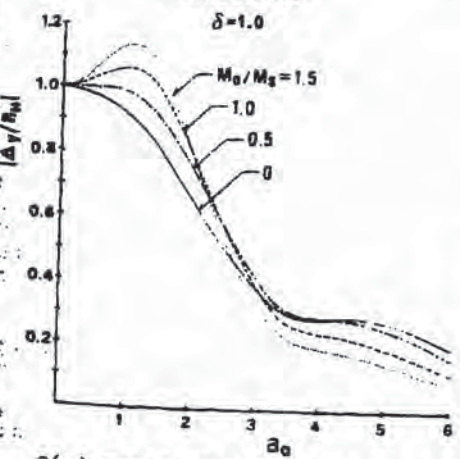


3(a) Horizontal Displacement.

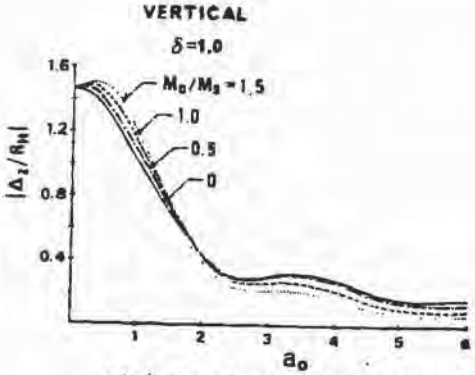


3(b) Vertical Displacement.

Calc. No. 03.7.316-2.0
Page B.9 of B.9

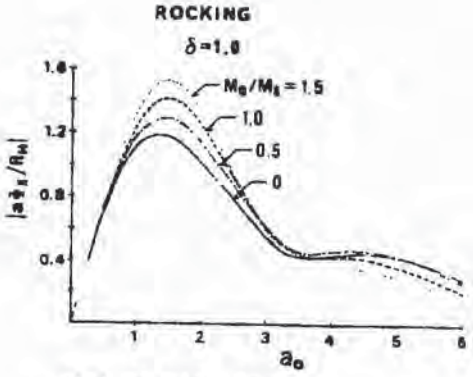


3(c) Rocking Angle.

Fig. 3 Effect of Mass Ratio on Seismic Responses of the Foundation. ($\nu$ = 0.25)

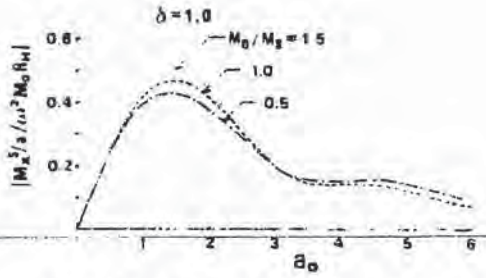


Fig. 5 Seismic Moment Acting on the Cylindrical Embedded Foundation. ($\nu$ = 0.25)

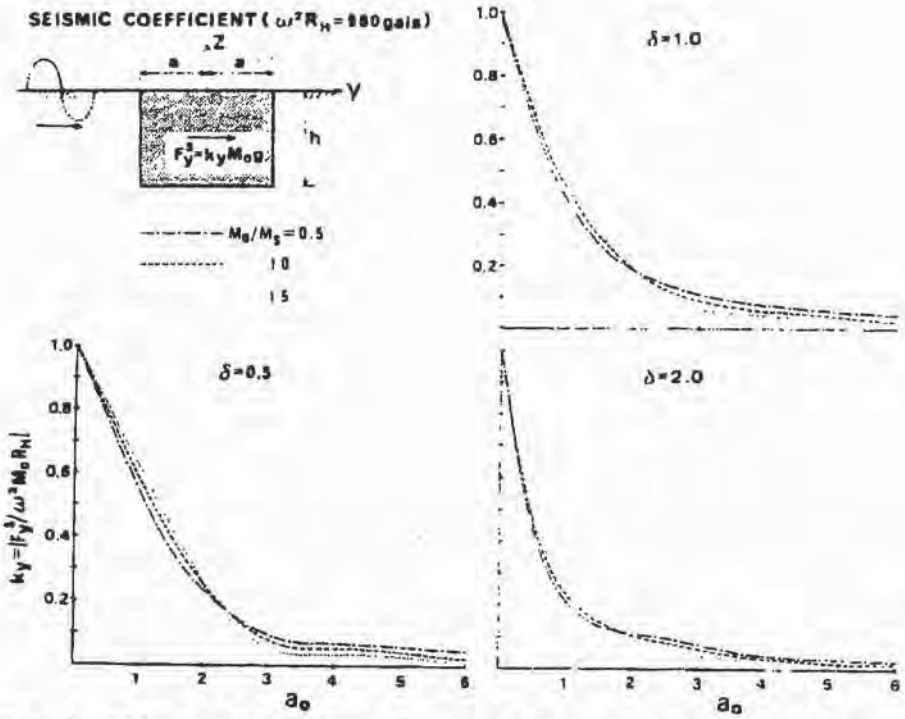


Fig. 4 Effects of Embedment Ratio and Mass Ratio on the Lateral Seismic Forces Acting on the Cylindrical Embedded Foundation. ($\nu$ = 0.25)

EARTHQUAKE ENGINEERING AND STRUCTURAL DYNAMICS, VOL. 6, 3–16 (1978)

Reference 10

# DYNAMIC RESPONSE OF RECTANGULAR FOUNDATIONS TO OBLIQUELY INCIDENT SEISMIC WAVES

H. L. WONG

*Department of Civil Engineering, School of Engineering, University of Southern California, Los Angeles, California, U.S.A.*

AND

J. E. LUCO

*Department of Applied Mechanics and Engineering Sciences, University of California, San Diego, La Jolla, California, U.S.A.*

## SUMMARY

A study is made of the harmonic response of a rigid massless rectangular foundation bonded to an elastic half-space and subjected to the action of both external forces and obliquely incident plane seismic waves. The associated mixed boundary value problem is discretized and solved numerically. The results obtained indicate that the angle of incidence of the seismic wave has a marked effect on the nature and magnitude of the foundation response.

## INTRODUCTION

Most studies of the interaction between structures and the soil during earthquakes are based on the assumption of vertically incident seismic waves. This assumption is generally justified on the grounds that the refraction of the seismic waves by the softer layers of soil closer to the soil surface would lead to essentially vertically incident waves. It is possible to think of circumstances under which such justification is not valid, e.g. hard soil deposits, shallow earthquake sources. Also, recent analyses of strong-motion records have shown that surface waves contribute in a significant amount to the earthquake motions recorded at intermediate and long epicentral distances.[1,2] Under such circumstances, it becomes important to study the effects of non-vertically incident seismic waves.

This study is directed at the evaluation of the dynamic response of a rigid massless rectangular foundation perfectly bonded to an elastic half-space and subjected to the action of both external forces and obliquely incident seismic waves. The external forces may correspond in a complete soil-structure interaction problem to the forces and moments that the superstructure and the foundation exert on the soil. The seismic excitation will be represented by plane compressional and shear waves impinging on the foundation with the angles of incidence shown in Figure 1. Both types of excitation will be assumed to have harmonic time dependence.

The evaluation of the response of the rigid foundation to external forces involves the determination of the compliance matrix for the foundation-soil system. Similarly, the evaluation of the response of the rigid massless foundation to plane seismic waves involves the determination of the 'input motion' matrix for the foundation.[3] The compliance and input motion matrices constitute a complete characterization of the interaction between the rigid foundation and the supporting soil. Once these matrices have been determined the complete soil-structure interaction problem for non-vertically incident seismic waves and for any configuration of the superstructure may then be formulated and solved.[3]

While a large number of publications dealing with the dynamic response of rigid foundations to external forces has appeared in the literature,[4] very few studies have been conducted on the related problem of diffraction of seismic waves by rigid movable foundations. A transient solution for the diffraction of an incident wave by a smooth rigid strip in contact with an elastic half-space has been presented by Flitman.[5]

0098–8847/78/0106–0003$01.00

*Received 24 February 1976*
*Revised 2 August 1976*

The corresponding harmonic problem under bonded contact conditions has been studied by Oien.[6] Thau and Umek[7,8] and Dravinski and Thau[9,10] have studied the response of a two-dimensional rigid foundation embedded in an elastic half-space and excited by non-vertically incident plane waves. Kobori *et al.*[11] have analysed the harmonic response of a rigid circular disc placed on an elastic half-space and subjected to the action of non-vertically incident plane SH-waves. A study of the torsional response of a rigid circular disc and a rigid semi-spherical foundation generated by harmonic plane SH-waves has been presented by Luco.[12,13] Approximate evaluations of the response of rigid foundations to non-vertically incident seismic waves have been presented by Newmark,[14] Tani *et al.*[15] and Iguchi.[16] The effects of non-vertically incident waves on the earthquake response of structures have been studied by Newmark,[14] Kobori *et al.*,[17] Iguchi[16] and Luco.[12,13]

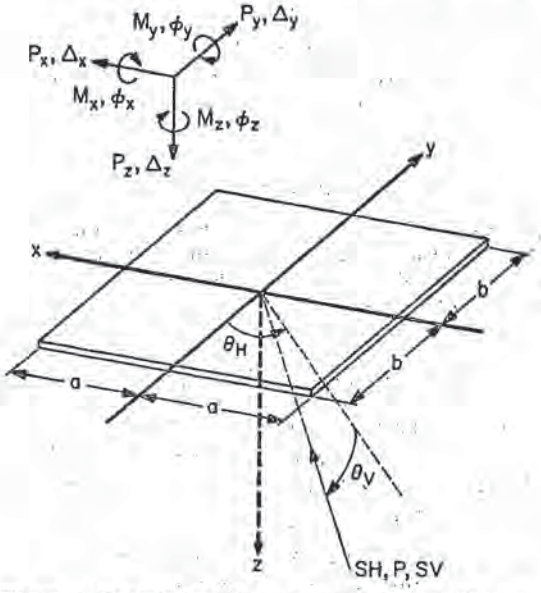


Figure 1. Description of the system and co-ordinates

The procedure employed here to determine the response of rigid foundations is based on formulating the corresponding dynamic mixed-boundary value problem by means of the Green's functions for the elastic half-space. Discretization of the integral equations representing the boundary condition is used to obtain approximate values for the tractions acting at the contact between the foundation and the soil.[4,18] Once the surface tractions have been determined the other quantities of interest are easily obtained. One of the advantages of this procedure is that it is equally applicable to arbitrarily shaped flat foundations.

## FORMULATION OF THE PROBLEM

Consider the vector displacement field in the elastic half-space $z \geqslant 0$ when excited by a plane compressional or shear wave in absence of the rigid rectangular foundation. If the plane incident wave is characterized by the vertical and horizontal angles of incidence, $\theta_V$ and $\theta_H$, respectively, as shown in Figure 1, then the total displacement field, including the reflection of the incident wave on the free surface, may be expressed in the form

$$\{\mathbf{u}^g(\bar{x})\}\exp(i\omega t) = \{\mathbf{U}^g\}\exp\left[i\omega\left(t-\frac{x}{c}\sin\theta_H-\frac{y}{c}\cos\theta_H\right)\right] \tag{1}$$

on the surface $z = 0$. In equation (1), $\omega$ is the frequency of the plane wave excitation, $\{\mathbf{U}^g\} = (U_x^g, U_y^g, U_z^g)^T$ is the amplitude vector of the free-field motion $\{\mathbf{u}^g\}$ at the origin of the co-ordinate system and $c$ is the apparent velocity of the incident wave as observed on the free-surface and along the direction of propagation of the wave. The apparent velocity $c$ takes the form $c = \alpha/\cos\theta_V$ or $c = \beta/\cos\theta_V$, where $\alpha$ and $\beta$ are the compressional

and shear wave velocities in the elastic medium, depending on whether the incident waves are compressional or shear waves. The free-field motion $\{\mathbf{u}^g(\bar{x})\}$ gives rise to no surface tractions on $z = 0$. For brevity the harmonic time factor $\exp(i\omega t)$ will be omitted in the following work.

Now consider the case in which a rigid rectangular foundation is bonded to the elastic half-space in the region $|x| < a$, $|y| < b$, $z = 0$.

In this case the total displacement field may be written in the form

$$\{\mathbf{u}(\bar{x})\} = \{\mathbf{u}^g(\bar{x})\} + \{\mathbf{u}^s(\bar{x})\} \tag{2}$$

where $\{\mathbf{u}^s(\bar{x})\}$ represents the scattered field generated by the rigid foundation. The surface traction $\{\mathbf{T}^s(\bar{x})\} = -(\sigma_{zx}(\bar{x}), \sigma_{zy}(\bar{x}), \sigma_{zz}(\bar{x}))^{\mathrm{T}}$ associated with the scattered field must vanish on the free surface exterior to the foundation. Also, the total displacement field $\{\mathbf{u}(\bar{x})\}$ in the contact region between the foundation and the half-space must be equal to the rigid-body motion of the foundation, i.e.

$$\{\mathbf{u}^g(\bar{x})\} + \{\mathbf{u}^s(\bar{x})\} = [\mathbf{A}(a^{-1}\bar{x})]\{\mathbf{U}\}, \quad z = 0, \quad |x| \leqslant a, \quad |y| \leqslant b \tag{3}$$

where $[\mathbf{A}(a^{-1}\bar{x})]$ is the $3 \times 6$ matrix defined by

$$[\mathbf{A}(a^{-1}\bar{x})] = \begin{bmatrix} 1 & 0 & 0 & 0 & 0 & -y/a \\ 0 & 1 & 0 & 0 & 0 & x/a \\ 0 & 0 & 1 & y/a & -x/a & 0 \end{bmatrix} \tag{4}$$

and $\{\mathbf{U}\}$ is the $6 \times 1$ vector

$$\{\mathbf{U}\} = (\Delta_x, \Delta_y, \Delta_z, a\phi_x, a\phi_y, a\phi_z)^{\mathrm{T}} \tag{5}$$

describing the rigid-body motion of the foundation. In equation (5), $\Delta_x, \Delta_y$ and $\Delta_z$ are the displacement components of the centre of the rigid foundation, while $\phi_x$, $\phi_y$ and $\phi_z$ represent the small angles of rotation about the $x$, $y$ and $z$ axes, respectively, as shown in Figure 1.

Introducing the Green's function for the elastic half-space it is possible to express the scattered field $\{\mathbf{u}^s(\bar{x})\}$ in terms of the contact tractions $\{\mathbf{T}^s(\bar{x})\}$ by means of the following relation

$$\{\mathbf{u}^s(\bar{x})\} = -\int_S \int [\mathbf{G}(\bar{x} - \bar{x}'; \kappa, \nu)]\{\mathbf{T}^s(\bar{x}')\}\,\mathrm{d}S' \tag{6}$$

where $[\mathbf{G}(\bar{x} - \bar{x}'; \kappa, \nu)]$ represents the $3 \times 3$ matrix of Green's functions for the elastic half-space.[4,18] In equation (6), $\kappa = \omega/\beta$, $\nu$ is the Poisson ratio for the elastic medium and $S$ represents the contact area $|x| \leqslant a$, $|y| \leqslant b$, $z = 0$. Substitution from equations (1) and (6) into the displacement boundary conditions (3) and rearranging leads to the following integral equation for $\{\mathbf{T}^s\}$

$$a^2 \int_{S'} \int [\mathbf{G}(\bar{\xi} - \bar{\xi}'; a_0, \nu)]\{\mathbf{T}^s(\bar{\xi}')\}\,\mathrm{d}S'$$

$$= -[\mathbf{A}(\bar{\xi})]\{\mathbf{U}\} + \exp\left[-ia_0 \frac{\beta}{c}(\xi \sin\theta_{\mathrm{H}} + \eta \cos\theta_{\mathrm{H}})\right]\{\mathbf{U}^g\}, \quad |\xi| \leqslant 1, \quad |\eta| \leqslant b/a \tag{7}$$

where $\bar{\xi} = (\xi, \eta, 0) = (x/a, y/a, 0)$, $a_0 = \omega a/\beta$ and $S'$ represents the region $|\xi| \leqslant 1$, $|\eta| \leqslant b/a$. In deriving equation (7) the relationship $[\mathbf{G}(x; \kappa, \nu)] = a[\mathbf{G}(a^{-1}x; a\kappa, \nu)]$ has been used.

Since the integral equation (7) is linear, the surface traction $\{\mathbf{T}^s\}$ may be decomposed into

$$\{\mathbf{T}^s(a\bar{\xi})\} = \mu a^{-1}[\mathbf{T}^{\mathrm{R}}(a\bar{\xi})]\{\mathbf{U}\} - \mu a^{-1}[\mathbf{T}^{\mathrm{D}}(a\bar{\xi})]\{\mathbf{U}^g\} \tag{8}$$

where $[\mathbf{T}^{\mathrm{R}}]$ and $[\mathbf{T}^{\mathrm{D}}]$ are $3 \times 6$ and $3 \times 3$ matrices, respectively, defined by the integral equations

$$\mu a^2 \int_{S'} \int [\mathbf{G}(\bar{\xi} - \bar{\xi}'; a_0, \nu)]\,[\mathbf{T}^{\mathrm{R}}(a\bar{\xi}')]\,\mathrm{d}S' = -[\mathbf{A}(\bar{\xi})] \tag{9}$$

$$\mu a^2 \int_{S'} \int [\mathbf{G}(\bar{\xi} - \bar{\xi}'; a_0, \nu)]\,[\mathbf{T}^{\mathrm{D}}(a\bar{\xi}')]\,\mathrm{d}S' = -[\mathbf{I}] \exp[-ia_0 \frac{\beta}{c}(\xi \sin\theta_{\mathrm{H}} + \eta \cos\theta_{\mathrm{H}}), \quad |\xi \leqslant 1, \quad |\eta| \leqslant b/a \tag{10}$$

In equation (10), [I] is the $3\times3$ identity matrix. The first term of the right-hand side of equation (8) corresponds to the surface tractions generated by the rigid-body motion of the rectangular foundation in the absence of incident waves; the second term corresponds to the surface tractions that are produced when the foundation is kept fixed while under the effects of the incident waves. This decomposition first suggested by Thau[19] has the advantage of allowing the evaluation of $[\mathbf{T}^{\mathrm{R}}]$ and $[\mathbf{T}^{\mathrm{D}}]$ without regard to the amplitudes of the rigid-body motion and of the free-field motion.

Postponing the discussion of the solution of equations (9) and (10), it may be said that once these equations are solved it is possible to evaluate the total forces and moments that the rigid foundation exerts on the soil by means of the following expression

$$\{\mathbf{F}^{\mathrm{s}}\} = a^2 \int_{S'} \int [\mathbf{A}(\bar{\xi}')]^{\mathrm{T}} \{\mathbf{T}^{\mathrm{s}}(a\bar{\xi}')\}\, \mathrm{d}S' \tag{11}$$

in which, $\{\mathbf{F}^{\mathrm{s}}\}$ is the $6\times1$ vector

$$\{\mathbf{F}^{\mathrm{s}}\} = (P_x, P_y, P_z, M_x/a, M_y/a, M_z/a)^{\mathrm{T}} \tag{12}$$

representing the total forces $P_x, P_y, P_z$ and the total moments $M_x, M_y, M_z$ acting on the soil. The sign convention for these forces and moments is illustrated in Figure 1.

Substitution from equation (8) into equation (11) leads to the force-displacement relationship

$$\{\mathbf{F}^{\mathrm{s}}\} = \mu a[\mathbf{K}]\{\mathbf{U}\} - \mu a[\mathbf{K}^*]\{\mathbf{U}^{\mathrm{g}}\} \tag{13}$$

where $[\mathbf{K}]$ is the $6\times6$ impedance matrix for the rigid foundation defined by

$$[\mathbf{K}] = \iint_{S} [\mathbf{A}(\xi')]^{\mathrm{T}} [\mathbf{T}^{\mathrm{R}}(a\bar{\xi}')]\, \mathrm{d}S' \tag{14}$$

and, $[\mathbf{K}^*]$ is the $6\times3$ 'driving force' matrix given by

$$[\mathbf{K}^*] = \iint_{S'} [\mathbf{A}(\bar{\xi}')]^{\mathrm{T}} [\mathbf{T}^{\mathrm{D}}(a\bar{\xi}')]\, \mathrm{d}S' \tag{15}$$

The force-displacement relationship for the rigid rectangular foundation given by equation (13) plays a key role in the study of the dynamic interaction between structures and the supporting soil. In equation (13), the term $\mu a[\mathbf{K}]\{\mathbf{U}\}$ represents the forces and moments that the rigid foundation exerts on the soil when moving with rigid-body motion $\{\mathbf{U}\}$ in absence of seismic excitation ($\{\mathbf{U}^{\mathrm{g}}\} = 0$). The term $\mu a[\mathbf{K}^*]\{\mathbf{U}^{\mathrm{g}}\}$ corresponds to the forces and moments that the soil exerts on the rigid foundation when the foundation is kept fixed ($\{\mathbf{U}\} = 0$) while under the effects of the seismic excitation.

The factor $(\mu a)$ appearing on the right-hand side of equation (13) has been introduced to render the matrices $[\mathbf{K}]$ and $[\mathbf{K}^*]$ dimensionless. The impedance matrix $[\mathbf{K}]$ defined by equation (14) depends on the geometry of the rigid foundation, the elastic properties of the soil and on the frequency of the excitation. The 'driving force' matrix $[\mathbf{K}^*]$ given by equation (15) depends, in addition, on the vertical and horizontal angles of incidence of the seismic waves.

An alternative form of the force-displacement relationship may be obtained by premultiplying both sides of equation (13) by $(\mu a)^{-1}[\mathbf{K}]^{-1}$, leading to

$$\{\mathbf{U}\} = (\mu a)^{-1}[\mathbf{C}]\{\mathbf{F}^{\mathrm{s}}\} + [\mathbf{S}^*]\{\mathbf{U}^{\mathrm{g}}\} \tag{16}$$

where $[\mathbf{C}]$ is the $6\times6$ compliance matrix for the rigid rectangular foundation

$$[\mathbf{C}] = [\mathbf{K}]^{-1} \tag{17}$$

and $[\mathbf{S}^*]$ is the $6\times3$ 'input motion' matrix defined by

$$[\mathbf{S}^*] = [\mathbf{C}][\mathbf{K}^*] \tag{18}$$

Equation (16) indicates that the total displacement of the rigid foundation $\{\mathbf{U}\}$ may be decomposed into two terms: the first term $(\mu a)^{-1}[\mathbf{C}]\{\mathbf{F}^{\mathrm{s}}\}$ corresponds to the displacement of the foundation associated with the forces $\{\mathbf{F}^{\mathrm{s}}\}$ that the foundation exerts on the soil; the second term corresponds to the effects of the seismic

waves. In particular, $[\mathbf{S}^*]\{\mathbf{U}^g\}$ represents the motion of a rigid massless foundation free from external forces ($\{\mathbf{F}^s\} = 0$) when excited by the free-field motion $\{\mathbf{U}^g\}$.

The compliance matrix $[\mathbf{C}]$ for a rigid rectangular foundation depends on the geometry of the foundation $(b/a)$, on the Poisson's ratio $\nu$ of the soil and on the dimensionless frequency $a_0 = \omega a/\beta$. The 'input motion' matrix $[\mathbf{S}^*]$ defined by equation (18) depends in addition on the relative phase velocity $c/\beta$ and on the horizontal angle of incidence $\theta_H$. Once the matrices $[\mathbf{C}]$ and $[\mathbf{S}^*]$ have been obtained the motion of the rigid foundation can be easily computed for any combination of inertial properties of the foundation. For instance, for a rigid foundation having a mass matrix $[\mathbf{M}_0]$ (referred to the centre of the base of the foundation), the force $\{\mathbf{F}^s\}$ that the foundation exerts on the soil is given by

$$\{\mathbf{F}^s\} = \omega^2[\mathbf{M}_0]\{\mathbf{U}\} \tag{19}$$

Substitution from equation (19) into equation (16) leads to the response

$$\{\mathbf{U}\} = \left([\mathbf{I}] - \frac{\omega^2}{\mu a}[\mathbf{C}][\mathbf{M}_0]\right)^{-1}[\mathbf{S}^*]\{\mathbf{U}^g\} \tag{20}$$

where $[\mathbf{I}]$ is the $6 \times 6$ identity matrix. If a superstructure is attached to the foundation, equation (20) is still valid, except that in this case the matrix $[\mathbf{M}_0]$ is frequency-dependent and involves not only the inertial properties of the foundation but also the inertial and elastic properties of the superstructure.

Equation (20) shows the importance of the 'input motion' matrix $[\mathbf{S}^*]$ in determining the response at the level of the foundation. Due to the lack of information of the 'input motion' matrix most previous studies on the interaction between structures and the soil were restricted to the case of vertically incident seismic waves for which

$$[\mathbf{S}^*]\{\mathbf{U}^g\} = (U_x^g, U_y^g, U_z^g, 0, 0, 0)^T \tag{21}$$

Such an assumption excludes all the rocking and torsional components of the input motion.

## NUMERICAL EVALUATION OF THE SURFACE TRACTIONS

The numerical procedure used here to solve the integral equations (9) and (10) is based upon sub-dividing the contact area into a number $N$ of smaller square sub-regions and in assuming that the contact tractions $\{\mathbf{T}^D\}$ and $\{\mathbf{T}^S\}$ within each sub-region may be considered to be constant. Imposition of the boundary conditions at the centres of the $N$ sub-regions reduces the integral equations (9) and (10) into systems of linear algebraic equations having for unknowns the constant values of the contact tractions within each of the $N$ sub-regions. Once these equations have been solved, the impedance matrix $[\mathbf{K}]$, and the 'driving force' matrix $[\mathbf{K}^*]$ may be evaluated by numerical integration of the integrals appearing in equations (14) and (15). The compliance matrix $[\mathbf{C}]$ and the 'input motion' matrix $[\mathbf{S}^*]$ may then be easily evaluated. Further details on this numerical procedure may be found elsewhere.[4,18]

## COMPLIANCE MATRIX FOR A SQUARE FOUNDATION

The procedure described in the previous section has been used to determine the compliance matrix $[\mathbf{C}]$ for a rigid square foundation $(a = b)$ bonded to an elastic half-space. Because of the symmetry of the square foundation, the compliance matrix reduces in this case to

$$[\mathbf{C}] = \begin{bmatrix} C_{HH} & 0 & 0 & 0 & C_{HM} & 0 \\ 0 & C_{HH} & 0 & -C_{HM} & 0 & 0 \\ 0 & 0 & C_{VV} & 0 & 0 & 0 \\ 0 & -C_{MH} & 0 & C_{MM} & 0 & 0 \\ C_{MH} & 0 & 0 & 0 & C_{MM} & 0 \\ 0 & 0 & 0 & 0 & 0 & C_{TT} \end{bmatrix} \tag{22}$$

where the coupling compliances $C_{MH}$ and $C_{HM}$ are equal. Thus, only five functions determine the complete compliance matrix in the case under consideration. These functions are the horizontal, vertical, rocking, torsion and coupling compliances denoted respectively by $C_{HH}$, $C_{TT}$, $C_{MM}$, $C_{TT}$ and $C_{MH} = C_{HM}$. The real and imaginary parts of these compliances for an elastic half-space with a Poisson's ratio of $\frac{1}{3}$ are presented in Figure 2 for values of the dimensionless frequency $a_0 = \omega a/\beta$ ranging from 0 to 4. It may be noticed in Figure 2 that the coupling compliances have values considerably lower than those for the other compliance functions. It should be emphasized that the compliance matrix as defined here has been rendered dimensionless in such a way that the force-displacement relationship in the absence of seismic wave excitation is given by

$$(\Delta_x, \Delta_y, \Delta_z, a\phi_x, a\phi_y, a\phi_z)^{\mathrm{T}} = (\mu a)^{-1}[\mathbf{C}](P_x, P_y, P_z, \mathbf{M}_x/a, \mathbf{M}_y/a, \mathbf{M}_z/a)^{\mathrm{T}} \tag{23}$$

The results presented in Figure 2 for the bonded square foundation differ from those obtained previously for a square foundation under relaxed boundary conditions.[4,18] The bonded compliances are in general lower than the corresponding relaxed functions. Differences of less than 2 per cent are obtained for values of $a_0$ less than two; for higher values of $a_0$ larger differences may be observed.

The numerical results just presented were obtained by sub-dividing the square foundation into 64 equal square elements. The symmetry or the skew-symmetry of the problem was also employed.

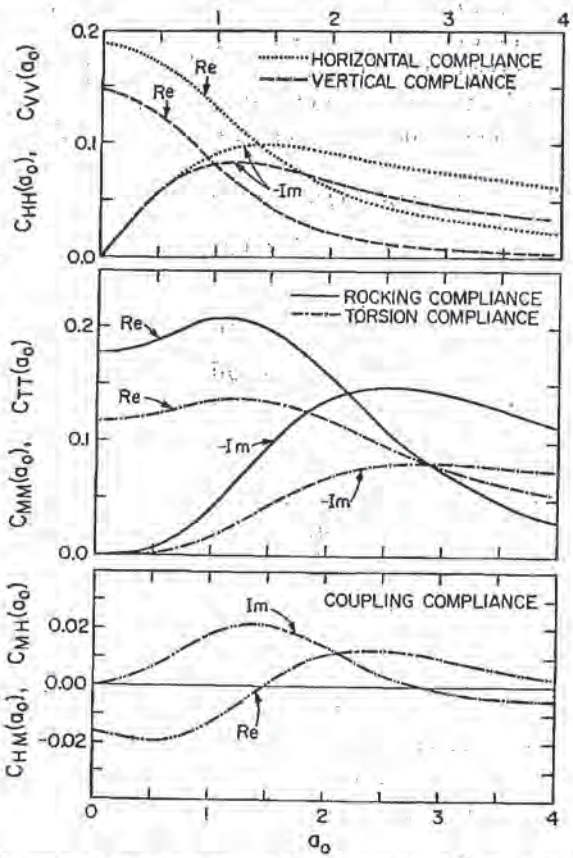


Figure 2. Compliance functions for a rigid square foundation bonded to an elastic half-space ($\nu = \frac{1}{3}$)

## INPUT MOTION MATRIX

It has been mentioned that the 'input motion' matrix [S*] depends on the geometry of the rectangular foundation ($b/a$), the value of the Poisson's ratio $\nu$ for the soil, the horizontal angle of incidence $\theta_H$ of the seismic waves, the relative phase velocity $c/\beta$ and on the dimensionless frequency $a_0$. For brevity, a detailed discussion will be presented only for the case of a square foundation ($b/a = 1$) subjected to plane waves with

wavefronts perpendicular to the plane $x = 0$, i.e. for $\theta_H = 0$. Also, numerical results will be presented only for the case $\nu = \frac{1}{3}$.

The 'input motion' matrix $[\mathbf{S}^*(a_0, \beta/c, \theta_H)]$ for a square foundation subjected to plane waves with horizontal angles of incidence $\theta_H = 0$ takes the form

$$[\mathbf{S}^*(a_0, \beta/c, 0)] = \begin{bmatrix} S_{xx}(a_0, \beta/c, 0) & 0 & 0 \\ 0 & S_{yy}(a_0, \beta/c, 0) & S_{yz}(a_0, \beta/c, 0) \\ 0 & S_{zy}(a_0, \beta/c, 0) & S_{zz}(a_0, \beta/c, 0) \\ 0 & R_{xy}(a_0, \beta/c, 0) & R_{xz}(a_0, \beta/c, 0) \\ R_{yx}(a_0, \beta/c, 0) & 0 & 0 \\ R_{zx}(a_0, \beta/c, 0) & 0 & 0 \end{bmatrix} \tag{24}$$

Thus, for $\theta_H = 0$, the 'input motion' matrix has only nine non-zero elements. Numerical values for the non-zero elements as a function of the dimensionless frequency $a_0$ are presented in Figures 3–7 for different values of the parameter $\beta/c$ reflecting the vertical angle of incidence.

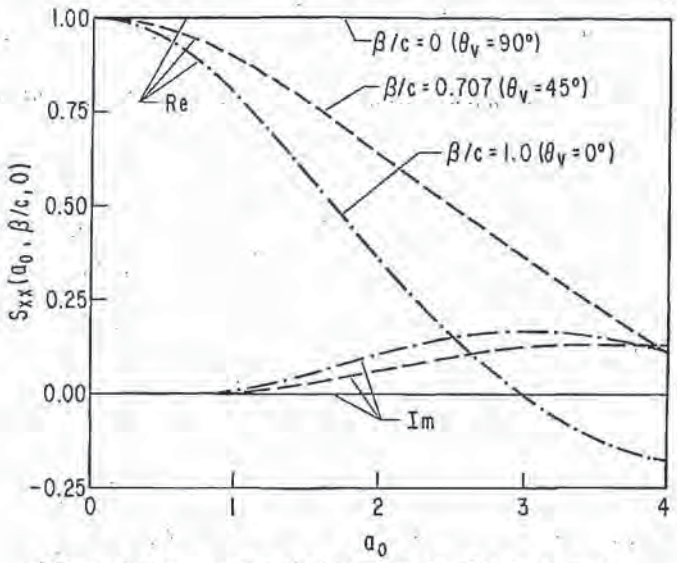


Figure 3. Input motion coefficient $S_{xx}(a_0, \beta/c, 0)$, $(\nu = \frac{1}{3})$

To give a physical interpretation to the different elements appearing in the 'input motion' matrix [S*], consider first the case of a rigid massless foundation free from external forces ($[\mathbf{F}^s] = 0$) and subjected to the action of an incident plane SH-wave of amplitude $u_0$ with particle motion polarized along the $x$-axis and with vertical angle of incidence $\theta_v$. In this case, the amplitude of the free-field motion at the centre of the foundation is $(U_x^g, U_y^g, U_z^g) = (2u_0, 0, 0)$, and the apparent velocity is $c = \beta/\cos\theta_v$. The response of the rigid massless foundation as obtained from equations (16) and (24) is then

$$\left.\begin{aligned} U_x &= S_{xx}(a_0, \beta/c, 0)\, 2u_0 \\ a\phi_z &= R_{zx}(a_0, \beta/c, 0)\, 2u_0 \\ a\phi_y &= R_{yx}(a_0, \beta/c, 0)\, 2u_0 \\ U_y &= U_z = a\phi_x = 0 \end{aligned}\right\} \tag{25}$$

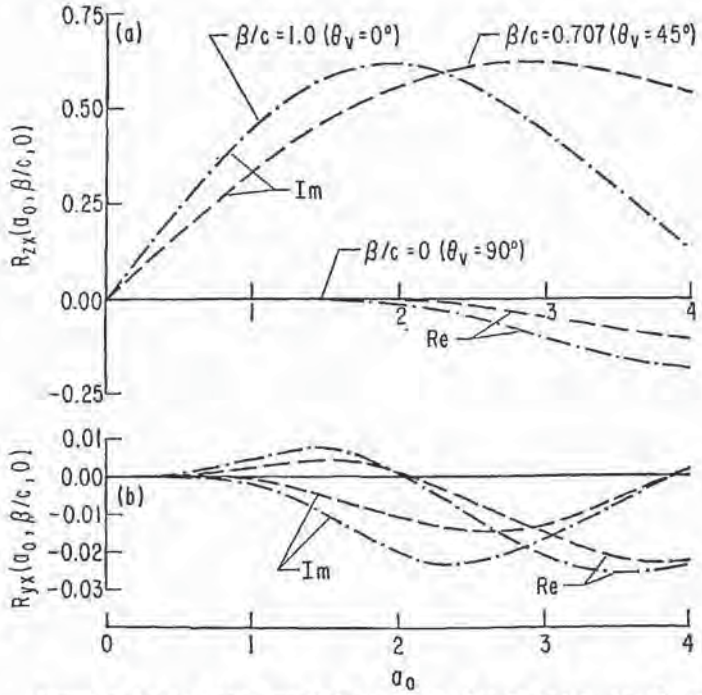


Figure 4. Input motion coefficients $R_{zx}(a_0, \beta/c, 0)$ and $R_{yx}(a_0, \beta/c, 0)$, $(\nu = \frac{1}{3})$

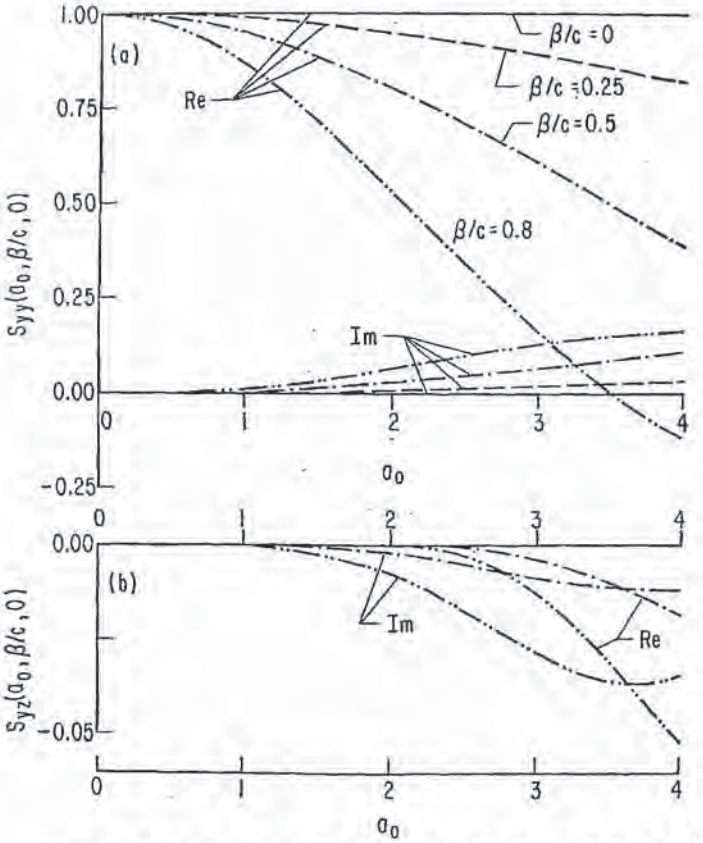


Figure 5. Input motion coefficients $S_{yy}(a_0, \beta/c, 0)$ and $S_{yz}(a, \beta/c, 0)$, $(\nu = \frac{1}{3})$

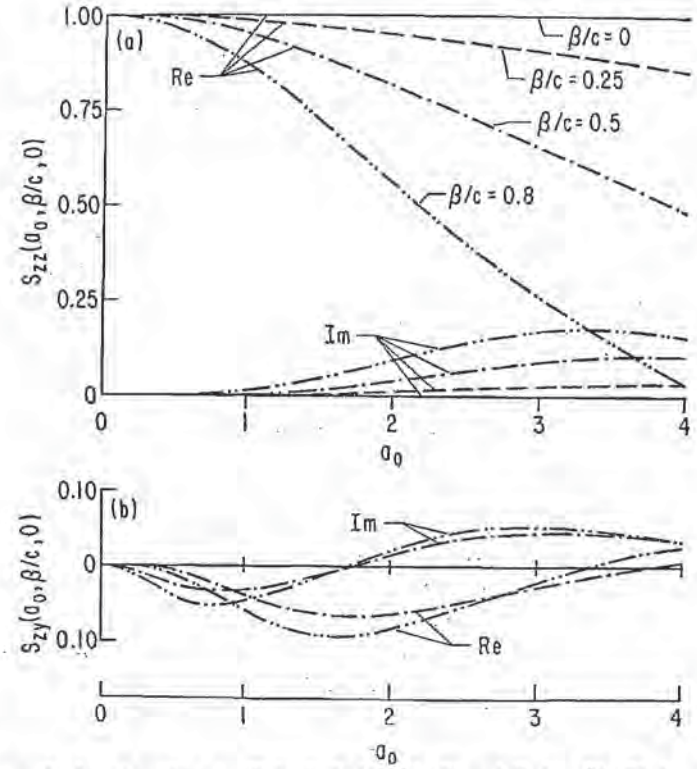


Figure 6. Input motion coefficients $S_{zz}(a_0, \beta/c, 0)$ and $S_{zy}(a_0, \beta/c, 0)$, $(\nu = \frac{1}{3})$

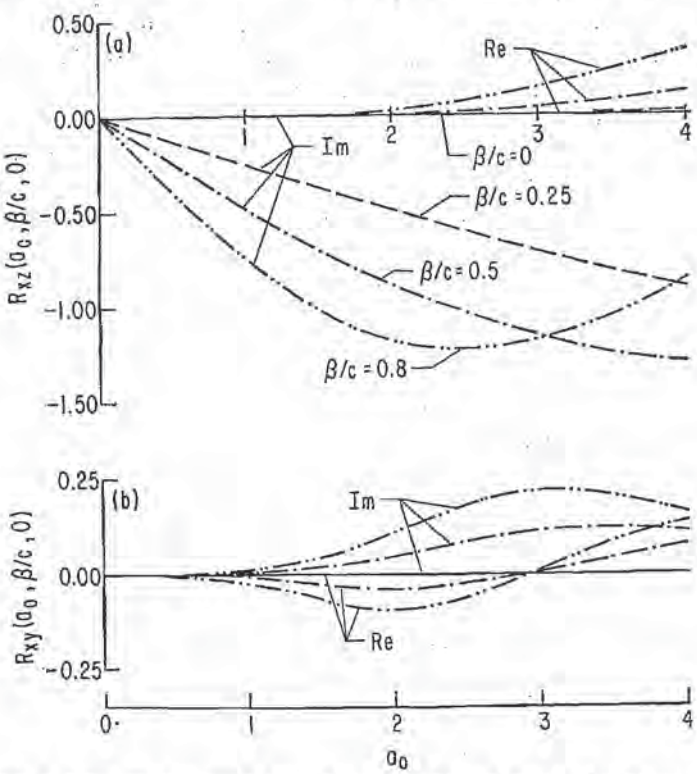


Figure 7. Input motion coefficients $R_{xz}(a_0, \beta/c, 0)$ and $R_{xy}(a_0, \beta/c, 0)$, $(\nu = \frac{1}{3})$

Thus, for the case under consideration, the response of the massless foundation consists of translation along the $x$-axis plus torsion about the vertical $z$-axis. A small rocking component about the $y$-axis is also obtained. Equation (25) shows that $S_{xx}(a_0, \beta/c, 0)$ corresponds to the ratio between the amplitude of the response along the $x$-axis and the amplitude $2u_0$ of the free-field motion. The results presented in Figure 3 indicate that the real part of $S_{xx}$ is dominant implying that at low frequencies the translational response is essentially in phase with the free-field motion at the centre of the foundation. For vertical incidence ($\theta_v = 90$ degrees), $S_{xx} = 1$ for all frequencies; however, for other angles of incidence $S_{xx}$ exhibits a marked decrease with frequency, the associated decrease in response being largest for horizontally propagating waves ($\theta_v = 0$ degrees). It is interesting to point out that studies of the response of the Hollywood Storage Building show for intermediate and high frequencies a strong reduction of the basement motion as compared with the free-field motion for both the Arvin–Tehachapi earthquake of 1952 and the San Fernando earthquake of 1971.[20–22] Housner[20] and Crouse[22] have suggested that such a reduction may be explained by non-vertically incident seismic waves. Such an explanation is in agreement with the results presented in Figure 3.

Equation (25) indicates that $R_{zx}(a_0, \beta/c, 0)$ defines the torsional response of the rigid massless foundation for SH excitation. In particular, $R_{zx}$ is equal to the ratio between the amplitude $a\phi_z$ of the tangential displacements associated with the torsional response at the points $(\pm a, 0, 0)$ and $(0, \pm a, 0)$ and the amplitude $2u_0$ of the free-field motion. The results presented in Figure 4($a$) show that $R_{zx}$ is complex, the imaginary part being dominant. Thus the torsional response is essentially 90 degrees out of phase with the free-field motion at the centre of the foundation. The torsional response is zero for vertically incident waves ($\theta_v = 90$ degrees) and it reaches its highest values for horizontally incident waves ($\theta_v = 0$ degrees). In particular, for horizontally propagating waves the maximum torsional response occurs at $a_0 \sim 1{\cdot}9$, i.e. when the wavelength is almost about 1·5 times the width of the foundation. In this case, the amplitude $a\phi_z$ of the induced tangential motion at the points $(\pm a, 0, 0)$ and $(0, \pm a, 0)$ may be as high as 60 per cent of the free-field amplitude $2u_0$. The results presented in Figure 4($a$) are consistent with those obtained by Kobori *et al.*[11] and Luco[12] for a rigid circular foundation. It is important to mention that for some massive structures, such as those in nuclear power plants, the value of $a_0$ at the fundamental fixed-base torsional frequency may be in the range of one to two indicating that large torsional effects can be expected for SH waves with shallow angles of incidence.[12,13]

The term $R_{yx}(a_0, \beta/c, 0)$, shown in Figure 4($b$), defines the rocking response about the $y$-axis as indicated in equation (25). In particular, $R_{yx}$ corresponds to the ratio of the rocking induced vertical displacement $a\phi_y$ along the edges $x = \pm a$ of the foundation to the amplitude of the free-field motion. The results presented in Figure 4($b$) indicate that this rocking response is quite small and may be neglected for most practical purposes.

To interpret the last two columns of the 'input motion' matrix $[\mathbf{S}^*(a_0, \beta/c, 0)]$ consider the case of a rigid massless foundation free from external loads ($\{\mathbf{F}^s\} = 0$) and subjected to the action of a non-vertically incident plane P-wave of amplitude $p$, vertical angle of incidence $\theta_v = e$, and particle motion polarized in the plane $x = 0$, i.e. $\theta_H = 0$. In this case the amplitude of the free-field motion ($U_x^g, U_y^g, U_z^g$) at the centre of the foundation is given by[23]

$$\left.\begin{aligned} U_x^g &= 0 \\ U_y^g &= p\cos e[1 + R_{pp} - R_{sp}\tan f] \\ U_z^g &= -p\sin e[1 - R_{pp} - R_{sp}\tan e] \end{aligned}\right\} \tag{26}$$

where $\tan f$ is defined by

$$1 + \tan^2 f = [2(1-\nu)/(1-2\nu)](1 + \tan^2 e) \tag{27}$$

and

$$\left.\begin{aligned} R_{pp} &= [4\tan e\tan f - (\tan^2 f - 1)^2]/R \\ R_{sp} &= -[4\tan f(\tan^2 f - 1)]/R \\ R &= 4\tan e\tan f + (\tan^2 f - 1)^2 \end{aligned}\right\} \tag{28}$$

The relative amplitudes $U_y^g/p$ and $U_z^g/p$ of the free-field motion are shown in Figure 8 for different angles of incidence $\theta_v = e$ and for different values of Poisson's ratio $\nu$. Figure 8 indicates that for shallow angles of

incidence the horizontal component of the free-field motion is more pronounced, while for angles of incidence close to 90 degrees the vertical component becomes predominant. The phase velocity $c$ associated with the non-vertically incident P-waves is given by

$$c = \alpha/\cos e = [2(1-\nu)/(1-2\nu)]^{\frac{1}{2}}\beta/\cos e \tag{29}$$

Values of $\beta/c$, $U_y^g/p$ and $U_z^g/p$ for a few selected angles of incidence $\theta_v = e$ are listed in Table I.

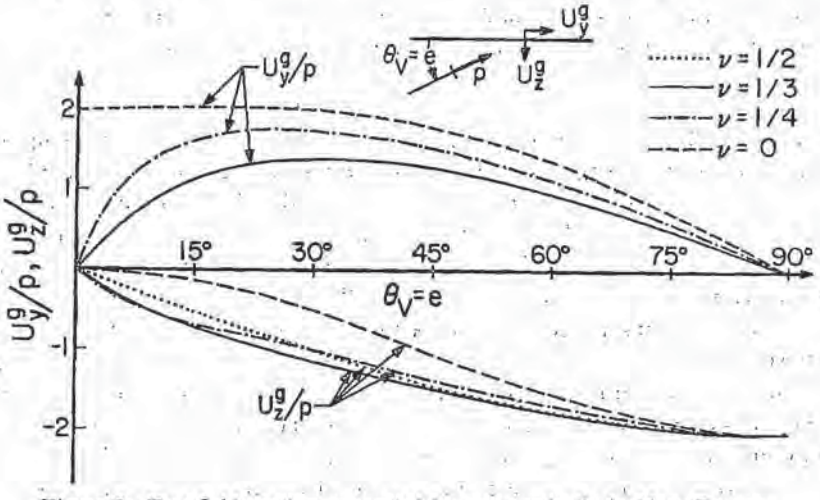


Figure 8. Free-field motion generated by non-vertically incident P waves

Table I. Values of $\beta/c$, $U_y^g$, $U_z^g$ for incident P-waves ($\nu = \frac{1}{3}$)

| $\beta/c$ | $\theta_v = e$ | $U_y^g/p$ | $U_z^g/p$ |
|---|---|---|---|
| 0·00 | 90° | 0·00 | −2·00 |
| 0·25 | 60° | 0·96 | −1·74 |
| 0·40 | 36·9° | 1·38 | −1·28 |
| 0·50 | 0° | 0·00 | 0·00 |

For the case under consideration, the response of the rigid massless foundation may be obtained by use of equations (16), (24) and (26), leading to

$$\left.\begin{aligned} \Delta_y &= S_{yy}U_y^g + S_{yz}U_z^g \\ \Delta_z &= S_{zy}U_y^g + S_{zz}U_z^g \\ a\phi_x &= R_{xy}U_y^g + R_{xz}U_z^g \\ \Delta_x &= a\phi_y = a\phi_z = 0 \end{aligned}\right\} \tag{30}$$

Equation (30) indicates that the response of the massless foundation consists of translations along the $y$- and $z$-axes and of rocking about the $x$-axis. The role of the 'input motion' coefficients $S_{yy}$, $S_{yz}$, $S_{zy}$, $S_{zz}$, $R_{xy}$ and $R_{xz}$ is clearly determined by equation (30). In particular, $S_{yy}(a_0, \beta/c, 0)$ determines the contribution of the horizontal component of the free-field motion $U_y^g$ to the horizontal response $\Delta_y$ of the foundation, while $S_{yz}(a_0, \beta/c, 0)$ determines the contribution of the vertical component of the free-field motion $U_z^g$ to the horizontal response. Similar roles are played by $S_{zy}(a_0, \beta/c, 0)$ and $S_{zz}(a_0, \beta/c, 0)$ with respect to the vertical component of response $\Delta_z$. The coefficients $R_{xy}$ and $R_{xz}$ determine the rocking response $a\phi_x$ associated with the horizontal and vertical components of the free-field motion. Numerical values for these coefficients plotted *vs* the dimensionless frequency $a_0 = \omega a/\beta$ are presented in Figures 5–7 for different values of $\beta/c$.

Only the results shown for $0 \leqslant \beta/c \leqslant 0{\cdot}5$ have a physical meaning for P-wave excitation and for a soil characterized by $\nu = \frac{1}{3}$, as indicated by equation (29) and Table I.

One of the interesting results obtained is that the coefficients $S_{yy}$ and $S_{zz}$ are essentially real and that their behaviour is similar to that of $S_{xx}$. For vertical incidence, $\beta/c = 0$ and $S_{yy} = S_{zz} = 1$ for all frequencies; for non-vertical incidence $S_{yy}$ and $S_{zz}$ show a decrease in amplitude with increasing frequency as illustrated in Figures 5(a) and 6(a).

The coefficients $S_{yz}$, $S_{zy}$ and $R_{xy}$ are complex as shown in Figures 5–7, respectively, and their amplitudes are considerably lower than the amplitudes of $S_{yy}$, $S_{zz}$ and $R_{xx}$. It follows that for all practical purposes the influence of these terms may be neglected allowing equation (30) to be written in the simplified form

$$\Delta_y \approx S_{yy} U_y^g, \quad \Delta_z \approx S_{zz} U_z^g, \quad a\phi_x \approx R_{xx} U_z^g \tag{31}$$

It has been mentioned that the coefficient $R_{xx}(a_0, \beta/c, 0)$ is associated with the rocking response generated by non-vertically incident P-waves. In particular, $R_{xx}$ is equal to the ratio of the vertical response $a\phi_x$ at the points $(0, \pm a, 0)$ due to rocking about the $x$-axis and the amplitude of the vertical component of the free-field motion $U_z^g$. Inspection of Figure 7(a) shows that $R_{xx}$ is in general complex and that the imaginary part of $R_{xx}$ is dominant. For vertical incidence ($\beta/c = 0$) $R_{xx}$ is zero, while for other angles of incidence $R_{xx}$ is considerably different from zero. Considering that $a\phi_x \approx R_{xx} U_z^g$, it results from Figures 7 and 8 that the maximum rocking response is obtained for P-waves with angles of incidence between 30 and 60 degrees ($\beta/c$ between 0·25 and 0·4).

The last two columns of the 'input motion' matrix $[\mathbf{S}^*(a_0, \beta/c, 0)]$ are also helpful in determining the response of the rigid foundation to non-vertically incident plane SV-waves. Consider a plane SV-wave of amplitude $s$, vertical angle of incidence $\theta_v = f$ and particle motion polarized in the plane $x = 0$, i.e. $\theta_H = 0$. In this case the response of the rigid massless foundation is also given by equation (30), except that for SV-waves the free-field motion is characterized by[23]

$$\left.\begin{aligned} U_x^g &= 0 \\ U_y^g &= s \sin f [1 - R_{pp} - R_{sp} \tan f] \\ U_z^g &= s \cos f [1 + R_{pp} - R_{sp} \tan e] \end{aligned}\right\} \tag{32}$$

where $\tan e$, $R_{pp}$ and $R_{sp}$ are defined by equations (27) and (28), respectively. The relative amplitudes $U_y^g/s$ and $U_z^g/s$ of the free-field motion are shown in Figure 9 for different angles of incidence $\theta_v = f$ for the case $\nu = \frac{1}{3}$. Notice that if $f < 60$ degrees, i.e. if $f$ is less than the critical angle for SV waves, the amplitudes of $U_y^g$

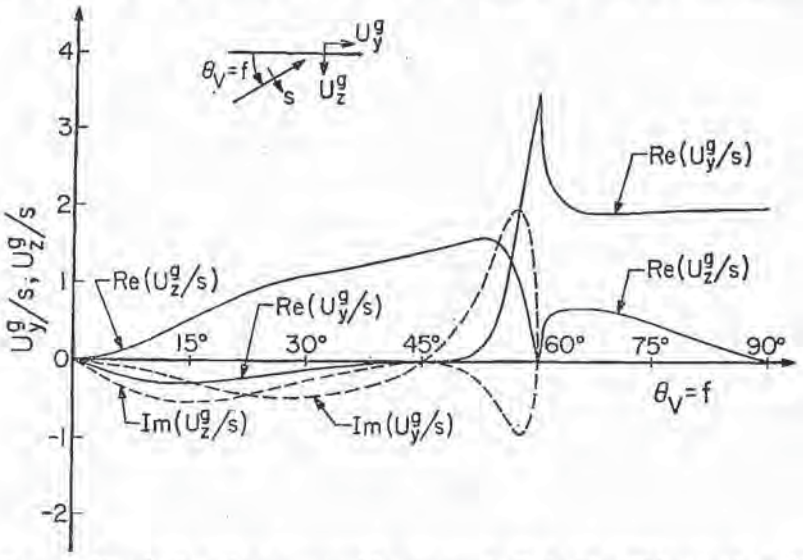


Figure 9. Free-field motion generated by non-vertically incident SV waves ($\nu = \frac{1}{3}$)

and $U_x^g$ are complex. In the case of incident SV-waves, the phase velocity $c$ is $c = \beta/\cos f$. Values of $\beta/c$, $U_y^g$ and $U_z^g$ are summarized in Table II for some particular values of $\theta_v = f$. Since the elements of the 'input motion' matrix presented in Figures 5–7 depend only on $\beta/c$ they may also be used to determine the response for non-vertically incident SV-waves. The results presented in Figures 7 and 9 indicate, for instance, that SV-waves impinging on the foundation with angles of incidence of 30–60 degrees ($\beta/c = 0{\cdot}5$–$0{\cdot}9$) will cause a considerable amount of rocking about the $x$-axis.

The results presented above for the 'input motion' matrix $[\mathbf{S}^*(a_0, \beta/c, \theta_H)]$ are strictly valid only for plane waves with horizontal angles of incidence of $\theta_H = 0$. The same procedure described herein may be used to determine the 'input motion' matrix for other horizontal angles of incidence and for other types of excitation such as Rayleigh waves.[24]

Table II. Values of $\beta/c$, $U_y^g$, $U_z^g$ for incident SV-waves ($\nu = \frac{1}{3}$)

| $\beta/c$ | $\theta_v = f$ | $U_y^g/s$ | $U_z^g/s$ |
|---|---|---|---|
| 0·00 | 90° | 2·00 | 0·00 |
| 0·25 | 75·5° | 1·95 | 0·48 |
| 0·40 | 66·4° | 1·95 | 0·69 |
| 0·50 | 60° | 3·46 | 0·00 |
| 0·80 | 36·9° | 0·00 | 0·00 |

## CONCLUSIONS

The problem of the forced vibrations of a rigid rectangular foundation bonded to an elastic half-space and subjected to the action of external forces and non-vertically incident seismic waves has been analysed. It has been shown that the solution of the problem under general loading conditions reduces to the determination of the compliance and 'input motion' matrices. Numerical values for the elements of these matrices have been presented for the particular case of a square foundation.

The results obtained indicate that the dynamic response of a rigid massless foundation subjected to non-vertically incident seismic waves differs both in magnitude and nature from the corresponding response for vertically incident waves. In particular, non-vertically incident SH waves generate a marked torsional response, while non-vertically incident P and SV-waves may cause a considerable amount of rocking of the foundation. These components of motion are not excited by vertically incident waves. The non-vertical incidence of the seismic waves also causes a notable decrease of the translational response for high frequencies. The results presented here suggest that soil-structure interaction studies should not be limited to seismic excitations with vertical incidence.

### ACKNOWLEDGEMENTS

The authors are indebted to M. D. Trifunac for his critical reading of the manuscript.

This research has been supported by grants from the National Science Foundation, the U.S. Geological Survey and the Earthquake Research Affiliates Program at the California Institute of Technology.

### REFERENCES

1. M. D. Trifunac, 'Response envelope spectrum and interpretation of strong earthquake ground motion', *Bull. Seism. Soc. Am.* **61**, 343–356 (1971).
2. T. C. Hanks, 'Strong ground motion following the San Fernando, California, earthquake: ground displacements', *Bull. Seism. Soc. Am.* **65**, 193–225 (1975).
3. J. E. Luco, H. L. Wong and M. D. Trifunac, 'A note on the dynamic response of rigid embedded foundations', *Earthq. Engng Struct. Dyn.* **4**, 119–128 (1975).
4. H. L. Wong, 'Dynamic soil-structure interaction', Report EERL–75–01, Earthquake Research Lab., California Institute of Technology, Pasadena, California, 1975.

5. L. M. Flitman, 'On the motion of a rigid strip-mass lying on an elastic half space and excited by a seismic wave', *J. Appl. Math. Mech.* **26**, 1583–1604 (1962).
6. M. A. Oien, 'Steady motion of a rigid strip bonded to an elastic half-space', *J. Appl. Mech., ASME*, **38**, 328–344 (1971).
7. S. A. Thau and A. Umek, 'Transient response of a buried foundation to antiplane shear waves', *J. Appl. Mech., ASME*, **40**, 1061–1066 (1973).
8. S. A. Thau and A. Umek, 'Coupled rocking and translating vibrations of a buried foundation', *J. Appl. Mech., ASME*, **41**, 697–702 (1974).
9. M. Dravinski and S. A. Thau, 'Multiple diffractions of elastic shear waves by a rigid rectangular foundation embedded in an elastic half-space', *J. Appl. Mech., ASME*, **43**, 295–299 (1976).
10. M. Dravinski and S. A. Thau, 'Multiple diffractions of elastic waves by a rigid rectangular foundation: plane-strain model', *J. Appl. Mech., ASME*, **43**, 291–294 (1976).
11. T. Kobori, R. Minai and Y. Shinozaki, 'Vibration of a rigid circular disc on an elastic half-space subjected to plane waves', *Proc. 21st Japan Nat. Cong. for Appl. Mech.*, 109–119 (1971).
12. J. E. Luco, 'Torsional response of structures to obliquely incident seismic SH waves', *Earthq. Engng Struct. Dyn.* **4**, 207–219 (1976).
13. J. E. Luco, 'Torsional response of structures for SH waves: the case of hemispherical foundations', *Bull. Seism. Soc. Am.* **66**, 109–123 (1976).
14. N. M. Newmark, 'Torsion of symmetrical buildings', *Proc. 4th Wld Conf. Earthq. Engng*, Santiago, Chile, **2**, (1969).
15. S. Tani, J. Sakurai and M. Iguchi, 'The effect of plane shape and size of buildings on the input earthquake motions', *Proc. 5th Wld Conf. Earthq. Engng*, Rome (1973).
16. M. Iguchi, 'Seismic response with consideration of both phase differences of ground motion and soil-structure interaction', *Proc. Japan Earthq. Engng Symp.*, Tokyo, Japan (1973).
17. T. Kobori, R. Minai and Y. Shinozaki, 'Dynamic response of a structure on an elastic half-space excited by SH-waves', *Proc. Japan Architectural Soc.* (1973).
18. H. L. Wong and J. E. Luco, 'Dynamic response of rigid foundations of arbitrary shape', *Earthq. Engng Struct. Dyn.* **4**, 579–587 (1976).
19. S. A. Thau, 'Radiation and scattering from a rigid inclusion in an elastic medium', *J. Appl. Mech., ASME*, **89**, 509–511 (1967).
20. G. W. Housner, 'Interaction of building and ground during an earthquake', *Bull. Seism. Soc. Am.* **47**, 179–186 (1957).
21. C. M. Duke, J. E. Luco, A. R. Carriveau, P. J. Hradilek, R. Lastrico and D. Ostrom, 'Strong earthquake motion and site conditions: Hollywood', *Bull. Seism. Soc. Am.* **60**, 1271–1289 (1970).
22. C. B. Crouse, 'Engineering studies of the San Fernando earthquake', Report EERL–73–04, Earthquake Engineering Research Lab., California Institute of Technology, Pasadena, California, 1973.
23. W. M. Ewing, W. S. Jardetzky and F. Press, *Elastic Waves in Layered Media*, McGraw-Hill, New York, 1957.
24. J. E. Luco and H. L. Wong, 'Dynamic response of rectangular foundations for Rayleigh wave excitation', *Proc. 6th Wld Conf. Earthq. Engng*, New Delhi (1977).

EARTHQUAKE ENGINEERING AND STRUCTURAL DYNAMICS, VOL. 14, 891–908 (1986)

Reference 11.

# RESPONSE OF A RIGID FOUNDATION TO A SPATIALLY RANDOM GROUND MOTION

J. E. LUCO

*Department of Applied Mechanics and Engineering Sciences, University of California, San Diego, La Jolla, California* 92093, *U.S.A.*

AND

H. L. WONG

*Department of Civil Engineering, University of Southern California, Los Angeles, California, U.S.A.*

## SUMMARY

A method to obtain the dynamic response of an extended rigid foundation supported on an elastic half-space when subjected to a spatially varying ground motion including both random and deterministic effects is presented. The method relies on an integral representation of the response of the foundation in terms of the free-field ground motion. Numerical results for a rigid square foundation and for a ground motion characterized by a particular spatial coherence function are described. The results obtained indicate that the spatial randomness of the ground motion produces effects similar to the deterministic effects of wave passage including reduction of the translational components of the response at high frequencies and creation of rocking and torsional response components. The possibility of defining an effective apparent horizontal velocity which produces effects equivalent to those from a given spatial randomness is explored.

## INTRODUCTION

Strong motion records obtained in dense arrays (Tamura *et al.*,[1] Tsuchida *et al.*,[2,3] Bycroft,[4] Smith *et al.*,[5] King,[6] King and Tucker,[7] Bolt *et al.*,[8–10] Hoshiya and Ishii,[11,12]) reveal a somewhat unexpected degree of variability over short distances. The observed spatial variation of the free-field motion over short distances may have important implications for the seismic response of structures supported on extended foundations or multiple supports and for various types of pipelines. In particular, for structures supported on sufficiently rigid extended foundations the inclusion of the effects associated with the spatial variation of ground motion may lead to a reduction of the translational response at foundation level and to some increase in the rocking and torsional response. For structures supported on flexible foundations or multiple supports, and, for pipelines, the spatial variation of the free-field ground motion may cause increased localized deformations and strains.

Comparisons of records obtained in buildings with those recorded on the free-field show some filtering of high frequencies which can be explained only in part by inertial soil–structure interaction effects (Housner,[13] Duke *et al.*,[14] Yamahara,[15] Shioya and Yamahara,[16] Ishii *et al.*,[17]). The rest of the filtering must be attributed to embedment effects and to the lateral spatial variation of the free-field ground motion. The free-field motion on the ground surface varies from point to point as a result of non-vertical incidence of body-wave energy, surface-wave propagation, waves arriving from different points on an extended source, and amplitude changes and time delays due to inhomogeneities along the propagation path. The effects that the first two factors, i.e. non-vertical incidence of body-wave energy and surface-wave energy, have on the response of foundations and structures are relatively well documented (e.g. Newmark,[18] Luco,[19,20] Luco and Wong,[21,22] Wong and Luco,[23] Luco and Sotiropoulos[24]). The information obtained from dense arrays suggests that, under certain conditions, the variability of ground motion resulting from inhomogeneities along the path and from incidence from different directions may be equally or even more significant than the variability associated with non-vertically incident waves from a fixed azimuth.

0098–8847/86/060891–18$09.00


*Received 6 September 1985*
*Revised 13 January 1986*

Several approaches have been proposed to estimate the effects of spatial variation of the free-field ground motion on the response of extended foundations. One approach is purely empirical and relies on observation of the motion of light foundations and on comparisons with observed free-field ground motion. A second approach, typically used to estimate the effects on the translational response of the foundation, consists in using spatial averages of observed free-field ground motion directly, or, of functionals of the observed ground motion such as response or Fourier spectra. Smith *et al.*[5] used the ratio of the pseudo-velocity response spectrum of the spatial average of the recorded accelerations to the corresponding average spectrum. King[6] and King and Tucker[7] used the same type of ratio except for the use of Fourier amplitude spectra instead of response spectra and for the introduction of weights to account for unequal spacing of the stations. Loh *et al.*[25] in an analysis of a structure supported at two points have considered the ratio of the pseudo-acceleration response spectrum for a linear combination of the acceleration recorded at the two points to the corresponding average spectrum. Hoshiya and Ishii[12] have used the ratio of the Fourier amplitude spectrum of the spatial average of the recorded accelerations to the spectrum of the recorded acceleration at a central point in the array. All of these measures indicate a reduction in translational response which increases with frequency and with the overall spatial dimension over which the average is taken. The major difficulties with this second approach are: (i) the spatial averages are usually calculated over a line while most foundations are two dimensional in plan, (ii) the spatial dimensions are controlled by the geometry of the arrays which, in many cases, have minimum spacing larger than the length of interest for many foundations, and, (iii) a simple average may not properly represent the contact problem between a rigid foundation and the elastic soil.

A third approach to estimate the effects of spatial variation of the free-field ground motion on the response of extended foundations relies on an analytic representation of the spatial variation of ground motion in the frequency domain and on the use of spatial weighted averages including weights which are, typically, linear functions of position. In the case of wave passage effects, the spatial variation of ground motion is typically represented in the form of plane waves. For random spatial variation, the stochastic spatial characteristics of the ground motion are represented by the cross-correlation or coherence function between the motion at two points. For wave passage effects this approach has been used, among others, by Iguchi,[26] Scanlan[27] and Luco and Sotiropoulos.[24] For random spatial variation this approach has been utilized by Matsushima[28] and Hoshiya and Ishii.[12] The procedure is simple and can accommodate foundations of different geometries. The limitations are: (i) the results depend on the appropriateness of the assumed spatial variation of the ground motion, and (ii) weighted averages may not account for the actual contact problem between the foundation and the soil.

A fourth approach also relies on an analytic representation of the spatial variation of ground motion but addresses the contact problem between the foundation and the soil as a mixed boundary-value problem. For wave passage effects, this approach have been used, among others, by Luco,[19,20] Luco and Wong[21] and Wong and Luco.[23]

The objective of this study is to determine the response of a rigid foundation bonded to a visco-elastic half-space when subjected to a spatially varying ground motion including both random and deterministic effects. The proposed method follows the fourth approach described above and relies on the use of a coherence function. Special emphasis is given to the effects of spatial randomness on the translational and rocking components of the response and on the correlation between the various response components. The relationship between wave passage and spatial randomness effects is examined and a procedure to account for the interaction effects due to the presence of a superstructure is also described.

## CHARACTERIZATION OF THE FREE-FIELD GROUND MOTION

A Cartesian coordinate system $x_1x_2x_3$ located on the surface ($x_3 = 0$) of the half-space ($x_3 \leqslant 0$) representing the soil is utilized to describe the free-field ground motion (Figure 1). The complex Fourier amplitude of the free-field ground motion vector at a point $\mathbf{x} = (x_1, x_2, 0)$ on the ground surface is represented by

$$\{U_g(\mathbf{x}, \omega)\} = (U_{g1}(\mathbf{x}, \omega), U_{g2}(\mathbf{x}, \omega), U_{g3}(\mathbf{x}, \omega))^T \tag{1}$$

in which $\omega$ is the frequency and $U_{gm}(\mathbf{x}, \omega)$ represents the component of motion along the $x_m$-axis ($m = 1, 2, 3$).

The superscript $T$ denotes transposition. The components of the free-field ground motion are considered to be random functions of position $\mathbf{x}$ such that

$$E[U_{gm}(\mathbf{x}, \omega)] = 0 \qquad (m = 1, 2, 3) \tag{2}$$

in which $E[\cdot]$ denotes expected value.

The second order properties of the random field are described by the covariance matrix

$$[B(\mathbf{x}, \mathbf{x}', \omega)] = E[\{U_g(\mathbf{x}, \omega)\}\{\tilde{U}_g(\mathbf{x}', \omega)\}^T] \tag{3}$$

in which the tilde denotes complex conjugate. The components $B_{mn}$ of the matrix $[B]$ are given by

$$B_{mn}(\mathbf{x}, \mathbf{x}', \omega) = E[U_{gm}(\mathbf{x}, \omega)\,\tilde{U}_{gn}(\mathbf{x}', \omega)] \qquad (m, n = 1, 2, 3). \tag{4}$$

In the derivation which follows it is assumed that the covariance functions $B_{mn}$ can be expressed in the form

$$B_{mn}(\mathbf{x}, \mathbf{x}', \omega) = \mu_{gm}\mu_{gn}\rho_{gmn}f_{mn}(|\mathbf{x}-\mathbf{x}'|, \omega)\exp[-i\omega(x_1/c_m - x_1'/c_n)] \tag{5}$$

in which the variances

$$\mu_{gm}^2(\omega) = E[|U_{gm}(\mathbf{x}, \omega)|^2] \tag{6}$$

and the normalized correlation coefficients

$$\rho_{gmn} = \tilde{\rho}_{gnm} = \frac{E[U_{gm}(\mathbf{x}, \omega)\tilde{U}_{gn}(\mathbf{x}, \omega)]}{\mu_{gm}\mu_{gn}}\exp[i\omega x_1(c_m^{-1} - c_n^{-1})] \tag{7}$$

are considered to be independent of $\mathbf{x}$. Clearly, $\rho_{g11} = \rho_{g22} = \rho_{g33} = 1$. The spatial coherence functions $f_{mn}$ for two points $\mathbf{x}$ and $\mathbf{x}'$ on the ground surface are assumed to depend only on the distance $|\mathbf{x}-\mathbf{x}'|$ between the two points. These functions are such that $f_{mn}(0, \omega) = 1$.

The exponential factor appearing in equation (5) represents a deterministic spatial variation of ground motion due to wave passage. The form of this factor is based on the assumptions that: (i) the $x_1$-axis has been selected in the direction from the source to the site, (ii) the local variation of ground motion due to wave passage effects can be described by the simple phase shift for plane waves, and, (iii) the $U_{gm}$ component of motion is characterized by the apparent horizontal velocity $c_m$. The exponential factor appearing in equation (7) represents a correction for deterministic wave passage effects.

A major difficulty in the use of the characterization given by equation (5) is that the functional dependence of the coherence functions $f_{mn}$ on distance and frequency has not been fully established. Analyses of array data indicate that $f_{mm}$ $(m = 1, 2, 3)$ are decreasing functions of distance and also decreasing functions of frequency for frequencies above 1–2 Hz (Smith *et al.*,[5] King and Tucker,[7] Hoshiya and Ishii,[12] Harichandran and Vanmarcke[29]). Matsushima[28] and Hoshiya and Ishii[12] have suggested exponentially decreasing functions of distance for $f_{mn}$ and, in particular, Hoshiya and Ishii[12] have used the form $f_{mm} = \exp[-(a' + b'\omega)|\mathbf{x}-\mathbf{x}'|/\beta]$ in which $a'$ and $b'$ are constants and $\beta$ is a representative shear wave velocity in the soil. Harichandran and Vanmarcke[29] have found it necessary to use a weighted sum of two exponential functions. No information is available on the cross coherence functions $f_{mn}$ $(m \neq n)$. Given this uncertain situation, which will only be settled when sufficient data have accumulated, it is convenient to use as guidance the functional forms resulting from theoretical models. For (scalar) shear waves propagating a distance $H$ through a random medium, the coherence function is given by (Uscinski[30])

$$f(|\mathbf{x}-\mathbf{x}'|, \omega) = \exp\{-l[1 - \exp(-|\mathbf{x}-\mathbf{x}'|^2/r_0^2)]\} \tag{8}$$

where $r_0$ is the scale length of the random inhomogeneities along the path, and

$$l \approx \omega^2 r_0 H\mu^2/\beta^2 \tag{9}$$

in which $\beta$ is an estimate of the elastic wave velocity and $\mu^2$ is a measure of the relative variation of elastic properties. For $|\mathbf{x}-\mathbf{x}'| < r_0$, equation (8) can be approximated by

$$f(|\mathbf{x}-\mathbf{x}'|, \omega) = \exp[-(\gamma\omega|\mathbf{x}-\mathbf{x}'|/\beta)^2] \tag{10}$$

in which $\gamma = \mu(H/r_0)^{1/2}$. Crude comparisons with data indicate that $\gamma/\beta \sim (2-3)\times 10^{-4}\ \mathrm{m}^{-1}\,\mathrm{s}$ may be a reasonable value for this ratio. The numerical results presented below are based on the simplifying assumption $f_{mn} = f(m, n = 1, 2, 3)$ and on the use of the functional dependence given by equation (10).

The data on the correlation coefficients $\rho_{gmn}$ $(m \neq n; m, n = 1, 2, 3)$ are also scarce. Hadjian[31] has found that the orientation of axes which minimizes the correlation between two perpendicular horizontal components corresponds approximately to the source–station direction. For this orientation, the correlation between the azimuthal and vertical components is minimized while the correlation between the radial and vertical components is maximized.

## RESPONSE OF A FLAT RIGID FOUNDATION

To quantify the effects of the spatial variation of ground motion on the dynamic response of foundations, the case of a flat massless rigid foundation bonded to a uniform viscoelastic half-space is considered. The free-field ground motion is assumed to involve both deterministic and random variations with respect to space. The response of the rigid foundation, in the frequency domain, can be represented by the $6 \times 1$ generalized displacement vector

$$\{U_0^*(\omega)\} = (U_{01}^*, U_{02}^*, U_{03}^*, U_{04}^*, U_{05}^*, U_{06}^*)^T \tag{11}$$

where $(U_{01}^*, U_{02}^*, U_{03}^*)$ correspond to the three translational components of motion at a point of reference on the foundation and $(U_{04}^*, U_{05}^*, U_{06}^*) = (a\theta_{01}^*, a\theta_{02}^*, a\theta_{03}^*)$, in which $a$ is a characteristic length of the foundation, correspond to normalized rotations about the $x_1$-, $x_2$- and $x_3$-axes, respectively.

The deterministic relation between the response of the foundation $\{U_0^*\}$ and the free-field ground motion $\{U_g(\mathbf{x}, \omega)\}$ is given by the integral representation (Bycroft,[32] Luco[33,34])

$$\{U_0^*\} = [C(\omega)] \int_S [T(\mathbf{x})]^T \{U_g(\mathbf{x}, \omega)\}\, dS(\mathbf{x}) \tag{12}$$

valid for flat foundations in which $[C(\omega)]$ is the symmetric $6 \times 6$ compliance matrix for the foundation and $[T(\mathbf{x})]$ is a $3 \times 6$ traction matrix in which each column corresponds to the traction vector on the contact area $S$ between the foundation and the soil for unit rigid-body motions of the foundation in the order $(U_{01}, U_{02}, U_{03}, a\theta_{01}, a\theta_{02}, a\theta_{03})$. The matrix $[T(\mathbf{x})]$, which also depends on frequency, can be obtained by numerical solution of an integral equation as presented by Wong and Luco.[35] For later use it is convenient to write equation (12) in the form

$$U_{0p}^* = \sum_{m=1}^{3} \int_S F_{mp}(\mathbf{x}, \omega)\, U_{gm}(\mathbf{x})\, dS(\mathbf{x}) \qquad (p = 1, 2, \ldots, 6) \tag{13}$$

in which $F_{mp}$ $(m = 1, 2, 3;\ p = 1, 2, \ldots, 6)$ is an element of the $3 \times 6$ matrix $[F(\mathbf{x}, \omega)]$ defined by

$$[F] = [T(\mathbf{x})][C(\omega)] \tag{14}$$

Each column of the matrix $[F]$ corresponds to the traction vector at a point $\mathbf{x}$ on $S$ for unit generalized forces and moments applied to the rigid foundation in the order $(F_1, F_2, F_3, M_1/a, M_2/a, M_3/a)$.

The linear relation between the response of the foundation and the free-field motion given by equations (12) and (13), and the zero-mean assumption [equation (2)] for the free-field ground motion, indicate that

$$E[U_{0p}^*(\omega)] = 0 \qquad (p = 1, 2, \ldots, 6) \tag{15}$$

The second order characteristics of the response of the foundation are described by the covariance matrix

$$[A] = E[\{U_0^*\}\{\bar{U}_0^*\}^T] \tag{16}$$

which has for elements

$$A_{pq} = E[U_{0p}^* \bar{U}_{0q}^*] = \mu_{0p}^* \mu_{0q}^* \rho_{0pq}^* \qquad (p, q = 1, 2, \ldots, 6) \tag{17}$$

in which $\mu_{0p}^{*2}$ $(p = 1, 2, \ldots, 6)$ are the variances and $\rho_{0pq}^{*}$ $(p, q, = 1, 2, \ldots, 6)$ are the correlation coefficients $(\rho_{0pp}^{*} = 1, p = 1, 2, \ldots, 6)$.

Substitution from equations (13) and (4) into equation (17) leads to

$$\mu_{0p}^{*}\mu_{0q}^{*}\rho_{0pq}^{*} = \sum_{m=1}^{3}\sum_{n=1}^{3}\int_S\int_S F_{mp}(\mathbf{x}, \omega)B_{mn}(\mathbf{x}, \mathbf{x}', \omega)\bar{F}_{nq}(\mathbf{x}', \omega)\,dS(\mathbf{x})\,dS(\mathbf{x}') \tag{18}$$

which when combined with equation (5) results in

$$\mu_{0p}^{*2} = \sum_{m=1}^{3}\sum_{n=1}^{3} A_{mn}^{pp}(\omega)\mu_{gm}\mu_{gn}\rho_{gmn} \qquad (p = 1, 2, \ldots, 6) \tag{19}$$

and

$$\rho_{0pq}^{*} = \sum_{m=1}^{3}\sum_{n=1}^{3} A_{mn}^{pq}(\omega)\mu_{gm}\mu_{gn}\rho_{gmn}/\mu_{0p}^{*}\mu_{0q}^{*} \qquad (p \neq q;\ p, q = 1, 2, \ldots, 6) \tag{20}$$

in which

$$A_{mn}^{pq}(\omega) = \int_S\int_S F_{mp}(\mathbf{x}, \omega)\bar{F}_{nq}(\mathbf{x}', \omega)f_{mn}(|\mathbf{x} - \mathbf{x}'|, \omega) \times \exp\left[-i\omega(x_1/c_m - x_1'/c_n)\right]dS(\mathbf{x})\,dS(\mathbf{x}') \quad (p, q = 1, 2, \ldots, 6;\ m, n = 1, 2, 3) \tag{21}$$

are frequency dependent covariance coefficients. Equations (19) and (20) give the relation between the second order characteristics of the response of the foundation and the characteristics of the free-field ground motion. This relation involves the coefficients $A_{mn}^{pq}(\omega)$ $(p, q = 1, 2, \ldots, 6;\ m, n = 1, 2, 3)$ which also depend on the coherence functions $f_{mn}$, the apparent velocities $c_m$, the geometrical characteristics of the foundation and on the soil properties. From equation (21), and from the assumption that the functions $f_{mn}(|\mathbf{x} - \mathbf{x}'|, \omega) = f_{nm}(|\mathbf{x} - \mathbf{x}'|, \omega)$ are real, it can be shown that

$$A_{nm}^{qp} = \bar{A}_{mn}^{pq} \tag{22}$$

which indicates that these coefficients are Hermitian with respect to the subscripts $m$ and $n$ for $p = q$. For $m = n$ and $p = q$, the coefficients $A_{mn}^{pq}$ are real (and non-negative).

Given the properties of $A_{mn}^{pp}$, equation (19) can be written in the form

$$\mu_{0p}^{*2} = A_{11}^{pp}\mu_{g1}^2 + A_{22}^{pp}\mu_{g2}^2 + A_{33}^{pp}\mu_{g3}^2 + 2\,\mathrm{Re}\left[A_{12}^{pp}\rho_{g12}\right]\mu_{g1}\mu_{g2} + 2\,\mathrm{Re}\left[A_{23}^{pp}\rho_{g23}\right]\mu_{g2}\mu_{g3} + 2\,\mathrm{Re}\left[A_{31}^{pp}\rho_{g31}\right]\mu_{g3}\mu_{g1} \qquad (p = 1, 2, \ldots, 6) \tag{23}$$

which, as expected, reveals that $\mu_{0p}^2$ is real.

To illustrate the physical interpretation of the coefficients $A_{mn}^{pq}$ consider the case in which the free-field ground motion has only one non-zero component along the $x_1$-axis, i.e. $\{U_g\} = (U_{g1}, 0, 0)^T$. In this case, $\mu_{g1} \neq 0$, $\mu_{g2} = \mu_{g3} = 0$, and from equations (19) and (20) it is found that

$$\mu_{0p}^{*2}/\mu_{g1}^2 = A_{11}^{pp}(\omega) \qquad (p = 1, 2, \ldots, 6) \tag{24}$$

and

$$\rho_{0pq}^{*} = \frac{A_{11}^{pq}(\omega)}{\sqrt{A_{11}^{pp}}\sqrt{A_{11}^{qq}}} \qquad (p \neq q;\ p, q = 1, 2, \ldots, 6) \tag{25}$$

Equation (25) indicates that, in this case, $A_{11}^{pq}$ $(p \neq q)$ determine the correlation between the $p$- and $q$-components of the response of the foundation. Equation (24) indicates that $A_{11}^{pp}$ determines the amplitude of the $p$-component of the foundation response. In particular, if the free-field ground motion can be represented as a stationary random process with respect to time then $\mu_{g1}^2$ and $\mu_{0p}^{*2}$ can be interpreted as the power spectral density of the ground motion and of the $p$-component of the foundation response, respectively. In this case, equation (24) indicates that $A_{11}^{pp}$ represents the ratio of the power spectral density of the $p$-component of the foundation response to the power spectral density of the free-field ground motion. Similar interpretations can be given to the terms $A_{22}^{pp}$ and $A_{33}^{pp}$ by considering the cases $\{U_g\} = (0, U_{g2}, 0)^T$ and $\{U_g\} = (0, 0, U_{g3})^T$, respectively.

Equations (19) and (20) indicate that the terms $A_{mn}^{pq}$ for $m \neq n$ need to be calculated only if the corresponding free-field correlation coefficients $\rho_{gmn}$ are non-zero. The terms $A_{mn}^{pq}$ for $m \neq n$ are associated with the effect that the correlation between the $m$- and $n$-components of the free-field ground motion has on the response of the rigid foundation.

## ESTIMATES OF THE COVARIANCE COEFFICIENTS $A_{mn}^{pp}$

To gain insight into the characteristics of the covariance coefficients $A_{mn}^{pq}$ it is desirable to obtain simple approximate expressions for these coefficients. Such estimates can be obtained by approximating the actual contact tractions $[F]$ defined by equation (14) and appearing in equation (21) by linear functions of position. For a rectangular foundation ($-a < x_1 < a$, $-b < x_2 < b$, $x_3 = 0$), the approximation to $[F]$ is

$$[F]^T \approx \frac{1}{4ab} \begin{bmatrix} 1 & 0 & 0 \\ 0 & 1 & 0 \\ 0 & 0 & 1 \\ 0 & 0 & 3\left(\frac{a}{b}\right)^2\left(\frac{x_2}{a}\right) \\ 0 & 0 & -3\left(\frac{x_1}{a}\right) \\ -3\left(\frac{a^2}{a^2+b^2}\right)\left(\frac{x_2}{a}\right) & 3\left(\frac{a^2}{a^2+b^2}\right)\left(\frac{x_1}{a}\right) & 0 \end{bmatrix} \tag{26}$$

To obtain further simplicity it is assumed that $f_{mn} = f(m, n = 1, 2, 3)$ in which $f$ is the coherence function defined by equation (10). In addition, only terms up to second order in $(\gamma\omega a/\beta)$ and $(\omega a/c_m)$ $(m = 1, 2, 3)$ are

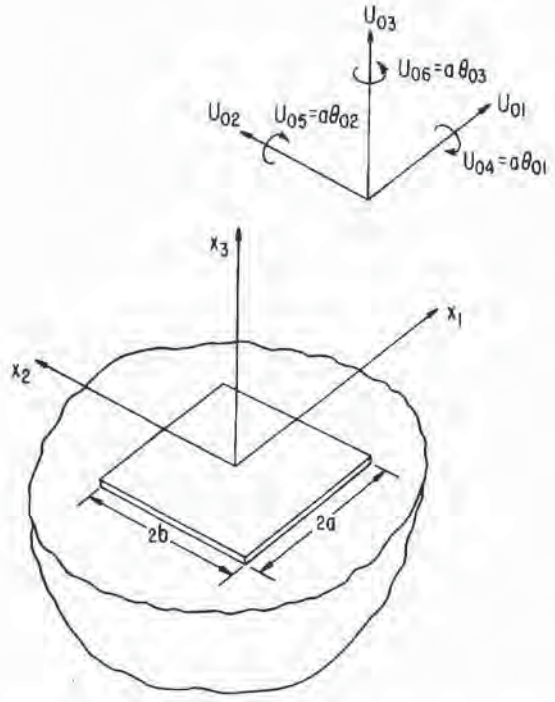


Figure 1. Description of the foundation and soil model, and coordinate systems

included. The resulting non-vanishing coefficients $A_{mn}^{pp}$ ($p = 1, 2, \ldots, 6$; $m, n = 1, 2, 3$) are

$$A_{11}^{11} = 1 - \frac{2}{3}\gamma^2\left(\frac{a^2+b^2}{a^2}\right)\left(\frac{\omega a}{\beta}\right)^2 - \frac{1}{3}\left(\frac{\omega a}{c_1}\right)^2 \tag{27}$$

$$A_{22}^{22} = 1 - \frac{2}{3}\gamma^2\left(\frac{a^2+b^2}{a^2}\right)\left(\frac{\omega a}{\beta}\right)^2 - \frac{1}{3}\left(\frac{\omega a}{c_2}\right)^2 \tag{28}$$

$$A_{33}^{33} = 1 - \frac{2}{3}\gamma^2\left(\frac{a^2+b^2}{a^2}\right)\left(\frac{\omega a}{\beta}\right)^2 - \frac{1}{3}\left(\frac{\omega a}{c_3}\right)^2 \tag{29}$$

$$A_{33}^{44} = 2\gamma^2\left(\frac{\omega a}{\beta}\right)^2 \tag{30}$$

$$A_{33}^{55} = 2\gamma^2\left(\frac{\omega a}{\beta}\right)^2 + \left(\frac{\omega a}{c_3}\right)^2 \tag{31}$$

$$A_{11}^{66} = 2\gamma^2\left(\frac{b^2}{a^2+b^2}\right)^2\left(\frac{\omega a}{\beta}\right)^2 \tag{32}$$

$$A_{22}^{66} = 2\gamma^2\left(\frac{a^2}{a^2+b^2}\right)^2\left(\frac{\omega a}{\beta}\right)^2 + \left(\frac{a^2}{a^2+b^2}\right)^2\left(\frac{\omega a}{c_2}\right)^2 \tag{33}$$

The corresponding estimates for the coupling covariance coefficients $A_{mn}^{pq}$ ($p \neq q$) are listed in the Appendix.

## NUMERICAL RESULTS FOR A SQUARE FOUNDATION

The covariance coefficients $A_{mn}^{pq}(\omega)$ defined by equation (21) ($p, q = 1, 2, \ldots, 6$; $m, n = 1, 2, 3$) for a massless rigid square foundation ($-a < x_1 < a$, $-a < x_2 < a$, $x_3 = 0$) bonded to a viscoelastic half-space have been calculated for a range of frequencies. The viscoelastic half-space was characterized by a Poisson's ratio $\nu = 1/3$ and by material damping ratios $\xi_s = \xi_p = 0{\cdot}01$ ($Q_s = Q_p = 50$). In the calculations it was assumed that the coherence functions were defined by $f_{mn} = f$ ($m, n = 1, 2, 3$) in which $f$ is the coherence function defined by equation (10). The contact tractions $F_{mp}(\mathbf{x}, \omega)$ ($m = 1, 2, 3$; $p = 1, 2, \ldots, 6$) appearing in equation (21) were obtained by numerical solution of the contact integral equations following a procedure similar to that described by Wong and Luco.[35] The foundation was discretized into 256 equal subregions, the contact tractions were assumed to be constant within each of the subregions and the displacement conditions were imposed on the average displacement in each subregion. The double integrals over the contact area $S$ of the resulting contact tractions were calculated by Gaussian quadrature. The covariance coefficients $A_{mn}^{pq}$ depend on the dimensionless parameters $\gamma$, $\beta/c_1$, $\beta/c_2$, $\beta/c_3$ and $a_0 = \omega a/\beta$ where $\beta$ is the (real) shear wave velocity in the half-space. In the calculations it was assumed that $\beta/c_1 = \beta/c_2 = \beta/c_3 = \beta/c$.

*Results for the variance (or power spectral density) of the response*

The case $\beta/c_1 = \beta/c_2 = \beta/c_3 = \beta/c = 0$ is considered first. In this case, $A_{mn}^{pp} = 0$ for $m \neq n$ and $p = 1, 2, \ldots, 6$. Based on this result, equation (23) can be written in the form

$$\mu_{0p}^{*2} = A_{11}^{pp}\,\mu_{g1}^2 + A_{22}^{pp}\mu_{g2}^2 + A_{33}^{pp}\,\mu_{g3}^2 \qquad (p = 1, 2, \ldots, 6) \tag{34}$$

which indicates that, in this case, the variance of the $p$-component of the response depends on the coefficients $A_{11}^{pp}$, $A_{22}^{pp}$ and $A_{33}^{pp}$.

Numerical values for the square root of the coefficients $A_{mm}^{pp}$ are shown in Figures 2 and 3 versus the dimensionless frequency $a_0 = \omega a/\beta$ for values of the incoherence parameter $\gamma = 0, 0{\cdot}1, 0{\cdot}2, 0{\cdot}3, 0{\cdot}4$ and $0{\cdot}5$. It is noted that $\sqrt{A_{mm}^{pp}}$ ($p = 1, 2, \ldots, 6$; $m = 1, 2, 3$) can be interpreted as the amplitude of a transfer function between the $m$-component of the excitation and the $p$-component of the response. Inspection of Figures 2(a), 2(b) and 2(c) for $p = 1$ indicates that the translational response along the $x_1$-axis is mostly associated with the component of the free-field excitation along the $x_1$-axis. The $x_2$- and $x_3$-components of the excitation induce

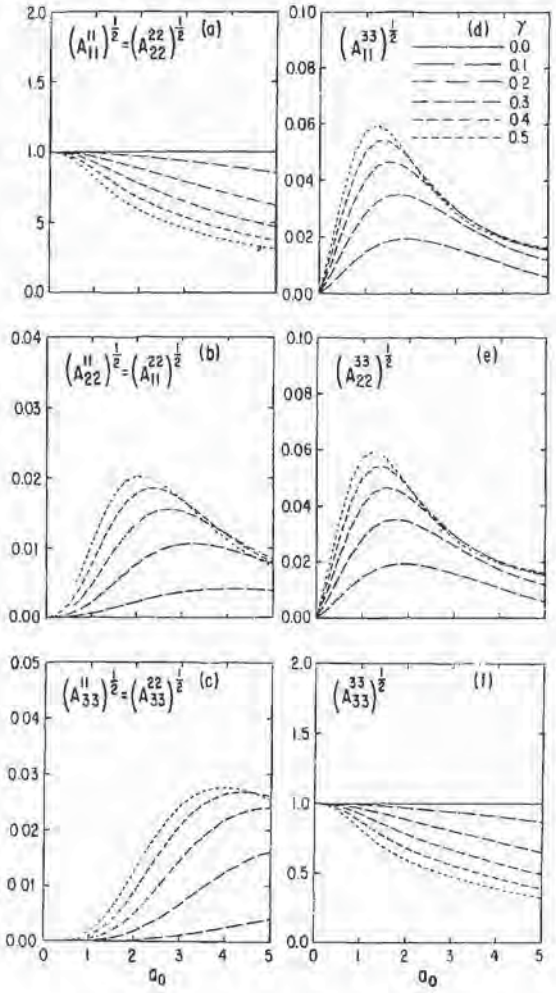


Figure 2. Square root of the covariance coefficients $A^{pp}_{mm}$ ($p = 1, 2, 3; m = 1, 2, 3$) for $\gamma = 0, 0{\cdot}1, 0{\cdot}2, 0{\cdot}3, 0{\cdot}4$ and $0{\cdot}5$ plotted versus $a_0 = \omega a/\beta$ ($\beta/c_1 = \beta/c_2 = \beta/c_3 = 0$)

extremely small responses in the $x_1$-direction [Figures 2(b) and 2(c)]. Given the symmetry of the square foundation, Figures 2(a), 2(b) and 2(c) also show that the translational response along the $x_2$-axis is mostly due to the $x_2$-component of the free-field excitation. Figures 2(d), 2(e) and 2(f) show that the dominant contribution to the translational response along the $x_3$-axis results from the $x_3$-component of the excitation. These results indicate that equation (34) for $p = 1$, 2 and 3 can be approximated by

$$\begin{aligned} \mu^{*2}_{01} &\approx A^{11}_{11}\,\mu^2_{g1} \\ \mu^{*2}_{02} &\approx A^{22}_{22}\,\mu^2_{g2} \\ \mu^{*2}_{03} &\approx A^{33}_{33}\,\mu^2_{g3} \end{aligned} \tag{35}$$

The most significant characteristic of the coefficients $A^{11}_{11} = A^{22}_{22}$ and $A^{33}_{33}$ is that they are decreasing functions of frequency for $\gamma \neq 0$. The reduction at a given frequency increases with the degree of incoherence of the free-field ground motion as measured by the parameter $\gamma$. This result indicates that the variance (or the power spectral density) of the translational response components can be lower than the variance (or power spectral density) of the corresponding component of the free-field ground motion. This loss of power is due to the kinematic constraint imposed by the rigid foundation. The extent of the loss of power depends on $\gamma$ and $a_0$

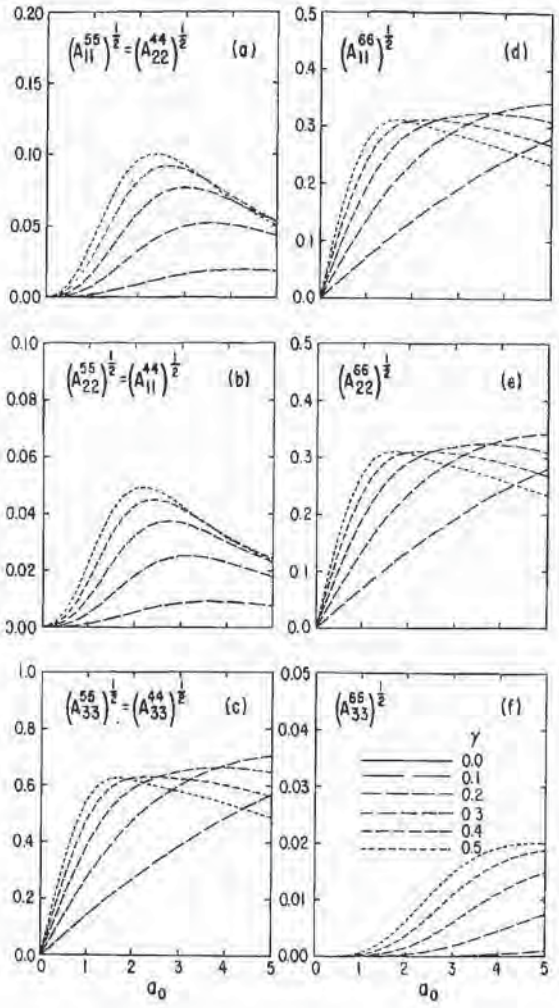


Figure 3. Square root of the covariance coefficients $A_{mm}^{pp}$ ($p = 4, 5, 6; m = 1, 2, 3$) for $\gamma = 0, 0{\cdot}1, 0{\cdot}2, 0{\cdot}3, 0{\cdot}4$ and $0{\cdot}5$ plotted versus $a_0 = \omega a/\beta$ ($\beta/c_1 = \beta/c_2 = \beta/c_3 = 0$)

$= \omega a/\beta$. For low values of $a_0$ and $\gamma$, the coefficients $A_{11}^{11} = A_{22}^{22}$ and $A_{33}^{33}$ can be approximated by the expressions given by equations (27), (28) and (29), respectively.

The square root of the coefficients $A_{mm}^{55} = A_{mm}^{44}$ and $A_{mm}^{66}$ ($m = 1,2,3$) associated with the rotational components of the foundation response are shown in Figure 3. The term $\sqrt{A_{mm}^{55}}$ can be interpreted as the amplitude of the transfer function between $U_{gm}$, the $m$-component of the free-field ground motion, and $U_{05}^* = a\theta_{02}^*$, the normalized rocking response about the $x_2$-axis. The terms $\sqrt{A_{mm}^{44}}$ and $\sqrt{A_{mm}^{66}}$ have similar interpretations. The results in Figure 3 indicate that the rocking responses about the $x_1$ and $x_2$-axis are mostly associated with the vertical component of the free-field ground motion, while the torsional response about the $x_3$-axis is associated with the $x_1$ and $x_2$-components of the ground motion. Given these results, equation (34) for $p = 4$, 5 and 6 can be approximated by

$$\begin{aligned} \mu_{04}^{*2} &\approx A_{33}^{44}\mu_{g3}^2 \\ \mu_{05}^{*2} &\approx A_{33}^{55}\mu_{g3}^2 \\ \mu_{06}^{*2} &\approx A_{11}^{66}\mu_{g1}^2 + A_{22}^{66}\mu_{g2}^2 \end{aligned} \tag{36}$$

The rotational response components induced by the spatial variation of the ground motion are quite large, and, at least for low frequencies, increase with frequency and with the degree of incoherence of the ground motion as measured by $\gamma$. For low values of $a_0$ and $\gamma$, the expressions given by equations (30), (31), (32) and (33) are good approximations to $A_{33}^{44}$, $A_{33}^{55}$, $A_{11}^{66}$ and $A_{22}^{66}$.

The effects of spatial randomness and wave passage on the response of rigid foundations are qualitatively similar in that both involve a reduction in the translational response of the foundation together with the creation of rocking and torsional response components. A more detailed comparison can be made by inspection of the results in Figures 2 and 3 for $\beta/c_1 = \beta/c_2 = \beta/c_3 = \beta/c = 0$ and $\gamma \neq 0$ with those in Figure 4 for $\gamma = 0$ and $\beta/c = 0, 0{\cdot}1, 0{\cdot}2, 0{\cdot}3, 0{\cdot}4$ and $0{\cdot}5$. The results in Figure 4 are for waves propagating along the $x_1$-axis with apparent velocity $c$. The most significant differences are that, while under spatial randomness both the $x_1$- and $x_2$-components of the excitation generate torsional response ($A_{11}^{66} = A_{22}^{66} \neq 0$ for $\gamma \neq 0$) and the vertical component induces rocking about both the $x_1$- and $x_2$-axes ($A_{33}^{44} = A_{33}^{55} \neq 0$ for $\gamma \neq 0$), for wave passage in the $x_1$-direction only the $x_2$-component of the ground motion induces torsion ($A_{22}^{66} \neq 0$, $A_{11}^{66} = 0$ for $\beta/c \neq 0$) and the vertical component induces rocking only about the $x_2$-axis ($A_{33}^{55} \neq 0$, $A_{33}^{44} = 0$ for $\beta/c = 0$).

The case in which random spatial variation and wave passage effects occur simultaneously is considered next. The wave passage effects are for propagation in the direction of the $x_1$-axis with apparent velocities $c_1/\beta = c_2/\beta = c_3/\beta = c/\beta$. In this case, $A_{12}^{pp} = \bar{A}_{21}^{pp} = 0$ and $A_{23}^{pp} = \bar{A}_{32}^{pp} = 0$ for $p = 1, 2, \ldots, 6$. Consequently,

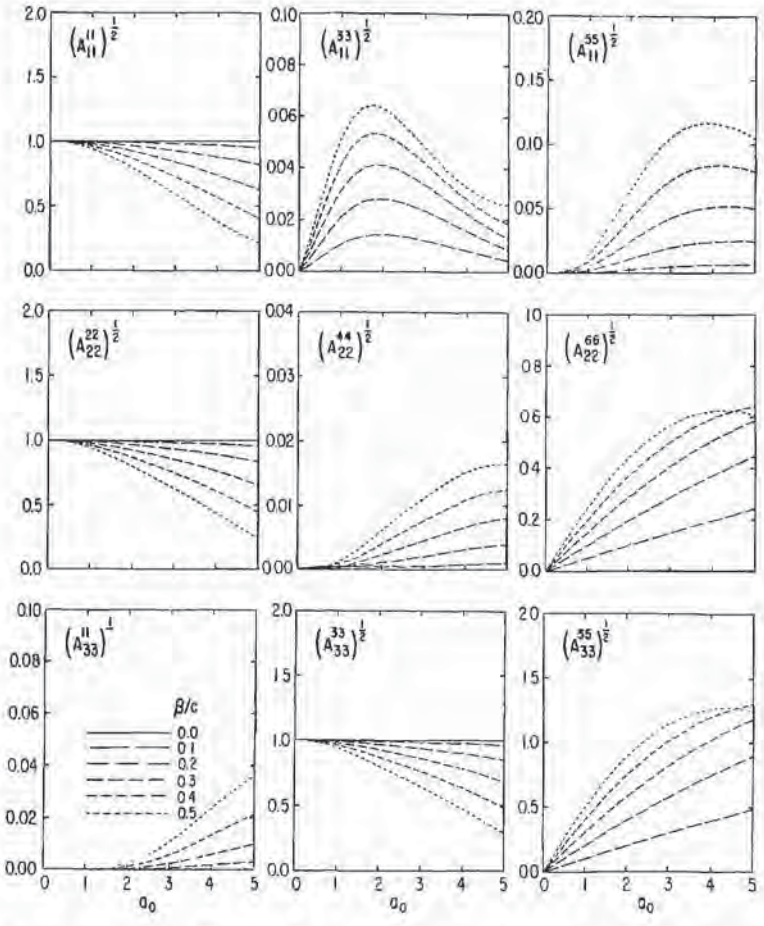


Figure 4. Square root of the non-vanishing coefficients $A_{mm}^{pp}$ ($p = 1, 2, \ldots, 6$; $m = 1, 2, 3$) for $\gamma = 0$ and $\beta/c = 0, 0{\cdot}1, 0{\cdot}2, 0{\cdot}3, 0{\cdot}4$, and $0{\cdot}5$ plotted versus $a_0 = \omega a/\beta$ ($\beta/c_1 = \beta/c_2 = \beta/c_3 = \beta/c$)

equation (23) can be written in the form

$$\mu_{0p}^{*2} = A_{11}^{pp}\mu_{g1}^2 + A_{22}^{pp}\mu_{g2}^2 + A_{33}^{pp}\mu_{g3}^2 + 2\,\mathrm{Re}\,[A_{13}^{pp}\rho_{g13}]\mu_{g1}\mu_{g3} \qquad (p = 1, 2, \ldots, 6) \tag{37}$$

which differs from equation (34) for the case $\beta/c = 0$ by the presence of the last term. This term makes $\mu_{0p}^{*2}$ dependent on the correlation $\rho_{g13}$ between the $x_1$- and $x_3$-components of the free-field ground motion. Calculation of the terms $A_{13}^{pp}$ $(p = 1, 2, \ldots, 6)$ for $\beta/c = 0{\cdot}1$ and $\gamma = 0, 0{\cdot}1, 0{\cdot}2, 0{\cdot}3, 0{\cdot}4$ and $0{\cdot}5$ shows that these terms are much smaller than the corresponding dominant terms $A_{11}^{11}$, $A_{22}^{22}$, $A_{33}^{33}$, $A_{33}^{44}$, $A_{33}^{55}$, $A_{11}^{66}$ and $A_{22}^{66}$, and consequently the contribution of the last term in equation (37) is small.

Comparison of the terms $A_{mm}^{pp}$ $(p = 1, 2, \ldots, 6; m = 1, 2, 3)$ for $\beta/c = 0{\cdot}1$ with those for $\beta/c = 0$ for $\gamma = 0, 0{\cdot}1, 0{\cdot}2, 0{\cdot}3, 0{\cdot}4$ and $0{\cdot}5$ indicates that the additional effects due to wave passage are significant for $\gamma = 0$ and $\gamma = 0{\cdot}1$, small for $\gamma = 0{\cdot}2$, and negligible for $\gamma = 0{\cdot}3, 0{\cdot}4$ and $0{\cdot}5$. For small values of $a_0$, $\gamma$ and $\beta/c$ the combination of the two effects is well described by equations (27) to (33).

*Results for the correlation between the components of the response*

The correlation between the $p$- and $q$-components of the response of the foundation given by equation (20) involves the coefficients $A_{mn}^{pq}$ $(p \neq q; p, q = 1, 2, \ldots, 6; m, n = 1, 2, 3)$. These coefficients have been calculated for various values of $\gamma$ and $\beta/c$. Given the large number of such coefficients it is possible to describe the properties of only a few. As an example, consider the case of a square foundation $(a = b)$, $\beta/c_1 = \beta/c_2 = \beta/c_3 = 0$ and $\rho_{g13} = \tilde{\rho}_{g31} \neq 0$ while all other correlation coefficients of the free-field ground motion are zero. In this case, the non-zero correlation coefficients of the response given by equation (20) are

$$\begin{aligned}
\rho_{013}^{*} &= \tilde{\rho}_{031}^{*} = (A_{13}^{13}\rho_{g13} + A_{31}^{13}\rho_{g31})\mu_{g1}\mu_{g3}/\mu_{01}^{*}\mu_{03}^{*} \\
\rho_{015}^{*} &= \tilde{\rho}_{051}^{*} = (A_{11}^{15}\mu_{g1}^2 + A_{22}^{15}\mu_{g2}^2 + A_{33}^{15}\mu_{g3}^2)/\mu_{01}^{*}\mu_{05}^{*} \\
\rho_{024}^{*} &= \tilde{\rho}_{042}^{*} = (A_{11}^{24}\mu_{g1}^2 + A_{22}^{24}\mu_{g2}^2 + A_{33}^{24}\mu_{g3}^2)/\mu_{02}^{*}\mu_{04}^{*} \\
\rho_{026}^{*} &= \tilde{\rho}_{062}^{*} = (A_{13}^{26}\rho_{g13} + A_{31}^{26}\rho_{g31})\mu_{g1}\mu_{g3}/\mu_{02}^{*}\mu_{06}^{*} \\
\rho_{035}^{*} &= \tilde{\rho}_{053}^{*} = (A_{13}^{35}\rho_{g13} + A_{31}^{35}\rho_{g31})\mu_{g1}\mu_{g3}/\mu_{03}^{*}\mu_{05}^{*} \\
\rho_{046}^{*} &= \tilde{\rho}_{064}^{*} = (A_{13}^{46}\rho_{g13} + A_{31}^{46}\rho_{g31})\mu_{g1}\mu_{g3}/\mu_{04}^{*}\mu_{06}^{*}
\end{aligned} \tag{38}$$

in which $\mu_{0p}^{*}$ $(p = 1, 2, \ldots, 6)$ are given by equation (34). For a square foundation and $\beta/c = 0$, $A_{11}^{24} = -A_{22}^{15}$, $A_{22}^{24} = -A_{11}^{15}$, $A_{33}^{24} = -A_{33}^{15}$ and $\rho_{015}^{*} = -\rho_{024}^{*}$.

The numerical values for the real and imaginary parts of $A_{mn}^{pq}$ $(p \neq q)$ presented in Figures 5, 6 and 7 have been divided by $\left[\sum_{l=1}^{3} A_{ll}^{pp}\right]^{1/2} \cdot \left[\sum_{l=1}^{3} A_{ll}^{qq}\right]^{1/2}$ and are shown versus the dimensionless frequency $a_0$ for five values of $\gamma$. The amplitudes of the normalized terms $A_{11}^{15}$, $A_{22}^{15}$ and $A_{33}^{15}$ shown in Figure 5 are small suggesting that $\rho_{015}^{*} = -\rho_{024}^{*} \approx 0$. The results for $A_{13}^{13}$ and $A_{31}^{13}$ presented in Figure 6 and equation (38) indicate that $\rho_{013}^{*} \approx \rho_{g13}$ while the values for the normalized coefficients $A_{13}^{46}$ and $A_{31}^{46}$ shown in Figure 7 and equation (38) indicate that $\rho_{046}^{*} \approx -0{\cdot}707\,\rho_{g31}$ for $\mu_{g1} \approx \mu_{g2}$. Finally, the calculated values for $A_{13}^{26}$, $A_{31}^{26}$, $A_{13}^{35}$ and $A_{31}^{35}$ (not shown) reveal that $\rho_{026}^{*} \approx 0$ and $\rho_{035}^{*} \approx 0$. These characteristics are consistent with the estimates for $\rho_{0pq}^{*}$ $(p \neq q)$ presented in the Appendix.

When the wave passage and spatial randomness effects are considered simultaneously $(\beta/c \neq 0, \gamma \neq 0)$, the correlation coefficients for the response $\rho_{0pq}^{*}$ differ from those for the case $\beta/c = 0$ and $\gamma \neq 0$. In particular, for the case in which $\rho_{g13} = \tilde{\rho}_{g31} \neq 0$ while all other correlation coefficients of the free-field ground motion are zero, the non-zero correlation coefficients of the response are given by

$$\rho_{0mn}^{*} = [A_{11}^{mn}\mu_{g1}^2 + A_{22}^{mn}\mu_{g2}^2 + A_{33}^{mn}\mu_{g3}^2 + (A_{13}^{mn}\rho_{g13} + A_{31}^{mn}\rho_{g31})\mu_{g1}\mu_{g3}]/\mu_{0m}^{*}\mu_{0n}^{*} \tag{39}$$

for the combinations of $(m, n) = (1, 3), (1, 5), (2, 4), (2, 6), (3, 5)$ and $(4, 6)$ and its reciprocals. These expressions differ from equation (38) for $\beta/c = 0$. Approximate expressions for $\rho_{0mn}^{*}$ for $\gamma \neq 0$ and $\beta/c \neq 0$ are given in the Appendix.

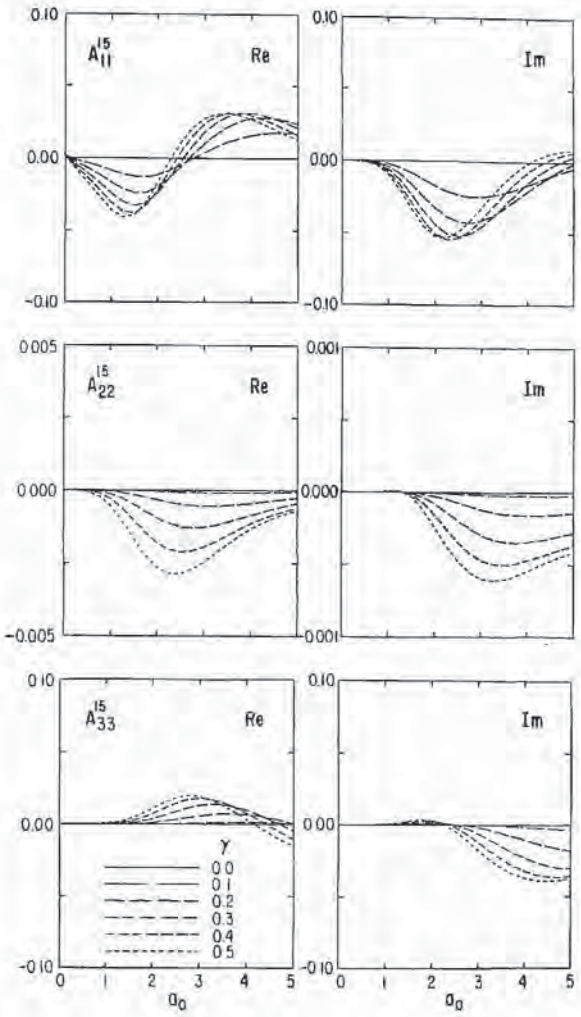


Figure 5. Real and imaginary parts of the normalized coefficients $A_{11}^{15}$, $A_{22}^{15}$ and $A_{33}^{15}$ for $\gamma = 0{\cdot}1, 0{\cdot}2, 0{\cdot}3, 0{\cdot}4$ and $0{\cdot}5$ plotted versus $a_0 = \omega a/\beta$ ($\beta/c_1 = \beta/c_2 = \beta/c_3 = 0$). The results are normalized by $\left[\left(\sum_{m=1}^{3} A_{mm}^{11}\right)\left(\sum_{m=1}^{3} A_{mm}^{55}\right)\right]^{1/2}$

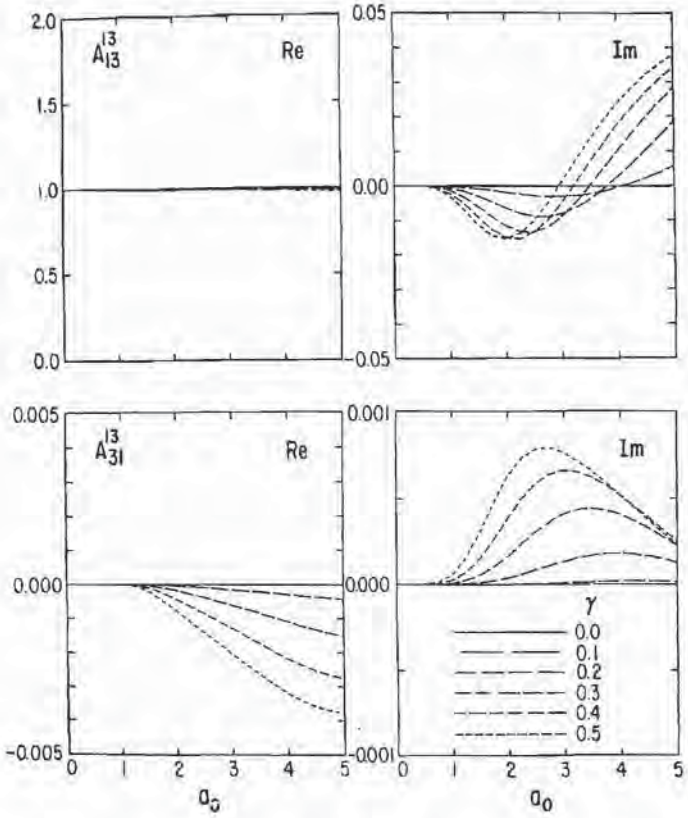


Figure 6. Real and imaginary parts of the normalized coefficients $A_{13}^{13}$ and $A_{31}^{13}$ for $\gamma = 0{\cdot}1, 0{\cdot}2, 0{\cdot}3, 0{\cdot}4$ and $0{\cdot}5$ plotted versus $a_0 = \omega a/\beta$ ($\beta/c_1 = \beta/c_2 = \beta/c_3 = 0$). The results are normalized by $\left[\left(\sum_{m=1}^{3} A_{mm}^{11}\right)\left(\sum_{m=1}^{3} A_{mm}^{33}\right)\right]^{1/2}$

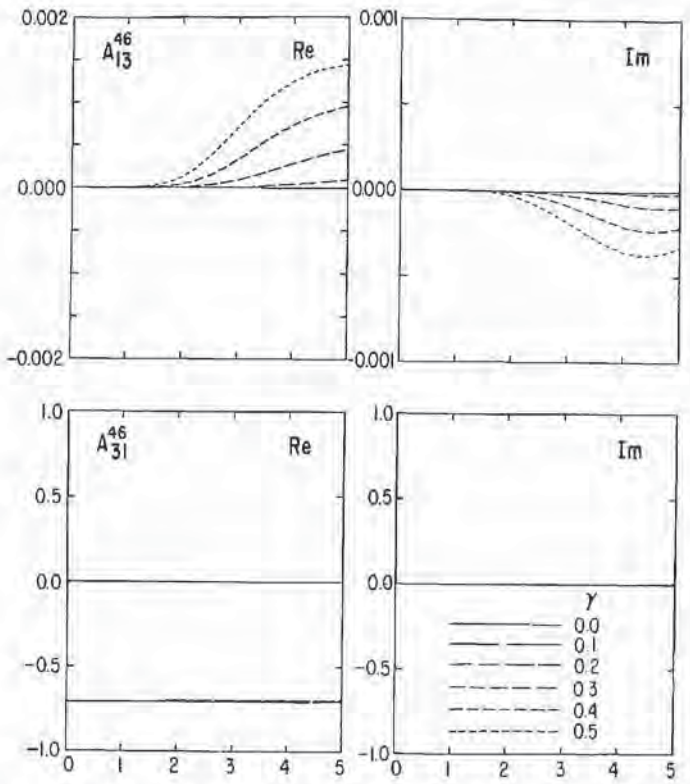


Figure 7. Real and imaginary parts of the normalized coefficients $A_{13}^{46}$ and $A_{31}^{46}$ for $\gamma = 0{\cdot}1, 0{\cdot}2, 0{\cdot}3, 0{\cdot}4$ and $0{\cdot}5$ plotted versus $a_0 = \omega a/\beta$ $(\beta/c_1 = \beta/c_2 = \beta/c_3 = 0)$. The results are normalized by $\left[\left(\sum_{m=1}^{3} A_{mm}^{44}\right)\left(\sum_{m=1}^{3} A_{mm}^{66}\right)\right]^{1/2}$

## EFFECTIVE APPARENT VELOCITY

It has been mentioned that the effects of wave passage and spatial randomness on the response of rigid foundations are qualitatively similar. Two questions of interest arise: (i) which of the two effects is stronger, and (ii) is it possible to find an effective apparent velocity such that the corresponding wave passage effects mimic the spatial randomness effects for a given spatial incoherence? Consider first the coefficients $A_{pp}^{pp}(\gamma, \beta/c_p, \omega)$ $(p = 1,2,3)$ which control the translational response of the foundation. The effective apparent velocity $c_p$ along the $x_1$-axis of the $p$-component of free-field motion can be defined by

$$A_{pp}^{pp}(0, \beta/c_p, \omega) = A_{pp}^{pp}(\gamma, 0, \omega) \quad (p = 1,2,3) \tag{40}$$

Based on the estimates of $A_{pp}^{pp}$ for rectangular foundations given by equations (27), (28) and (29) it is found that

$$\frac{\beta}{c_p} = \sqrt{2}\sqrt{\left(\frac{a^2+b^2}{a^2}\right)}\gamma \qquad (p = 1,2,3) \tag{41}$$

valid for small values of $(\gamma\omega a/\beta)$ and $(\omega a/c_p)$. For a square foundation $(a = b)$, the estimate given by equation (41) leads to $\beta/c_p = 2\gamma$. The effective apparent velocity $c_2$ based on equation (40) for $p = 2$ and on the results presented in Figures 2 and 4 is shown in Figure 8(a) versus the incoherence parameter $\gamma$ for different values of $a_0 = \omega a/\beta$. For $a_0 \leqslant 2$ or $\gamma < 0{\cdot}15$, the approximation $\beta/c_2 = 2\gamma$ appears to give excellent results. The effective velocities $c_1$ and $c_3$ based on equation (40) for $p = 1$ and 3, respectively, have values similar to $c_2$.

The apparent velocity $c_2$ necessary to produce an equivalent torsional effect can be defined by

$$A_{22}^{66}(0, \beta/c_2, \omega)\mu_{g2}^2 = A_{11}^{66}(\gamma, 0, \omega)\mu_{g1}^2 + A_{22}^{66}(\gamma, 0, \omega)\mu_{g2}^2 \tag{42}$$

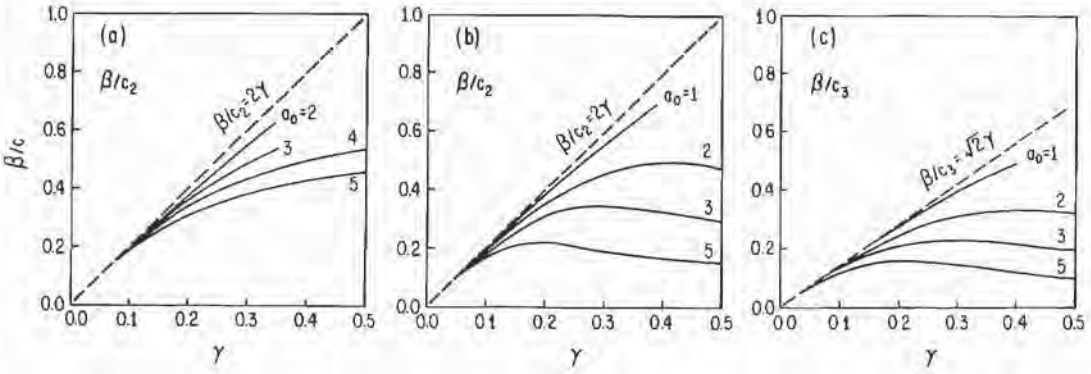


Figure 8. Effective apparent velocities along the $x_1$-axis for a square foundation subjected to a random free-field ground motion with spatial incoherence parameter $\gamma$: (a) $\beta/c_2$ based on translational response along $x_2$-axis; (b) $\beta/c_2$ based on torsional response about $x_3$-axis; and (c) $\beta/c_3$ based on rocking about $x_2$-axis

To eliminate $\mu_{g1}, \mu_{g2}$ from the definition of the effective velocity $c_2$, it is convenient to assume that $\mu_{g1}^2 = \mu_{g2}^2$, in which case

$$A_{22}^{66}(0, \beta/c_2, \omega) = A_{11}^{66}(\gamma, 0, \omega) + A_{22}^{66}(\gamma, 0, \omega) \tag{43}$$

Based on the estimates for $A_{11}^{66}$ and $A_{22}^{66}$ for a rectangular formation given by equation (32) and (33) it can be shown that equation (43) leads to

$$\beta/c_2 = \sqrt{2}\sqrt{\left(\frac{a^4+b^4}{a^4}\right)\gamma} \tag{44}$$

valid for small values of $(\gamma\omega a/\beta)$ and $(\omega a/c_2)$. For a square foundation, $\beta/c_2 = 2\gamma$, which coincides with the effective velocity based on the $x_2$-component of the translational response. The values of the ratio $\beta/c_2$ based on the equivalence given by equation (43) and on the results presented in Figures 3 and 4 for a square foundation are shown in Figure 8(b) versus the incoherence parameter $\gamma$ for various values of $a_0$. For $a_0 < 1$ or $\gamma < 0{\cdot}1$, the approximation $\beta/c_2 = 2\gamma$ appears to give excellent results.

Finally, the apparent velocity $c_3$ along the $x_1$-axis of the $x_3$-component of free-field ground motion necessary to generate the same rocking response about the $x_2$-axis can be defined by

$$A_{33}^{55}(0, \beta/c_3, \omega) = A_{33}^{55}(\gamma, 0, \omega) \tag{45}$$

Values of the ratio $\beta/c_3$ for a square foundation are shown in Figure 8(c) versus $\gamma$ for various values of $a_0$. In this case, the approximation $\beta/c_3 = \sqrt{2}\gamma$ based on the estimate given by equation (31) appears to be valid for $a_0 < 1$ or $\gamma < 0{\cdot}1$.

The previous results indicate that wave passage with velocities $c_1 = c_2 = c_3 = (\beta/2\gamma)$ along the $x_1$-axis produces effects on the variance (or power spectral density) of the translational and torsional response of the foundation similar to those resulting from spatial randomness with parameter $\gamma$. This choice of the effective apparent velocity $c_3$ leads to overestimation of the rocking response about the $x_2$-axis. On the other hand, wave passage along the $x_1$-axis does not excite a rocking response about the $x_1$-axis, while the spatially random vertical free-field component does create a significant rocking component about that axis. The partial equivalence just discussed gives a rational basis to compare the importance of the wave passage and spatial randomness effects. In general, if $c > \beta/2\gamma$ then the spatial randomness effects are stronger than the wave passage effects. Based on the limited information available it appears that $\gamma/\beta \sim (2\text{–}3) \times 10^{-4}$ m$^{-1}$ sec, leading to $\beta/2\gamma \sim (1{\cdot}7\text{–}2{\cdot}5)$ km/s. Analyses of array data (Tamura *et al.*,[1] Tsuchida *et al.*,[2] O'Rourke *et al.*,[36] O'Rourke and Dobry,[37] Spudich and Cranswick,[38] Harichandran and Vanmarcke[29]) as well as theoretical analyses (Luco and Sotiropoulos,[24] Hadjian and Hadley,[39] Bouchon and Aki,[40] Campillo and Bouchon,[41]) suggest that the apparent horizontal velocity $c$ in the source–site direction for the predominant motion is in the range $c$

$\sim$ (2–5) km/s. Based on limited data it appears that the effects of wave passage and spatial randomness on the response of rigid foundations are of comparable importance with the spatial randomness effects being perhaps slightly stronger.

## SOIL–STRUCTURE INTERACTION EFFECTS

The previous discussion considered a rigid massless foundation in the absence of a superstructure. If the mass of the foundation and the presence of the superstructure are considered, then the $6 \times 1$ generalized total displacement vector $\{U_0(\omega)\}$, in the frequency domain, at a point of reference on the foundation can be related to the foundation input motion $\{U_0^*\}$ (defined as the response of the massless foundation to the seismic excitation) through the equation (Luco and Wong[22])

$$\{U_0\} = [L(\omega)]\{U_0^*\} \tag{46}$$

in which

$$[L(\omega)] = ([I] - \omega^2 [C(\omega)]([M_0] + [M_b(\omega)]))^{-1} \tag{47}$$

where $[I]$ is the $6 \times 6$ identity matrix, $[C(\omega)]$ is the compliance matrix, $[M_0]$ is the mass matrix for the foundation and $[M_b(\omega)]$ is an equivalent frequency-dependent mass matrix for the superstructure.

From equations (46) and (16) it is found that $E[\{U_0\}] = 0$. The second order characteristics of the total response of the foundation are given by the covariance matrix

$$E[\{U_0\}\{\bar{U}_0\}^T] = [L(\omega)][A][\bar{L}(\omega)]^T \tag{48}$$

in which $[A]$ is the covariance matrix of the foundation input motion $\{U_0^*\}$ defined by equations (16), (17), (19), (20) and (21). Equation (48) and similar expressions for the superstructure can be used to obtain the effects of spatial randomness on the total response of the foundation and on the response of the superstructure.

## CONCLUSIONS

A method to obtain the dynamic response of a massless rigid foundation bonded to a viscoelastic half-space when subjected to a spatially varying ground motion including both random and deterministic effects has been presented. The method relies on an integral representation of the response of the foundation in terms of the free-field ground motion and the contact tractions for rigid-body motions of the foundation. The formulation involves a representation of the random spatial variation of the ground motion in terms of a coherence function and considers a possible correlation between the three components of the free-field ground motion. Numerical results describing the effects of random spatial variation of ground motion on the six components of the foundation response and on the correlation between response components have been presented for a square rigid foundation and for a particular spatial coherence function. Approximate analytical expressions describing these effects have been presented as well. The results obtained indicate that the spatial randomness of the ground motion produces effects similar to the deterministic effects of wave passage including reduction of the translational components of the response at high frequencies and creation of rocking and torsional response components. The extent of the effects is highly dependent on the degree of spatial incoherence of the free-field ground motion. The effects of random spatial variation and wave passage are additive (in a sense) only for small spatial incoherence and small apparent slowness of the wave. If the spatial incoherence is large the additional effect of wave passage is extremely small.

The possibility of defining an effective apparent horizontal velocity which would produce effects similar to those from a given random spatial variation was explored. It was found that it is not possible to find a unique effective velocity that would produce similarity of effects on all components of the response. For low frequencies and small spatial incoherence an effective apparent velocity was found for which the effects on the variance (or power spectral densities) of the three components of the translational response and the torsional response are similar. Since the effective apparent velocities appear to be similar or somewhat lower than

observed apparent velocities it appears that the effects of spatial randomness are of the same order or somewhat stronger than those resulting from wave passage.

Finally, the basic equations required to incorporate the effects of the mass of the foundations as well as those resulting from the presence of a superstructure were presented.

The numerical results obtained which show a strong dependency on the extent of the incoherence of the free-field ground motion suggest that practical applications of these results must wait until empirical data on the degree of incoherence and on its dependence on site and path conditions is fully established.

ACKNOWLEDGEMENT

The work described here has been supported by Grant ECE-83 12441 from the National Science Foundation.

## APPENDIX

Approximate expressions for the coupling coefficients $A_{mn}^{pq}$ ($p \neq q$; $p, q = 1, 2, \ldots, 6$; $m, n = 1,2,3$) defined by equation (21) and for the correlation coefficients $\rho_{0pq}^{*}$ ($p \neq q$) defined by equation (20) are given in this Appendix. The estimates for a rectangular foundation ($-a < x_1 < a$, $-b < x_2 < b$, $x_3 = 0$) are based on the linear approximation to $[F]$ given by equation (26), assuming that $f_{mn} = f$ ($m, n = 1,2,3$) in which $f$ is the coherence function defined by equation (10) and including only up to second order terms in $(\gamma\omega a/\beta)$ and $(\omega a/c_m)$ ($m = 1,2,3$). The resulting approximations to the non-vanishing coupling terms $A_{mn}^{pq}$ ($p \neq q$) are

$$A_{12}^{12} = 1 - \frac{2}{3}\gamma^2\left(\frac{a^2+b^2}{a^2}\right)\left(\frac{\omega a}{\beta}\right) - \frac{1}{6}\left[\left(\frac{\omega a}{c_1}\right)^2 + \left(\frac{\omega a}{c_2}\right)^2\right]$$

$$A_{13}^{13} = 1 - \frac{2}{3}\gamma^2\left(\frac{a^2+b^2}{a^2}\right)\left(\frac{\omega a}{\beta}\right)^2 - \frac{1}{6}\left[\left(\frac{\omega a}{c_1}\right) + \left(\frac{\omega a}{c_3}\right)^2\right]$$

$$A_{13}^{15} = -(i/2)(\omega a/c_3)$$

$$A_{12}^{16} = (i/2)[a^2/(a^2+b^2)]\,(\omega a/c_2) \tag{A1}$$

$$A_{21}^{21} = \bar{A}_{12}^{12}$$

$$A_{23}^{23} = 1 - \frac{2}{3}\gamma^2\left(\frac{a^2+b^2}{a^2}\right)\left(\frac{\omega a}{\beta}\right)^2 - \frac{1}{6}\left[\left(\frac{\omega a}{c_2}\right)^2 + \left(\frac{\omega a}{c_3}\right)^2\right]$$

$$A_{23}^{25} = -(i/2)\,(\omega a/c_3)$$

$$A_{22}^{26} = (i/2)[a^2/(a^2+b^2)]\,(\omega a/c_2) \tag{A2}$$

$$A_{31}^{31} = \bar{A}_{13}^{13}, \quad A_{32}^{32} = \bar{A}_{23}^{23}$$

$$A_{33}^{35} = -(i/2)\,(\omega a/c_3)$$

$$A_{32}^{36} = (i/2)\,[a^2/(a^2+b^2)]\,(\omega a/c_2) \tag{A3}$$

$$A_{31}^{46} = -2\gamma^2[b^2/(a^2+b^2)]\,(\omega a/\beta)^2 \tag{A4}$$

$$A_{31}^{51} = \bar{A}_{13}^{15}, \quad A_{32}^{52} = \bar{A}_{23}^{25}, \quad A_{33}^{53} = \bar{A}_{33}^{35}$$

$$A_{32}^{56} = -\left(\frac{a^2}{a^2+b^2}\right)\left[2\gamma^2\left(\frac{\omega a}{\beta}\right)^2 + \frac{(\omega a)^2}{c_2 c_3}\right] \tag{A5}$$

$$A_{21}^{61} = \bar{A}_{12}^{16}, A_{22}^{62} = \bar{A}_{22}^{26}, A_{23}^{63} = \bar{A}_{32}^{36}$$

$$A_{13}^{64} = \bar{A}_{31}^{46}, \quad A_{23}^{65} = \bar{A}_{32}^{56} \tag{A6}$$

The estimates of the correlation coefficients $\rho_{0pq}^{*}$ ($p \neq q$; $p, q = 1, 2, \ldots, 6$) between the $p$- and $q$-

components of the response of the foundation are

$$\rho^*_{012} = \rho_{g12}, \quad \rho^*_{013} = \rho_{g13}, \quad \rho^*_{014} = 0$$

$$\rho^*_{015} = -\left(\frac{i}{2}\right)\frac{(\beta/c_3)}{\sqrt{[(\beta/c_3)^2 + 2\gamma^2]}\sqrt{A^{11}_{11}}}\rho_{g13}$$

$$\rho^*_{016} = \left(\frac{i}{2}\right)\frac{(\beta/c_2)a^2\mu_{g2}}{g(\beta/c_2, \gamma, \mu_{g1}, \mu_{g2})\sqrt{A^{11}_{11}}}\rho_{g12} \tag{A7}$$

$$\rho^*_{021} = \rho_{g21}, \rho^*_{023} = \rho_{g23}, \quad \rho^*_{024} = 0$$

$$\rho^*_{025} = -\left(\frac{i}{2}\right)\frac{(\beta/c_3)}{\sqrt{[(\beta/c_3)^2 + 2\gamma^2]}\sqrt{A^{22}_{22}}}\rho_{g23}$$

$$\rho^*_{026} = \left(\frac{i}{2}\right)\frac{(\beta/c_2)a^2\mu_{g2}}{g(\beta/c_2, \gamma, \mu_{g1}, \mu_{g2})\sqrt{A^{22}_{22}}} \tag{A8}$$

$$\rho^*_{031} = \rho_{g31}, \quad \rho^*_{032} = \rho_{g32}, \quad \rho^*_{034} = 0$$

$$\rho^*_{035} = -\left(\frac{i}{2}\right)\frac{(\beta/c_3)}{\sqrt{[(\beta/c_3)^2 + 2\gamma^2]}\sqrt{A^{33}_{33}}}$$

$$\rho^*_{036} = \left(\frac{i}{2}\right)\frac{(\beta/c_2)a^2\mu_{g2}}{g(\beta/c_2, \gamma, \mu_{g1}, \mu_{g2})\sqrt{A^{33}_{33}}}\rho_{g32} \tag{A9}$$

$$\rho^*_{041} = \rho^*_{042} = \rho^*_{043} = \rho^*_{045} = 0$$

$$\rho^*_{046} = -\frac{\sqrt{2}\gamma b^2\mu_{g1}}{g(\beta/c_2, \gamma, \mu_{g1}, \mu_{g2})}\rho_{g31} \tag{A10}$$

$$\rho^*_{051} = \tilde{\rho}^*_{015}, \quad \rho^*_{052} = \tilde{\rho}^*_{025}, \quad \rho^*_{053} = \tilde{\rho}^*_{035}, \quad \rho^*_{054} = 0$$

$$\rho^*_{056} = -\frac{[\beta^2/(c_2c_3) + 2\gamma^2]a^2\mu_{g2}}{\sqrt{[(\beta/c_3)^2 + 2\gamma^2]}g(\beta/c_2, \gamma, \mu_{g1}, \mu_{g2})}\rho_{g32} \tag{A11}$$

$$\rho^*_{061} = \tilde{\rho}^*_{016}, \quad \rho_{062} = \tilde{\rho}^*_{026}, \quad \rho^*_{063} = \tilde{\rho}^*_{036}, \quad \rho^*_{064} = \tilde{\rho}^*_{046}, \quad \rho^*_{065} = \tilde{\rho}^*_{056} \tag{A12}$$

in which

$$g(\beta/c_2, \gamma, \mu_{g1}, \mu_{g2}) = \sqrt{[(\beta/c_2)^2a^4\mu^2_{g2} + 2\gamma^2(a^4\mu^2_{g2} + b^2\mu^2_{g1})]} \tag{A13}$$

and $A^{11}_{11}$, $A^{22}_{22}$, $A^{33}_{33}$ are given by equations (27) to (33).

## REFERENCES


1. C. Tamura, T. Noguchi and K. Kato, 'Earthquake observations along measuring lines on the surface of alluvial soft ground, *Proc. 6th world conf. earthquake eng.* New Delhi, India, **I**, 389–394 (1977).
2. H. Tsuchida, E. Kurata and S. Hayashi, 'Observation of earthquake response of ground with horizontal and vertical seismometer arrays', *Proc. 6th world conf. earthquake eng.* New Delhi, India, **I**, 509–515 (1977).
3. H. Tsuchida, S. Noda, S. Tsai and E. Kurata, 'Observation of earthquake response of ground with horizontal and vertical seismometer arrays, 2nd report', *Proc. 7th world conf. earthquake eng.* Istanbul, Turkey **2**, 475–482 (1980).
4. G. N. Bycroft, 'El Centro differential ground motion array', *U.S. Geological Survey, Open File Report* 80-919, 1980.
5. S. W. Smith, J. E. Ehrenberg and E. N. Hernandez, 'Analysis of the El Centro differential array for the 1979 Imperial Valley earthquake', *Bull. seism. soc. Am.* **72**, 237–258 (1982).
6. J. L. King, 'Observations on the seismic response of sediment-filled valleys', *Ph.D. Dissertation*, University of California, San Diego, CA, 1981.
7. J. L. King and B. E. Tucker, 'Analysis of differential array data from El Centro, USA and Garm USSR', *Proc. third int. conf. microzonation* Seattle, Washington **II**, 611–622 (1982).
8. B. A. Bolt, J. Penzien and Y. B. Tsai, 'Preliminary results from the strong motion accelerograph array in Taiwan', *Newsletter, earthquake eng. res. inst.* **15** (5) 24–27 Sept. (1981).
9. B. A. Bolt, C. H. Loh, J. Penzien, Y. B. Tsai and Y. T. Yeh, 'Preliminary report on the SMART 1 strong motion array in Taiwan', *Report No. UCB/EERC-82/13*, Earthquake Engineering Research Center, University of California, Berkeley CA, 1982.

10. B. A. Bolt, Y. B. Tsai, K. Yeh and M. K. Hsu, 'Earthquake strong motions recorded by a large near-source array of digital seismographs', *Earthquake eng. struct. dyn.* **10**, 561–573 (1982).
11. M. Hoshiya and K. Ishii, 'Potential loss of ground motion due to kinematic interaction in a 4-story RC building', *Trans. JSCE appl. mech. struct. eng. div.* **14**, 129 (1982).
12. M. Hoshiya and K. Ishii, 'Evaluation of kinematic interaction of soil–foundation systems by a stochastic model', *Soil dyn. earthquake eng.* **2**, 128–134 (1983).
13. G. W. Housner, 'Interaction of building and ground during an earthquake', *Bull. seism. soc. Am.* **47**, 179–186 (1957).
14. C. M. Duke, J. E. Luco, A. R. Carriveau, P. J. Hradilek, R. Lastrico and D. Ostrom, 'Strong earthquake motion and site conditions: Hollywood', *Bull. seism. soc. Am.* **60**, 1271–1289 (1970).
15. H. Yamahara, 'Ground motions during earthquakes and the input loss of earthquake power to an excitation of building', *Soils and Foundations*, Japan Society of Soil Mechanics and Foundation Engineering, **10**, No. 2, 145–161 (1970).
16. K. Shioya and H. Yamahara, 'Study of filtering effect of foundation slab based on observational records', *Proc. 7th world conf. earthquake eng.* Istanbul, Turkey **5**, 181 (1980).
17. K. Ishii, T. Itoh and J. Suhara, 'Kinematic interaction of soil–structure system based on observed data', *Proc. 8th world conf. earthquake eng.* San Francisco, CA (1984).
18. N. M. Newmark, 'Torsion of symmetrical buildings', *Proc. 4th world conf. earthquake eng.* Santiago, Chile (1969).
19. J. E. Luco, 'Torsional response of structures for obliquely incident seismic waves,' *Earthquake eng. struct dyn.* **4**, 207–219 (1976).
20. J. E. Luco, 'Torsional response of structures for SH-waves: the case of hemispherical foundations', *Bull. seism. soc. Am.* **66**, 109–123 (1976).
21. J. E. Luco and H. L. Wong, 'Dynamic response of rectangular foundations for Rayleigh wave excitation', *Proc. 6th world conf. earthquake eng.* New Delhi, India **II**, 1542–1547 (1977).
22. J. E. Luco and H. L. Wong, 'Response of structures to nonvertically incident seismic waves', *Bull. seism. soc. Am.* **72**, 275–302 (1982).
23. H. L. Wong and J. E. Luco, 'Dynamic response of foundations to obliquely incident seismic waves', *Earthquake eng. struct. dyn.* **6**, 3–16 (1978).
24. J. E. Luco and D. A. Sotiropoulos 'Local characterization of free field ground motion and effects of wave passage', *Bull. seism. soc. Am.* **70**, 2229–2244 (1980).
25. C. H. Loh, J. Penzien and Y. B. Tsai, 'Engineering analyses of SMART 1 array accelerograms', *Earthquake eng. struct. dyn.* **10**, 575–591 (1982).
26. M. Iguchi 'Seismic response with consideration of both phase differences of ground motion and soil–structure interaction', *Proc. Japan earthquake eng. symp.* Tokyo, Japan **B-16** (1973).
27. R. H. Scanlan 'Seismic wave effects on soil–structure interaction', *Earthquake eng. struct. dyn.* **4**, 379–388 (1976).
28. Y. Matsushima, 'Stochastic response of structure due to spatially variant earthquake excitations', *Proc. 6th world conf. earthquake eng.* New Delhi, India **II**, 1077–1082 (1977).
29. R. Harichandran and E. Vanmarcke, 'Space–time variation of earthquake ground motion', *Research Report R84-12*, Department of Civil Engineering, Massachusetts Institute of Technology, Cambridge, MA, 1984.
30. B. J. Uscinski, *The Elements of Wave Propagation in Random Media*, McGraw-Hill, New York, 1977.
31. A. H. Hadjian, 'On the correlation of the components of strong motion', *Proc. 2nd int. conf. microzonation*, San Francisco, CA (1978).
32. G. N. Bycroft 'Soil–foundation interaction and differential ground motions', *Earthquake eng. struct. dyn.* **8**, 397–404 (1980).
33. J. E. Luco 'Linear soil–structure interaction', *Report UCRL-15272, PSA #* 7249809, Lawrence Livermore Laboratory, Livermore, CA, 1980.
34. J. E. Luco, 'On the relation between radiation and scattering problems for foundations embedded in an elastic half-space', *Soil dyn. earthquake eng.* **5**, 97–101 (1986).
35. H. L. Wong and J. E. Luco 'Dynamic response of foundations of arbitrary shape', *Earthquake eng. struct. dyn.* **4**, 579–587 (1976).
36. M. J. O'Rourke, M. Bloom and R. Dobry, 'Apparent propagation velocity of body waves', *Earthquake eng. struct. dyn.* **10**, 283–294 (1982).
37. M. J. O'Rourke and R. Dobry, 'Apparent horizontal propagation velocity for the 1979 Imperial Valley earthquake', *Bull. seism. soc. Am.* **72**, 2377–2380 (1982).
38. P. Spudich and E. Cranswick, 'Use of near source seismic array data to reveal details of earthquake rupture process', *Earthquake notes*, **53**, 39 (1982).
39. A. H. Hadjian and D. M. Hadley, 'Studies of apparent seismic wave velocity', *Int. conf. recent adv. geotech. earthquake eng. soil dyn.* St. Louis (1981).
40. M. Bouchon and K. Aki, 'Strain, tilt and rotation associated with strong motion in the vicinity of earthquake fault', *Bull. seism. soc. Am.* **72**, 1717–1738 (1982).
41. M. Campillo and M. Bouchon, 'A theoretical study of the radiation from small strike-slip earthquakes at close distances', *Bull. seism. soc. Am.* **73**, 83–96 (1983).